

An introduction to symmetries in stellarators

Lise-Marie Imbert-Gérard, Elizabeth Paul, Adelle Wright

Contents

1	Introduction	3
2	Background	4
2.1	Plasma	4
2.2	Fusion reactions and power source	5
2.3	Charged particles and trajectories	6
2.4	Magnetic confinement for fusion	6
2.5	Separation of length and time scales	7
3	Electric and magnetic fields: Maxwell's equations	8
3.1	Electro-magnetics	8
3.2	Electrostatics	8
3.3	Magnetostatics	9
3.4	Vacuum fields	9
3.5	Summary	9
4	Classical mechanics	10
4.1	Newton's laws	10
4.2	Lagrangian mechanics	10
4.3	Hamiltonian mechanics	12
5	Single particle motion in electro-magnetic fields	13
5.1	Motion in a straight and uniform magnetic field	13
5.2	Gyroaveraged Lagrangian	15
5.2.1	Adiabatic invariant for gyromotion	18
5.2.2	Energy conservation	18
5.2.3	Particle trapping	19
5.3	Guiding center motion	19
5.3.1	Parallel guiding center motion	20
5.3.2	Perpendicular guiding center motion	20
5.4	Introduction to toroidal confinement	21
6	Coordinate systems	22
6.1	Magnetic field lines and flux surfaces	23
6.2	Canonical cylindrical coordinates	24
6.3	Flux surfaces and flux functions	24
6.4	Flux coordinates	25
6.5	Cheat sheet for non-orthogonal coordinates	27
7	Toroidal magnetic confinement	30
7.1	Axisymmetry	30
7.2	Particle confinement in axisymmetry	30
7.3	Tokamak	31
7.4	Stellarator	32
7.5	Rotational transform	32
7.6	Producing rotational transform	33
7.6.1	With axisymmetry	34
7.6.2	Without axisymmetry	35

8	Coupling of particles and electro-magnetic fields: MHD models	36
8.1	Ideal MHD	36
8.2	Flux freezing	37
8.3	Ideal MHD equilibrium	38
8.4	MHD equilibrium in a tokamak: Grad-Shafranov	39
8.5	Summary	39
9	Magnetic coordinates	40
9.1	Contravariant form	40
9.2	Covariant form	41
9.3	Boozer coordinates	43
9.3.1	Radial covariant component	44
9.4	Summary	45
10	Challenges associated with 3D equilibrium fields	45
10.1	From existence to non-existence of magnetic surfaces	45
10.1.1	Analysis of the vector potential	46
10.1.2	Variational principle for field line flow	47
10.1.3	Relation to Hamiltonian dynamics	47
10.2	Integrability of a Hamiltonian system	48
10.2.1	Defining integrability	48
10.2.2	Hamilton-Jacobi method	49
10.2.3	Perturbations about integrability	51
10.2.4	Persistence of some flux surfaces: KAM theory	53
10.3	Singularities and surface currents in 3D MHD	54
10.4	Constructing 3D MHD equilibria near the magnetic axis	56
11	Models of 3D equilibrium magnetic fields	60
11.1	Variational principle for MHD equilibria	60
11.2	3D MHD equilibrium with assumption of surfaces	62
11.3	3D MHD equilibria without assumption of surfaces	63
11.4	Force-free fields	63
11.5	Stepped pressure equilibrium (MRxMHD)	65
11.6	Vacuum fields	67
11.7	Summary and analogy with steady Euler flow	68
12	Symmetries in stellarators	69
12.1	Quasisymmetry	69
12.1.1	Guiding center motion in quasisymmetry	70
12.1.2	Remark on “quasi”	71
12.1.3	Types of quasisymmetry	71
12.2	N_P symmetry	72
12.3	Stellarator symmetry	72
A	Debye shielding	75

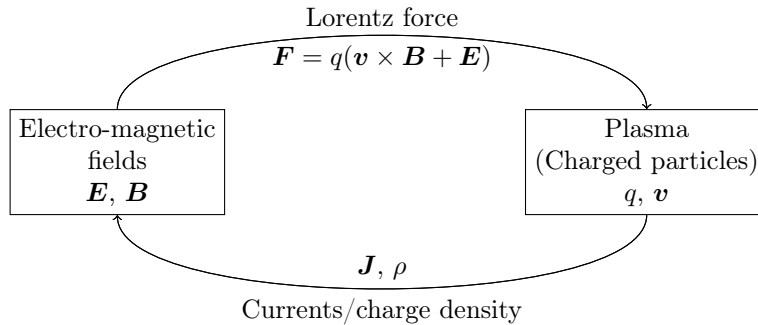


Figure 1: Diagram representing the coupling between particles (left box) and fields (right box). An arrow pointing to a box represents inputs, while an arrow starting from a box represents an action.

1 Introduction

The field of plasma physics is broad, with applications in astrophysical and solar phenomena, laser experiments, electronics, and nuclear fusion. Rather than provide a comprehensive introduction to plasma physics, the goal of this document is to explain several important concepts for magnetic confinement in a stellarator. Specifically, we aim to provide the requisite background material in order to discuss challenges related to stellarator equilibrium models in Sections 10 and 11, as well as quasisymmetry in Section 12. Both of these concepts are related to ‘hidden symmetries’ in 3D systems. Tokamaks have a symmetry with respect to rotation about the toroidal angle, ensuring the existence of continuously nested magnetic surfaces and single particle confinement. While stellarators lack this symmetry, we will discuss how magnetic fields in a stellarators can be approximately integrable, providing some nested magnetic surfaces. Furthermore, single particle confinement can also be comparable to that in a tokamak through application of the quasisymmetry concept.

Much of the research efforts in magnetic confinement of plasmas has focused on the tokamak configuration, which features much simpler geometry than the stellarator due to its symmetry with respect to one coordinate. Conversely, the stellarator relies on breaking of this symmetry in order to provide confinement. While stellarators tend to be more difficult to design because of their lack of inherent symmetry, they provide several advantages over tokamak configurations as they do not require a large current in the confinement region. Modern stellarators have been designed to take advantage of hidden symmetries, allowing these configurations to have confinement properties similar to tokamaks. The [Simons Collaboration on Hidden Symmetries and Fusion Energy](#) has been formed to foster collaboration between experts in numerical optimization, dynamical systems, PDE analysis, and plasma physics in order to find stellarator configurations with hidden symmetries. We hope that this document will serve as an introduction for those with interests in stellarator confinement.

Along the way, we motivate magnetic confinement for fusion with the stellarator concept. Many models and corresponding hypotheses will be discussed. As often as possible, the ideas will be presented using equations and pictures. References to other relevant introductory material will be included. Our hope is for the material to be accessible for those who may not have a physics background but are interested in applications of mathematical and computational tools to stellarator research.

The general setting of plasma modeling is represented in Figure 1, representing the interaction between electro-magnetic fields and charged particle motion. Charged particle motion depends on electro-magnetic fields through the Lorentz force, and electro-magnetic fields depend on charged particle motion through the resulting current and density which appear in Maxwell’s equations. While such a set of equations provides a complete picture of how a coupled system evolves, it is hopeless to solve these equations in practice for any physical system of interest, as all of the particles are coupled through the fields. To glean physical understanding and for computational tractability, it is therefore necessary to make approximations. The choice of approximations depends on the problem at hand or physical regime of interest, leading to a hierarchy of models which are used to describe the physics of plasmas. In this way, there is a wealth of interesting open problems related

to the mathematical properties and numerical approximations used to model magnetic confinement plasmas.

Section 2, we provides basic terminology for plasmas and their relation to magnetic confinement. Section 3 presents the set of equations that govern the evolution of electro-magnetic fields, namely Maxwell's equations. Section 4 reviews the equations of motion that describe the trajectory of a charged particle in electro-magnetic fields and their relation to the variational principles associated with the Lagrangian and Hamiltonian. Under the assumption that electro-magnetic fields can be imposed without feedback from the particles on the fields, Section 5 discusses the motion of charged particles within these given fields. Section 6 introduces convenient coordinate systems to describe toroidal confinement devices. In Section 7, these ideas are applied to discuss concepts related to magnetic confinement. Here we provide motivation for stellarator confinement. Section 8 discusses the coupling of the electro-magnetic fields with particles through the magneto-hydrodynamic (MHD) model, including the set of equations used to describe the equilibrium state. Section 9 introduces coordinate systems relying on additional assumptions on the magnetic field related to MHD equilibria. Section 10 focuses on the existence of surfaces in stellarator devices and their associated consequences for MHD equilibria. Several models for MHD equilibria in stellarators are presented in Section 11. These models provide the equations which determine the time-independent fields, from which the particle trajectories and other physical quantities of interest can be computed. Finally, several symmetries common to stellarator configurations and their consequences are described in Section 12.

2 Background

In this Section we will define and discuss central ideas to the field of plasma physics and magnetic confinement. This will not include many mathematical details, but will simply provide some background and motivation for what will follow.

2.1 Plasma

A plasma is a partially or fully ionized gas that exhibits some collective behavior, in contrast to a neutral gas where the particle dynamics are determined essentially by collisions between nearest neighbors. As the behavior of a plasma is rather different from that of a gas, plasma is often called the fourth state of matter. In an ionized gas, some electrons are stripped off of the nuclei, and ions and those electrons move independently rather than bound together as atoms.

Ionization can occur due to the collision of an atom with an electron or the absorption of a photon with sufficient energy, causing an electron to be removed from the atom. The inverse processes can also occur, in which an atom and two electrons collide to form an atom and one electron, or an electron and ion can combine, releasing a photon. In equilibrium, these processes balance each other to determine the degree of ionization. The fraction of ionized atoms depends on the temperature and density of the gas. At room temperature, the ionization fraction of a typical gas is negligibly small. At the typical densities and temperatures relevant for fusion experiments, the ionization fraction is large enough that collisions between charged particles dominate over those between charged and neutral particles. For this reason, we will focus our attention on charged particle motion when discussing plasmas in this document. See Chapter 10 in [31] for a further discussion on ionization.

On earth, naturally occurring plasmas are not especially common but can be found in lightning and auroras. Laboratory created plasmas are widely used in many industrial processing applications [68] such as the deposition of thin layers of metal on surfaces like in solar panels or watches, or for processing of materials including the etching of superconductors. In medicine, plasma is used to treat certain cells [57]. On the other hand, plasmas are ubiquitous in space and astrophysical environments. For example, the earth's upper atmosphere (the ionosphere) is ionized and plays a critical role in shielding the planet from potentially harmful radiation from the sun. More generally, the magnetospheres of magnetized astronomical objects are important for determining the interaction of the body with the surrounding medium. Plasma thrusters have also been explored for use in satellite propulsion [66].

A hot, fusion-relevant plasma is typically fully ionized, with the ions and electrons in thermal equilibrium. If we consider the temperature, T , of each species, we often find that $T_e \approx T_i$ if the plasma is confined long enough for the temperatures to equilibrate. Temperature can be thought

of as being a measure of the energy per particle; thus temperature equilibration corresponds to the equal partition of energy among particles. A classical plasma must be hot enough that the electrons have the necessary energy to overcome the potential of the nucleus to ionize, and diffuse enough that the plasma appears neutral on length scales larger than the Debye length (see Appendix A). This is known as quasineutrality,

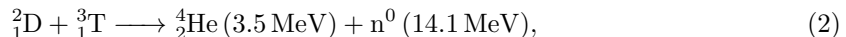
$$\sum_s n_s q_s = 0, \quad (1)$$

where n_s and q_s are the number density and charge of species s , respectively, and the sum is taken over species. We call this quasineutrality rather than neutrality, since if one considers short enough length scales this assumption is violated.

2.2 Fusion reactions and power source

Stars, including the sun, are giant balls of plasmas, the convection of which produces a magnetic field. The majority of stars, including our sun, are fuelled by nuclear fusion reactions, when two atomic nuclei combine to form atomic nuclei in addition to other products. This process leads to a slight decrease in mass, resulting in the release of energy according to the famous $E = mc^2$ equation, where E is the energy released, m is the mass, and c is the speed of light (a physical constant).

In order for two particles to undergo a fusion reaction, they must be brought close enough together for the strong force, which acts on the scale length of protons and neutrons, to act. This requires overcoming the repulsive Coulomb force, which makes like charges repel and opposite charges attract, and acts over much larger length scales. In stars, the combination of high temperature and strong gravitational field ensures the probability, or cross-Section, of a fusion reaction occurring is sufficient to power the star. At standard conditions on earth, however, the probability of a fusion reaction is negligibly small. To realize terrestrial fusion power, we therefore need to create conditions which sufficiently increase the fusion reaction cross-Section. In practice, this is achieved by increasing temperatures, up to ten times hotter than the center of the sun. The candidate reaction for terrestrial fusion with the largest cross-Section is the fusion of deuterium, ${}^2_1\text{D}$, and tritium, ${}^3_1\text{T}$, to produce helium, ${}^4_2\text{He}$, and an energetic neutron, n^0 ,



known as the D-T reaction. At the requisite temperatures for the D-T reaction to occur, matter exists in a plasma state. Therefore, we need to consider how to confine hot plasmas on earth. We will discuss magnetic confinement with the stellarator concept in detail in this document.

Nuclear fusion is one of the most energetic reactions known in nature. The D-T reaction produces 3.4×10^8 MJ of energy for every kg of fuel, in comparison with the combustion of gasoline, which produces 40 MJ [26]. If we could harness this mechanism as a power source on earth, it would yield numerous benefits. Fusion as a power source requires very little fuel, produces no greenhouse gasses, is safe, and produces no long-lived radioactive waste. In other words, it could provide a source of clean, virtually limitless energy. Both of the fuels necessary for the D-T reaction are readily available on earth: deuterium is found abundantly in the earth's oceans, and tritium can be produced with irradiation of lithium by an energetic neutron. There are now schemes proposed to produce tritium as a by-product of fusion reactions (see Section 5.5 in [26]).

Nuclear fission and fusion yield a similar amount of energy per kg of fuel. However, nuclear fusion has several advantages over nuclear fission. While the fusion reaction itself does not produce any radioactive by-products, isotopes result from the reaction of the fusion-produced neutrons with material structures in the plasma vessel. Isotopes associated with the production of fusion power have half-lives of around 10 years, compared to fission by-products which can have half-lives of over 10^4 years, eliminating challenges associated with long-lived radioactive waste. Unlike plutonium and uranium, the fuels of fission power, the fuel required for fusion power also have zero potential for enrichment or weaponization. Finally, compared to fission, fusion power is inherently safer as it does not depend on a chain reaction, is very sensitive to its conditions, and the amount of fuel present in a device at any given time is fairly small meaning there is no potential for runaway reactions.

2.3 Charged particles and trajectories

While not all plasmas are fully ionized, the interactions between charged particles dominate over those between charged and neutral particles. Thus for many applications, it suffices to only consider the behavior of charged particles, ions and electrons, rather than neutral atoms. In the plasma physics literature, the term ion refers to a positively charged nucleus while an electron is negatively charged. The bulk of fusion plasmas consist of hydrogen or one of its isotopes, deuterium and tritium. Other ions may exist in fusion plasmas, such as alpha particles, which are a product of a fusion reaction, or heavier impurities which enter the plasma through interaction with material structures. Charged particles are accelerated by electric fields and, when moving, interact with magnetic fields.

Trajectories, or orbits, refer to the motion of charged particles as the equations of motion that describe a particle's position and velocity are evolved in time. For example, in a straight magnetic field, particles exhibit helical trajectories, as will be discussed in Section 5.1. In Section 5.2 we will consider the trajectories of charged particles in the presence of strong magnetic fields. This provides a basis for confinement in the tokamak and stellarator configurations.

2.4 Magnetic confinement for fusion

In fusion experiments, the center of the device where fusion reactions take place is very hot and must be kept well away from the wall of the experimental vessel to avoid damage. The interaction of charged particles, which constitute a plasma, with electro-magnetic fields is one important property which can be exploited to control and contain plasmas. This is known as magnetic confinement (see Section 7), the focus of this document. Other principles for fusion plasma confinement include inertial confinement, as in the laser facility at the National Ignition Facility [1]. Regardless of the method, the ultimate goal of all fusion power devices is to produce more energy than what is required to initiate the reactions. This is measured by Q , the ratio of the fusion output power to the power used to heat the plasma. The break-even point corresponds to $Q = 1$ and ignition, a self-sustaining reaction, occurs as $Q \rightarrow \infty$. The goal of fusion research is to reach $Q \gg 1$. Magnetic confinement is one method to thermally insulate plasmas at temperatures and densities necessary for fusion to occur.

The first laboratory magnetic confinement fusion device was built in the late 1940s, a toroidal device known as a Z-pinch [12]. Many have been built around the world since, and there continues to be active experimental research at magnetic confinement fusion devices today. The largest magnetic confinement device in operation is the Joint European Torus (JET), a tokamak which has set the record for the largest value of $Q = 0.6$ [98].

The D-T fusion reaction (2) results in a helium nucleus (alpha particle) and a neutron. The neutron, being charge-neutral, is not confined by the magnetic fields and can leave the device. The alpha particle, on the other hand, may be confined by the magnetic fields and through collisions with the bulk plasma can deposit energy to the plasma. Ignition ($Q \rightarrow \infty$) is achieved if the energy deposited by the alpha particles is sufficient to sustain fusion plasma conditions without external heating.

The plasma conditions necessary for ignition to occur is described by the Lawson criterion, a lower bound on the fusion triple product,

$$nT\tau_E > 3 \times 10^{21} \text{ m}^{-3}\text{keVs}, \quad (3)$$

here n is the number density in m^{-3} , T is the temperature in keV ¹, and τ_E is the energy confinement time in seconds (the timescale of energy loss from the plasma). While magnetic confinement experiments can reach the conditions necessary for fusion to occur, the Lawson criteria has not been met in any experiments to date, though some have come close.

Ultimately, for electricity production, fusion power aims to achieve a burning plasma ($Q \geq 5$) operating regime where most of the energy required to heat the plasma is obtained from fusion reactions. The ITER project is a multi-national (35 countries) collaboration to demonstrate the scientific viability of fusion power. The experimental device is currently under construction in France and aims to demonstrate $Q > 10$ [2].

From the fusion triple product, it is clear that, for a given temperature, the Lawson criterion can be achieved by increasing confinement time. Increasing plasma temperature involves heating

¹The plasma temperature is typically measured in units of energy. If measured in Kelvin, we multiply by Boltzmann's constant $k_B = 1.38 \times 10^{-23} \text{ J/K}$

Parameter	W7-AS [72]	LHD [56]	W7-X [92]
$\lambda_{D,e}$ [cm]	3×10^{-3}	2×10^{-3}	9×10^{-3}
ρ_i [cm]	2×10^{-1}	3×10^{-1}	2×10^{-1}
a [cm]	20	60	50
Ω_i [s ⁻¹]	9×10^7	1×10^8	2×10^8
ν_{ee} [s ⁻¹]	1×10^5	2×10^5	4×10^3
τ_E^{-1} [s ⁻¹]	2	3	10

Table 1: This chart displays the range of length and time scales for several stellarator experiments. Here $\lambda_{D,e}$ is the electron Debye length (see Appendix A), ρ_i is the ion gyroradius (see Section 5.1), a is the average minor radius of the device (see Section 6.2), ν_{ee} is the electron-electron collision frequency, Ω_i is the ion gyrofrequency (see Section 5.1), and τ_E is the energy confinement time. Due to the large range of scales, it is intractable to model all of these scales simultaneously. This provides motivation for the application of reduced models.

which, if external, is expensive. One of the main challenges of magnetic confinement fusion is thus to achieve ignition by maximizing the energy confinement time which requires confining a hot, turbulent plasma for a sufficient period of time.

See Chapter 1 in [98] or Chapter 6 in [26] for a more complete overview of magnetic confinement for fusion.

2.5 Separation of length and time scales

In fusion plasmas, there is a good separation between length and time scale that has led to the development of reduced models. Table 1 provides a few typical length and time scales that exist in magnetic confinement fusion plasmas. The Debye length, λ_D , is much smaller than typical length scales for fusion devices, so the plasma can be assumed to be quasineutral, see Appendix A. The ion gyrofrequency, Ω_i , is much larger than typical frequencies, so motion can be averaged over the fast gyrofrequency to consider guiding center models, see Section 5.2.

Modeling plasma particles is another fundamental example. Under certain assumptions of length and time scales, charged particles can be modeled in various ways.

1. The *single particle approach* studies single particle motion in stationary background fields. Thus feedback of particles on the electro-magnetic fields or collisions between particles will be neglected. This approach is useful for discussing the confinement properties of several magnetic field configurations in the absence of plasma waves. Single particle trajectories are also considered when modeling a small population of particles whose feedback on the fields can be neglected. This approach will be discussed in Section 5.
2. The *kinetic approach* studies the evolution of distributions of particles in velocity and position space. Particles can interact with each other through collisions and are coupled to electro-magnetic fields. Rather than consider the equations of motion of individual particles, the distribution of the positions and velocities of particles are computed. This approach will not be discussed in this document. For an introduction, see Chapters 3-5 in [79] or Chapters 4-5 in [34].
3. The *fluid approach* studies the plasma at a macroscopic scale, as one or several fluids. The fluid is described by scalar density and pressure fields and vector flow velocity field rather than a distribution of all particles in velocity and position space. As the velocity distribution of particles is averaged over, a certain distribution of velocities must be assumed, such as an equilibrium distribution. If the velocity distribution is not in equilibrium, then this approach may not capture the necessary physics. The fluid approach is useful for studying large-scale effects and some waves. It provides a set of equations which is simpler than the kinetic approach. Some aspects of this approach will be discussed in Section 8.

3 Electric and magnetic fields: Maxwell's equations

We describe here models for the electro-magnetic fields, respectively denoted \mathbf{E} and \mathbf{B} , while the plasma density ρ and current density \mathbf{J} are considered inputs. In Section 5, we will discuss the trajectories of particles in static electro-magnetic fields, without considering the feedback of ρ and \mathbf{J} on the fields. A more realistic model would include this coupling: the Lorentz force describes how the electric and magnetic fields act on a charged particle motion, while Maxwell's equations describe how electric and magnetic fields evolve in the presence of ρ and \mathbf{J} . See Figure 1 and Section 8.

In the remainder of the text, we will use the SI system of units. Maxwell's equations are sometimes presented in Gaussian units such that the physical constants differ. See [45] for a comparison between the SI and Gaussian systems.

3.1 Electro-magnetics

Maxwell's equations describe how electric \mathbf{E} and magnetic \mathbf{B} fields propagate, interact together as well as with currents and charges. Maxwell's equations refer to the four following equations.

Gauss's law is

$$\nabla \cdot \mathbf{E} = \frac{\rho}{\epsilon_0}, \quad (4)$$

Ampere's law is

$$\nabla \times \mathbf{B} = \mu_0 \mathbf{J} + \frac{1}{c^2} \frac{\partial \mathbf{E}}{\partial t}, \quad (5)$$

Faraday's law is

$$\nabla \times \mathbf{E} = -\frac{\partial \mathbf{B}}{\partial t}, \quad (6)$$

and magnetic fields must be divergence-free,

$$\nabla \cdot \mathbf{B} = 0. \quad (7)$$

Here μ_0 is the permeability of free space, ϵ_0 is the permittivity of free space, and c is the speed of light. This set of PDEs describe how the electric and magnetic fields evolve in time, t , in response to charge density ρ and current density \mathbf{J} . Under further assumptions on time scales of interest, Maxwell's equations can be further reduced as we will see in the following Sections.

Often the electric and magnetic fields are expressed in terms of scalar and vector potentials. As \mathbf{B} is divergence-free from (7), it can always be written in terms of a vector potential,

$$\mathbf{B} = \nabla \times \mathbf{A}. \quad (8)$$

We note that there is some non-uniqueness in the choice of the vector potential, as the gradient of any scalar function can be added to \mathbf{A} without altering the magnetic field. A standard by which the vector potential is chosen is often referred to as the gauge in the physics literature. However, the gauge can not always be chosen arbitrarily, as other quantities of interest can be expressed in terms of the vector potential rather than the magnetic field (see for example, Sections 4.2 and 11.4).

Inserting (8) into (6), we see that \mathbf{E} can be written as $-\partial \mathbf{A} / \partial t$ with the addition of a curl-free vector field,

$$\mathbf{E} = -\nabla \Phi - \frac{\partial \mathbf{A}}{\partial t}. \quad (9)$$

Often Φ is referred to as the scalar potential and \mathbf{A} as the vector potential.

3.2 Electrostatics

In the static case ($\partial / \partial t = 0$), the equations satisfied by \mathbf{E} and \mathbf{B} decouple. As $\nabla \times \mathbf{E} = 0$ under this assumption, the electric field can be written in terms of only a scalar potential

$$\mathbf{E} = -\nabla \Phi. \quad (10)$$

From Gauss's law (4) the electrostatic potential satisfies Poisson's equation,

$$\Delta\Phi = -\frac{\rho}{\epsilon_0}. \quad (11)$$

Gauss's law can be written in an equivalent integral form by integrating over a volume Ω ,

$$\forall \text{ volume } \Omega \subset \mathbb{R}^3, \int_{\partial\Omega} \mathbf{E} \cdot \hat{\mathbf{n}} dA = \frac{1}{\epsilon_0} \int_{\Omega} \rho d^3x, \quad (12)$$

where $\hat{\mathbf{n}}$ is the outward unit normal on $\partial\Omega$.

3.3 Magnetostatics

Often the displacement current term, $\partial\mathbf{E}/\partial t$ in (5), can be neglected if the typical velocities of a system, v , are non-relativistic ($v/c \ll 1$). This is the assumption that the model does not need to include light waves, which are associated with very short time scales. Under this assumption, Ampere's law becomes

$$\nabla \times \mathbf{B} = \mu_0 \mathbf{J}. \quad (13)$$

This can be written in an equivalent integral form,

$$\forall \text{ surface } S \subset \mathbb{R}^3, \oint_{\partial S} \mathbf{B} \cdot d\mathbf{l} = \mu_0 \int_S \hat{\mathbf{n}} \cdot \mathbf{J} d^2x, \quad (14)$$

where for an open surface the line integral is taken along a closed curve forming the boundary of the surface S , while for a closed surface the left hand side is zero. Another integral form that is consistent with the magnetostatic equations is the Biot-Savart law,

$$\mathbf{B}(\mathbf{r}) = \frac{\mu_0}{4\pi} \int_{\mathbb{R}^3} \frac{\mathbf{J}(\mathbf{r}') \times (\mathbf{r} - \mathbf{r}')}{|\mathbf{r} - \mathbf{r}'|^3} d\mathbf{r}'. \quad (15)$$

For example, in a magnetic confinement fusion device, the integral is taken throughout the plasma volume and along the electro-magnetic coils.

3.4 Vacuum fields

The term vacuum field is used to describe the magnetic field in a region Ω without currents under the magnetostatics assumptions. In magnetic confinement fusion, this could be the region outside the plasma, not including the electro-magnetic coils. In this case, we have $\nabla \times \mathbf{B} = 0$, so a scalar potential can be used to describe the magnetic field,

$$\mathbf{B} = \nabla\Phi_B \text{ in } \Omega. \quad (16)$$

The magnetic field must also satisfy (7), so the scalar potential must satisfy Laplace's equation,

$$\Delta\Phi_B = 0 \text{ in } \Omega. \quad (17)$$

Laplace's equation is often solved with a Neumann boundary condition such that $\mathbf{B} \cdot \hat{\mathbf{n}} = \hat{\mathbf{n}} \cdot \nabla\Phi_B$ is prescribed on $\partial\Omega$. Depending on the topology of Ω , an additional scalar quantity must be specified to obtain a unique solution. The solution in a toroidal domain will be discussed in Section 11.6.

Instead of solving Laplace's equation, the magnetic field in the vacuum region can be determined using the Biot-Savart law (15), integrating over all currents outside of the vacuum region, that is to say over $\mathbb{R}^3 \setminus \Omega$.

3.5 Summary

Here we describe Maxwell's equations in the presence of some charge density ρ and current density \mathbf{J} . A realistic model would include coupling to a set of equations which describes the evolution of the charge and current density. Under various sets of hypotheses, Maxwell's equations can be reduced to simpler models. Common reduced models are gathered in the following Table. For each reduced model, the Table provides the hypotheses (Hyp.), the PDE model, a different formulation of the model, and the model data. Computational domains, as well as boundary conditions, will be addressed later (see Section 11.6).

	Maxwell	Electrostatics	Magnetostatics	Vacuum fields
Hyp.		$\partial \mathbf{E} / \partial t = 0$ $\partial \mathbf{B} / \partial t = 0$	$\partial \mathbf{E} / \partial t = 0$ $\partial \mathbf{J} / \partial t = 0$	$\partial \mathbf{E} / \partial t = 0$ $\mathbf{J} = 0$ in Ω
PDE model	$\nabla \cdot \mathbf{E} = \frac{\rho}{\epsilon_0}$ $\nabla \times \mathbf{B} = \mu_0 \mathbf{J} + \frac{1}{c^2} \frac{\partial \mathbf{E}}{\partial t}$ $\nabla \times \mathbf{E} = -\frac{\partial \mathbf{B}}{\partial t}$ $\nabla \cdot \mathbf{B} = 0$	$\nabla \cdot \mathbf{E} = \frac{\rho}{\epsilon_0}$ $\nabla \times \mathbf{E} = 0$	$\nabla \times \mathbf{B} = \mu_0 \mathbf{J}$ $\nabla \cdot \mathbf{B} = 0$	$\nabla \times \mathbf{B} = 0$ in Ω $\nabla \cdot \mathbf{B} = 0$ in Ω
Model \Leftrightarrow		$\mathbf{E} = -\nabla \Phi$ $\Delta \Phi = -\frac{\rho}{\epsilon_0}$	$\mathbf{B}(\mathbf{r}) = \frac{\mu_0}{4\pi} \times$ $\int_{\mathbb{R}^3} \frac{\mathbf{J}(\mathbf{r}') \times (\mathbf{r} - \mathbf{r}')}{ \mathbf{r} - \mathbf{r}' ^3} d\mathbf{r}'$	$\mathbf{B}(\mathbf{r}) = \frac{\mu_0}{4\pi} \times$ $\int_{\mathbb{R}^3 \setminus \Omega} \frac{\mathbf{J}(\mathbf{r}') \times (\mathbf{r} - \mathbf{r}')}{ \mathbf{r} - \mathbf{r}' ^3} d\mathbf{r}'$ $\Leftrightarrow \begin{cases} \mathbf{B} = \nabla \Phi_B \\ \Delta \Phi_B = 0 \end{cases}$ in Ω
Given	\mathbf{J}, ρ	ρ	\mathbf{J}	\mathbf{J} outside of Ω or $\mathbf{B} \cdot \hat{\mathbf{n}}$ on $\partial\Omega$

4 Classical mechanics

We briefly review concepts from classical mechanics. We begin in Section 4.1 with Newton's laws, a set of ODEs which describe the motion of a particle in the presence of a force. We will then show that these ODEs can be expressed in terms of two variational principles involving the Lagrangian and Hamiltonian functionals, respectively in Sections 4.2 and 4.3. These concepts will later be relevant to study single particle motion in electro-magnetic fields in Section 5 as well as magnetic field lines in Section 10.

4.1 Newton's laws

Newton's laws are a set of ODEs which describe the trajectory of a point particle of mass m ,

$$m \frac{d^2 \mathbf{r}(t)}{dt^2} = \mathbf{F}(\mathbf{r}(t), \dot{\mathbf{r}}(t)). \quad (18)$$

On the right hand side, \mathbf{F} is a force, which can in general depend on both the position, \mathbf{r} , and its time derivative, the velocity $\dot{\mathbf{r}}$. To study single particle motion in electric and magnetic fields, we will consider the Lorentz force,

$$\mathbf{F}(\mathbf{r}, \dot{\mathbf{r}}) = q(\dot{\mathbf{r}} \times \mathbf{B}(\mathbf{r}) + \mathbf{E}(\mathbf{r})), \quad (19)$$

which depends explicitly on $\dot{\mathbf{r}}$ and on \mathbf{r} through \mathbf{B} and \mathbf{E} . Newton's law can be solved to obtain the trajectory, $\mathbf{r}(t)$ and $\dot{\mathbf{r}}(t)$, of a particle given initial conditions \mathbf{r}_{init} and $\dot{\mathbf{r}}_{\text{init}}$.

4.2 Lagrangian mechanics

While Newton's laws, in principle, provide us with all of the information we need to obtain trajectories of charged particles, another more general approach is desirable. Specifically, we will discuss a variational formalism from which Newton's laws can be obtained. The Lagrangian approach will provide several advantages as we consider reduced models in Section 5.2. Further, calculations are simplified when manipulating the scalar Lagrangian as opposed to the vectorial equations

of motion. Working within the Lagrangian formalism will provide insight into certain conserved quantities as will be seen in Sections 5.2.1 and 5.2.2.

The equations of motion (18) follow from a variational principle involving a scalar function, the Lagrangian. To obtain the Lagrangian for motion in electro-magnetic fields, we first write the electric and magnetic fields in terms of vector and scalar potentials,

$$\mathbf{B} = \nabla \times \mathbf{A} \quad (20a)$$

$$\mathbf{E} = -\nabla\Phi - \frac{\partial\mathbf{A}}{\partial t}. \quad (20b)$$

The Lagrangian for charged particles in electro-magnetic fields is,

$$L : (\mathbf{r}, \dot{\mathbf{r}}, t) \in \mathbb{R}^3 \times \mathbb{R}^3 \times \mathbb{R} \mapsto \frac{m|\dot{\mathbf{r}}|^2}{2} + q\mathbf{A}(\mathbf{r}, t) \cdot \dot{\mathbf{r}} - q\Phi(\mathbf{r}, t). \quad (21)$$

Here we consider \mathbf{r} , $\dot{\mathbf{r}}$, and t to be independent coordinates (this will become important when we take partial derivatives of L). Along a given trajectory $\mathbf{r} \in \mathcal{C}^1(\mathbb{R}, \mathbb{R}^3)$, the Lagrangian is $L(\mathbf{r}(t), \dot{\mathbf{r}}(t), t)$, where $\dot{\mathbf{r}} = d\mathbf{r}/dt$ is the velocity along the trajectory, $\mathbf{r}(t)$.

Consider the following functional of a trajectory $\mathbf{r}(t)$ through L ,

$$\forall \mathbf{r} \in \mathcal{C}^1(\mathbb{R}, \mathbb{R}^3), \quad S[\mathbf{r}] := \int_{t_{\text{init}}}^{t_{\text{final}}} L(\mathbf{r}(t), \dot{\mathbf{r}}(t), t) dt, \quad (22)$$

called the action integral. We will show that trajectories which are stationary points of S correspond with those which satisfy Newton's laws; this is known as the principle of stationary action. We compute the first variation of S with respect to $\mathbf{r}(t)$, keeping the end points of the trajectory fixed. Consider the perturbation to S which results from perturbing the trajectory by $\delta\mathbf{r}(t)$,

$$\delta S[\mathbf{r}; \delta\mathbf{r}] = \int_{t_{\text{init}}}^{t_{\text{final}}} \left(\frac{\partial L(\mathbf{r}(t), \dot{\mathbf{r}}(t), t)}{\partial \mathbf{r}} \cdot \delta\mathbf{r}(t) + \frac{\partial L(\mathbf{r}(t), \dot{\mathbf{r}}(t), t)}{\partial \dot{\mathbf{r}}} \cdot \delta\dot{\mathbf{r}}(t) \right) dt, \quad (23)$$

where $\delta\dot{\mathbf{r}}(t) = d/dt(\delta\mathbf{r}(t))$. The second term on the right hand side can be integrated by parts, using the condition $\delta\mathbf{r}(t_{\text{init}}) = \delta\mathbf{r}(t_{\text{final}}) = 0$,

$$\delta S[\mathbf{r}; \delta\mathbf{r}] = \int_{t_{\text{init}}}^{t_{\text{final}}} \left(\frac{\partial L(\mathbf{r}(t), \dot{\mathbf{r}}(t), t)}{\partial \mathbf{r}} - \frac{d}{dt} \left(\frac{\partial L(\mathbf{r}(t), \dot{\mathbf{r}}(t), t)}{\partial \dot{\mathbf{r}}} \right) \right) \cdot \delta\mathbf{r}(t) dt. \quad (24)$$

In order for S to be stationary, it is necessary for $\delta S[\mathbf{r}; \delta\mathbf{r}]$ to vanish; thus, the above integral must vanish for all $\delta\mathbf{r}$. So we arrive at the following condition,

$$\frac{d}{dt} \left(\frac{\partial L(\mathbf{r}(t), \dot{\mathbf{r}}(t), t)}{\partial \dot{\mathbf{r}}} \right) = \frac{\partial L(\mathbf{r}(t), \dot{\mathbf{r}}(t), t)}{\partial \mathbf{r}}. \quad (25)$$

The above is referred to as the Euler-Lagrange equations.

We will next see that (25) is equivalent to Newton's laws. By computing $\partial L/\partial \mathbf{r}$ and $\partial L/\partial \dot{\mathbf{r}}$ from (21), we find

$$\frac{d}{dt} (m\dot{\mathbf{r}}(t) + q\mathbf{A}(\mathbf{r}(t))) = q\nabla(\dot{\mathbf{r}}(t) \cdot \mathbf{A}(\mathbf{r}(t))) - q\nabla\Phi(\mathbf{r}(t)). \quad (26)$$

We use the notation $\nabla = \partial/\partial \mathbf{r}$, noting that $\nabla \dot{\mathbf{r}} = 0$ as \mathbf{r} and $\dot{\mathbf{r}}$ are independent. To evaluate $\nabla(\dot{\mathbf{r}} \cdot \mathbf{A})$ we use the vector identity $\nabla(\mathbf{a} \cdot \mathbf{b}) = \mathbf{a} \times \nabla \times \mathbf{b} + \mathbf{b} \times \nabla \times \mathbf{a} + \mathbf{a} \cdot \nabla \mathbf{b} + \mathbf{b} \cdot \nabla \mathbf{a}$. We can also note that the total time derivative of \mathbf{A} along the trajectory is $d\mathbf{A}/dt = \partial\mathbf{A}/\partial t + \dot{\mathbf{r}} \cdot \nabla \mathbf{A}$. Thus we obtain the following equation of motion from the Euler-Lagrange equation,

$$m \frac{d^2 \mathbf{r}(t)}{dt^2} = q\dot{\mathbf{r}}(t) \times (\nabla \times \mathbf{A}(\mathbf{r}(t))) - q\nabla\Phi(\mathbf{r}(t)) - q \frac{\partial \mathbf{A}(\mathbf{r}(t))}{\partial t}. \quad (27)$$

Here we can use the expressions for the electro-magnetic fields in terms of vector and scalar potentials (20) to obtain the familiar Lorentz force (19). Therefore, we find that the Lagrangian reproduces Newton's law (18) for electro-magnetic fields with a force given by (19).

In Section 5.1 we will study trajectories within a uniform, straight magnetic field using the above ODEs directly. We will then consider motion in a strong magnetic field which is not necessarily straight or uniform in Section 5.2.

For further reading on Lagrangian mechanics, see the notes of David Tong [4] and Chapter 2 in [30].

4.3 Hamiltonian mechanics

Newton's laws can also be obtained from a variational principle involving the Hamiltonian functional. Rather than treating \mathbf{r} and $\dot{\mathbf{r}}$ as independent coordinates, in the Hamiltonian formalism we take the coordinate $\mathbf{q} := \mathbf{r}$ and the momentum, \mathbf{p} , which satisfies

$$\mathbf{p} = \frac{\partial L(\mathbf{q}, \dot{\mathbf{q}}, t)}{\partial \dot{\mathbf{q}}}. \quad (28)$$

The correspondence between the Hamiltonian and the Lagrangian thus reads

$$H(\mathbf{q}, \mathbf{p}, t) = \mathbf{p} \cdot \dot{\mathbf{q}}(\mathbf{q}, \mathbf{p}, t) - L(\mathbf{q}, \dot{\mathbf{q}}(\mathbf{q}, \mathbf{p}, t), t), \quad (29)$$

where we have used the transformation between Lagrangian $(\mathbf{q}, \dot{\mathbf{q}})$ and Hamiltonian (\mathbf{q}, \mathbf{p}) variables.

Consider the following functional,

$$\mathcal{W}[\mathbf{q}, \mathbf{p}] := \int_{t_{\text{init}}}^{t_{\text{final}}} \left(\mathbf{p}(t) \cdot \frac{d\mathbf{q}(t)}{dt} - H(\mathbf{q}(t), \mathbf{p}(t), t) \right) dt, \quad (30)$$

where \mathbf{p} and \mathbf{q} are independent functions of t and integration is taken along a trajectory, $\{\mathbf{q}(t), \mathbf{p}(t)\}$.

We consider the perturbation to \mathcal{W} due to the perturbation of the trajectory, using the boundary condition $\delta\mathbf{p}(t_{\text{init}}) = \delta\mathbf{q}(t_{\text{init}}) = \delta\mathbf{p}(t_{\text{final}}) = \delta\mathbf{q}(t_{\text{final}}) = 0$,

$$\delta\mathcal{W}[\mathbf{q}, \mathbf{p}; \delta\mathbf{q}, \delta\mathbf{p}] = \int_{t_{\text{init}}}^{t_{\text{final}}} \left(\delta\mathbf{p}(t) \cdot \frac{d\mathbf{q}(t)}{dt} + \mathbf{p}(t) \cdot \frac{d\delta\mathbf{q}(t)}{dt} - \frac{\partial H(\mathbf{q}(t), \mathbf{p}(t), t)}{\partial \mathbf{q}} \cdot \delta\mathbf{q}(t) - \frac{\partial H(\mathbf{q}(t), \mathbf{p}(t), t)}{\partial \mathbf{p}} \cdot \delta\mathbf{p}(t) \right) dt. \quad (31)$$

Upon integration by parts with respect to t we obtain

$$\delta\mathcal{W}[\mathbf{q}, \mathbf{p}; \delta\mathbf{q}, \delta\mathbf{p}] = \int_{t_{\text{init}}}^{t_{\text{final}}} \left(\delta\mathbf{p}(t) \cdot \frac{d\mathbf{q}(t)}{dt} - \frac{d\mathbf{p}(t)}{dt} \cdot \delta\mathbf{q}(t) - \frac{\partial H(\mathbf{q}(t), \mathbf{p}(t), t)}{\partial \mathbf{q}} \cdot \delta\mathbf{q}(t) - \frac{\partial H(\mathbf{q}(t), \mathbf{p}(t), t)}{\partial \mathbf{p}} \cdot \delta\mathbf{p}(t) \right) dt. \quad (32)$$

For $\delta\mathcal{W}$ to vanish for every $\delta\mathbf{p}$ and $\delta\mathbf{q}$, the following equations must be satisfied

$$\frac{d\mathbf{q}(t)}{dt} = \frac{\partial H(\mathbf{q}(t), \mathbf{p}(t), t)}{\partial \mathbf{p}} \quad (33a)$$

$$\frac{d\mathbf{p}(t)}{dt} = -\frac{\partial H(\mathbf{q}(t), \mathbf{p}(t), t)}{\partial \mathbf{q}}. \quad (33b)$$

These are known as Hamilton's equations. For an N -dimensional system such that $\mathbf{q} \in \mathbb{R}^N$, the Lagrangian provides a set of N second order ODEs while the Hamiltonian provides a set of $2N$ first order ODEs.

Using (33), the total time derivative of H is given by,

$$\begin{aligned} \frac{dH(\mathbf{q}(t), \mathbf{p}(t), t)}{dt} &= \frac{\partial H(\mathbf{q}(t), \mathbf{p}(t), t)}{\partial t} + \frac{\partial H(\mathbf{q}(t), \mathbf{p}(t), t)}{\partial \mathbf{q}} \cdot \frac{d\mathbf{q}(t)}{dt} + \frac{\partial H(\mathbf{q}(t), \mathbf{p}(t), t)}{\partial \mathbf{p}} \cdot \frac{d\mathbf{p}(t)}{dt} \\ &= \frac{\partial H(\mathbf{q}(t), \mathbf{p}(t), t)}{\partial t}, \end{aligned} \quad (34)$$

from which we note that if H does not depend explicitly on time, or is autonomous, then H is a constant of the motion. In many physical systems, H corresponds to total energy; a physical system which can be described by an autonomous Hamiltonian thus conserves energy.

Equivalence of the Hamiltonian and Lagrangian variational principles can be seen by showing that they lead to the same Euler-Lagrange equations. We will demonstrate by considering the Hamiltonian for charged particles in electro-magnetic fields. We first compute the momentum from (28) to be

$$\mathbf{p} = m\dot{\mathbf{q}} + q\mathbf{A}(\mathbf{q}), \quad (35)$$

from which we can note that $\dot{\mathbf{q}} = (\mathbf{p} - q\mathbf{A}(\mathbf{q}))/m$. The Hamiltonian is computed from (29),

$$H(\mathbf{q}, \mathbf{p}, t) = \frac{|\mathbf{p} - q\mathbf{A}(\mathbf{q})|^2}{2m} + q\Phi(\mathbf{q}). \quad (36)$$

We now apply Hamilton's equations (33) to obtain

$$\frac{d\mathbf{q}(t)}{dt} = \frac{(\mathbf{p}(t) - q(t)\mathbf{A}(\mathbf{q}(t)))}{m} \quad (37)$$

$$\frac{d\mathbf{p}(t)}{dt} = \frac{q}{m} (\mathbf{p}(t) - q\mathbf{A}(\mathbf{q}(t))) \times \mathbf{B}(\mathbf{q}(t)) + \frac{q}{m} (\mathbf{p}(t) - q\mathbf{A}(\mathbf{q}(t))) \cdot \nabla \mathbf{A}(\mathbf{q}(t)) - q\nabla\Phi(\mathbf{q}(t)), \quad (38)$$

where we use the notation $\nabla = \partial/\partial\mathbf{q}$. Using the transformation from $(\mathbf{q}, \dot{\mathbf{q}})$ to (\mathbf{q}, \mathbf{p}) and the expression of the fields in terms of the potentials (20), we therefore recover the same Euler-Lagrange equations (27).

For further reading on Hamiltonian mechanics, see [3] and Chapter 8 of [30].

5 Single particle motion in electro-magnetic fields

Magnetic fields can be designed to confine the orbits of charged particles. Examples of magnetic confinement configurations include the tokamak, see Section 7.3, stellarator, see Section 7.4, and mirror machines. In order to introduce the ideas behind these confinement concepts, we first study the motion of charged particles in the presence of electric and magnetic fields. We describe here models for individual charged particle motion with stationary electro-magnetic fields considered to be inputs. In practice, the electric and magnetic fields also depend on the charged particle motion, so a more realistic model would include the coupling between charged particle motion and electro-magnetic fields, see Section 8. We will also ignore the effects of collisions between particles.

We begin in Section 5.1 by considering the equations of motion a simple setting: a straight, uniform magnetic field. In Section 5.2, we discuss a reduction of the Lagrangian in the presence of a strong magnetic field which can vary in space, while consequences are discussed in Section 5.3. This model will become important as we discuss confinement of charged particles in toroidal magnetic confinement devices in Section 7. Finally Section 5.4 introduces the basic ideas of toroidal confinement.

5.1 Motion in a straight and uniform magnetic field

The concept of magnetic confinement can be illustrated by studying the trajectory of a particle in a straight, uniform magnetic field $\mathbf{B} = B\hat{\mathbf{e}}_1$. In practice, a solenoid, a cylindrical coil with several turns, can be used in order to generate a set of straight field lines in a given volume of space (see Figure 4). We will use the orthonormal coordinate system $(\hat{\mathbf{e}}_1, \hat{\mathbf{e}}_2, \hat{\mathbf{e}}_3)$ such that $\hat{\mathbf{e}}_1 \times \hat{\mathbf{e}}_2 = \hat{\mathbf{e}}_3$ (note that there remains much freedom in the definition of $\hat{\mathbf{e}}_2$ and $\hat{\mathbf{e}}_3$).

The Lorentz force (19) on a particle of charge q and velocity \mathbf{v} is given by $\mathbf{F} = qB(\mathbf{v} \times \hat{\mathbf{e}}_1)$, and the resulting trajectory obeys the following equations of motion from (27)

$$\frac{d\mathbf{r}(t)}{dt} = \mathbf{v}(t) \quad (39a)$$

$$m\frac{d\mathbf{v}(t)}{dt} = qB(\mathbf{v}(t) \times \hat{\mathbf{e}}_1). \quad (39b)$$

If a particle has initial velocity, $\mathbf{v}_{\text{init}} = v_{\parallel}\hat{\mathbf{e}}_1 + v_{\perp}(\sin(\varphi_{\text{init}})\hat{\mathbf{e}}_2 + \cos(\varphi_{\text{init}})\hat{\mathbf{e}}_3)$, it will spiral about the magnetic field in a helical orbit,

$$\mathbf{v}(t) = v_{\parallel}\hat{\mathbf{e}}_1 + v_{\perp}(\sin(\Omega t + \varphi_{\text{init}})\hat{\mathbf{e}}_2 + \cos(\Omega t + \varphi_{\text{init}})\hat{\mathbf{e}}_3). \quad (40)$$

Here $\Omega = qB/m$ is the gyrofrequency. The particle position is given by,

$$\begin{aligned} \mathbf{r}(t) = & (z_{\text{init}} + v_{\parallel}t)\hat{\mathbf{e}}_1 + \left(x_{\text{init}} + \frac{v_{\perp}}{\Omega} \cos(\varphi_{\text{init}}) - \frac{v_{\perp}}{\Omega} \cos(\Omega t + \varphi_{\text{init}}) \right) \hat{\mathbf{e}}_2 \\ & + \left(y_{\text{init}} - \frac{v_{\perp}}{\Omega} \sin(\varphi_{\text{init}}) + \frac{v_{\perp}}{\Omega} \sin(\Omega t + \varphi_{\text{init}}) \right) \hat{\mathbf{e}}_3, \end{aligned} \quad (41)$$

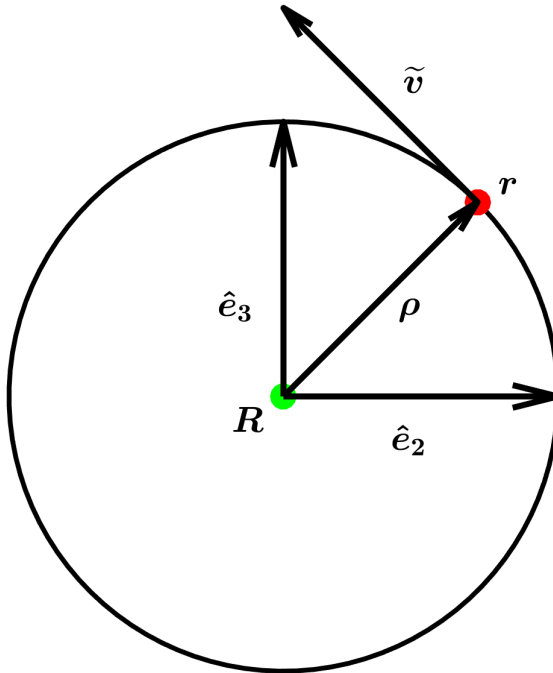


Figure 2: The motion in the plane perpendicular to the magnetic field. The quantity $\tilde{\mathbf{v}}$ describes the periodic velocity of the gyroradius, $\boldsymbol{\rho}$. The particle position is decomposed into periodic and non-periodic pieces, $\mathbf{r} = \mathbf{R} + \boldsymbol{\rho}$.

for initial position $\mathbf{r}_{\text{init}} = (x_{\text{init}}, y_{\text{init}}, z_{\text{init}})$.

Typically in experiments (see Table 1) the ion gyrofrequency is $\Omega_i \approx 10^8 \text{s}^{-1}$, and the electron gyrofrequency is $\Omega_e = (m_i/m_e)\Omega_i > 10^3\Omega_i$. When considering time scales $t \gg \Omega^{-1}$, it is often useful to separate the secular motion along a field line from the periodic motion. The velocity associated with the periodic motion is,

$$\tilde{\mathbf{v}}(t) = v_{\perp}(\sin(\Omega t + \varphi_{\text{init}})\hat{\mathbf{e}}_2 + \cos(\Omega t + \varphi_{\text{init}})\hat{\mathbf{e}}_3). \quad (42)$$

The position associated with this periodic motion, $\boldsymbol{\rho}(t)$, can be obtained by integrating $\tilde{\mathbf{v}}(t)$ with respect to time. The integration constants are chosen such that $\boldsymbol{\rho}(t) \cdot \hat{\mathbf{e}}_1 = 0$, as the gyromotion occurs in the plane perpendicular to the magnetic field, and $\tilde{\mathbf{v}}(t) \cdot \boldsymbol{\rho}(t) = 0$ for all t , as should be true for uniform periodic motion (see Figure 2),

$$\boldsymbol{\rho}(t) = \frac{v_{\perp}}{\Omega}(-\cos(\Omega t + \varphi_{\text{init}})\hat{\mathbf{e}}_2 + \sin(\Omega t + \varphi_{\text{init}})\hat{\mathbf{e}}_3). \quad (43)$$

The term *gyroradius* is often used to refer to $\boldsymbol{\rho}(t)$. The *guiding center* velocity, $\mathbf{V} = \mathbf{v}(t) - \tilde{\mathbf{v}}(t)$, accounts for the non-periodic motion along field lines,

$$\mathbf{V} = v_{\parallel}\hat{\mathbf{e}}_1. \quad (44)$$

The guiding center position, $\mathbf{R}(t)$, can be determined such that $\mathbf{r}(t) = \mathbf{R}(t) + \boldsymbol{\rho}(t)$,

$$\mathbf{R}(t) = (z_{\text{init}} + v_{\parallel}t)\hat{\mathbf{e}}_1 + \left(x_{\text{init}} + \frac{v_{\perp}}{\Omega}\cos(\varphi_{\text{init}})\right)\hat{\mathbf{e}}_2 + \left(y_{\text{init}} - \frac{v_{\perp}}{\Omega}\sin(\varphi_{\text{init}})\right)\hat{\mathbf{e}}_3. \quad (45)$$

The quantity $\mathbf{R}(t)$ is referred to as the *guiding center* position as it is the center about which the particle gyrates. The guiding center moves purely along the field line at the center of the helical motion. As $|\boldsymbol{\rho}| = v_{\perp}/\Omega$ is typically much smaller than most length scales of interest for a magnetic confinement device (see Section 2.5), considering the motion of the guiding center is a very good approximation. In Section 5.2 we will use this assumption to explore the trajectories of particles in the presence of more general electro-magnetic fields.

In a straight, uniform field, the motion of the guiding center is purely along a field line. In this way, the particle is confined in the direction perpendicular to the magnetic field (in an experiment it would stay away from the walls of the cylinder) but unconfined in the direction parallel to

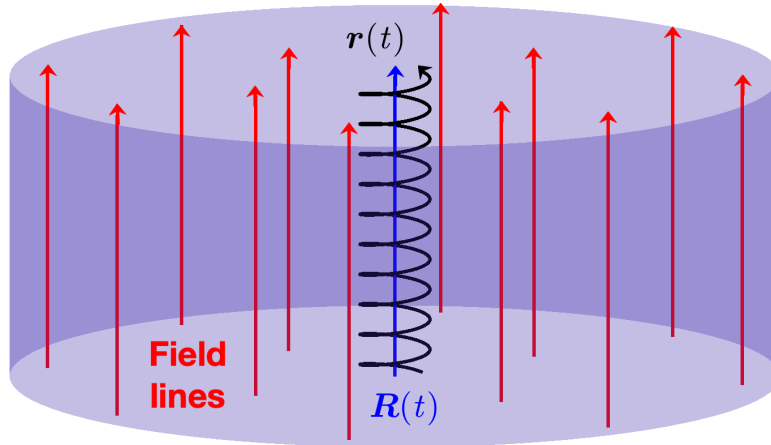


Figure 3: In a straight, uniform magnetic field, charged particles exhibit fast helical motion about field lines (red). All charged particles are confined in the direction perpendicular to the magnetic field, but are free to move in the direction parallel to the magnetic field. The guiding center trajectory (blue) describes the particle's motion (black) after averaging over the fast gyration.

the magnetic field (particles can escape out the ends). See Figure 3. An additional confining mechanism is needed to avoid losses of particles along the field lines, such as toroidal confinement or the mirror force. This will be discussed in Section 5.4.

5.2 Gyroaveraged Lagrangian

In this Section we consider the motion of charged particles in static electric and magnetic fields within the Lagrangian framework. Applying knowledge of the length and time scales involved, we will reduce the Lagrangian in order to gain insight about motion in a strong magnetic field. The results will be used to arrive at the well-known expressions for the drifts of particles across field lines in Section 5.3. While many sources simply average the Lorentz force in order to obtain the cross-field drifts, working within the Lagrangian framework will provide additional insight into the conserved quantities of the system.

We consider motion in a field $\mathbf{B}(\mathbf{r}) = B(\mathbf{r})\hat{\mathbf{e}}_1(\mathbf{r})$ that is no longer assumed to be straight and uniform. Here $\hat{\mathbf{e}}_1 = \hat{\mathbf{b}}$ is a local unit vector in the direction of the magnetic field at \mathbf{r} . The unit

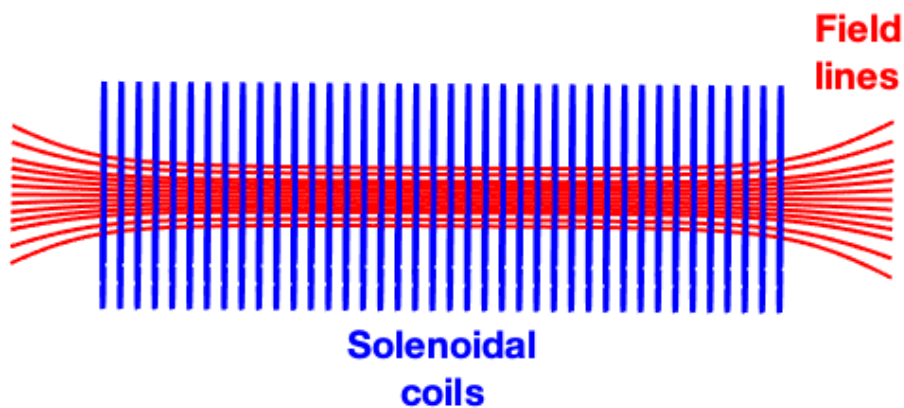


Figure 4: A solenoid is used to produce an (approximately) straight, uniform magnetic field.

vectors $\hat{e}_2(\mathbf{r})$ and $\hat{e}_3(\mathbf{r})$ form a basis of the plane perpendicular to $\mathbf{B}(\mathbf{r})$. At each point in $\mathbf{r} \in \mathbb{R}^3$, $(\hat{e}_1, \hat{e}_2, \hat{e}_3)$ forms a local orthonormal basis, independent of the motion.

Motivated by the calculation in Section 5.1, we would like to perform a similar coordinate transformation to study the motion of guiding centers in the Lagrangian framework. We separate the position coordinate into the guiding center position, \mathbf{R} , and gyroradius, $\boldsymbol{\rho}$,

$$\mathbf{r} = \mathbf{R} + \boldsymbol{\rho}. \quad (46)$$

The gyroradius lies in the plane perpendicular to \mathbf{B} and is parameterized by $(\rho, \varphi) \in \mathbb{R}^2$ as follows

$$\boldsymbol{\rho} = \rho(-\hat{e}_2(\mathbf{R}) \cos(\varphi) + \hat{e}_3(\mathbf{R}) \sin(\varphi)), \quad (47)$$

where φ is called the gyroangle and describes the angle of the gyroradius in the plane perpendicular to the magnetic field, while ρ describes the magnitude of the gyroradius in this plane. We have replaced one vector describing the position $\mathbf{r} \in \mathbb{R}^3$, for a vector coordinate $\mathbf{R} \in \mathbb{R}^3$ and two scalar coordinates $(\rho, \varphi) \in \mathbb{R}^2$ constrained by (46). We perform the coordinate transformation $(\mathbf{r}) \rightarrow (\mathbf{R}, \rho, \varphi)$,

$$L(\mathbf{r}, \dot{\mathbf{r}}) = \tilde{L}(\mathbf{R}, \rho, \varphi, \dot{\mathbf{R}}, \dot{\rho}, \dot{\varphi}). \quad (48)$$

The Lagrangian in this new set of coordinates can now be expressed as

$$\begin{aligned} \tilde{L}(\mathbf{R}, \rho, \varphi, \dot{\mathbf{R}}, \dot{\rho}, \dot{\varphi}) = & \frac{m}{2} \left(\dot{\mathbf{R}} + \dot{\boldsymbol{\rho}}(\mathbf{R}, \rho, \varphi, \dot{\mathbf{R}}, \dot{\rho}, \dot{\varphi}) \right)^2 \\ & + q\mathbf{A}(\mathbf{R} + \boldsymbol{\rho}(\mathbf{R}, \rho, \varphi)) \cdot \left(\dot{\mathbf{R}} + \dot{\boldsymbol{\rho}}(\mathbf{R}, \rho, \varphi, \dot{\mathbf{R}}, \dot{\rho}, \dot{\varphi}) \right) - q\Phi(\mathbf{R} + \boldsymbol{\rho}(\mathbf{R}, \rho, \varphi)), \end{aligned} \quad (49)$$

where we have dropped any time dependence of the fields.

We will also perform an ordering in the small parameter

$$\epsilon \sim \frac{\rho}{L_B} \sim \frac{\omega_B}{\dot{\varphi}} \sim \frac{q\Phi}{T} \ll 1. \quad (50)$$

Here $L_B^{-1} = |\nabla B|/B$ is the typical length scale for the magnetic field variation and $\omega_B \sim v_t/L_B$ is the frequency associated with this variation, where $v_t = \sqrt{2T/m}$ is the thermal velocity associated with the temperature T . The thermal speed characterizes the typical speed of a particle in any direction.

- The assumption $\rho/L_B \ll 1$ means that the gyroradius is small compared with typical length scales of our system. This is justified considering Table 1.
- The assumption $\omega_B/\dot{\varphi} \ll 1$ means that the gyrofrequency is much larger than other frequencies of our system. This is also justified considering physical scales given in Table 1.
- The assumption $q\Phi/T \ll 1$ means that all of the drifts across the field lines are small compared with the velocity along the field lines, which is of similar order to the thermal speed, $v_{||} \sim v_t$.

We will also make the following assumptions based on the solution in a straight, uniform magnetic field.

- We assume that the parallel guiding center velocity $V_{||} = \hat{\mathbf{b}} \cdot \dot{\mathbf{R}}$ satisfies $V_{||} \sim v_t$ due to (44), as we found in the case of cylindrical confinement that the guiding center velocity is constant along field lines, $\hat{\mathbf{b}} \cdot \mathbf{V} = v_{||}$, and we can assume $v_{||} \sim v_t$. As the guiding center parallel velocity is the same as the particle parallel velocity, our assumption is sensible.
- We assume that the perpendicular guiding center velocity $\mathbf{V}_{\perp} = \dot{\mathbf{R}} - V_{||}\hat{\mathbf{b}}$ satisfies $|\mathbf{V}_{\perp}| \sim \epsilon v_t$, as we assume that the guiding center drifts are slow with respect to the velocity of the gyromotion or the motion along field lines. In a strong magnetic field, we expect the largest contribution to the guiding center motion to be in the parallel direction.
- We assume that $\dot{\varphi} \sim qB/m$ which arises from (42), as we found $\dot{\varphi} = \Omega = qB/m$ in the case of cylindrical confinement.

- We assume that $\dot{\rho} \sim \omega_B \rho$, which arises from (43), as we found $\rho = v_\perp / \Omega$ in the case of cylindrical confinement. Therefore, the time-variation of ρ arises due to the variation in B , which has characteristic frequency ω_B .

Under the assumption that $\omega_B / \dot{\varphi} \ll 1$, we wish to average the Lagrangian over the fast gyro-motion by performing the gyroaveraging operation

$$\langle F \rangle_\varphi = \frac{1}{2\pi} \int_0^{2\pi} F(\mathbf{R}, \rho, \varphi, \dot{\mathbf{R}}, \dot{\rho}, \dot{\varphi}) d\varphi. \quad (51)$$

As the gyroaverage is performed, the other coordinates are considered fixed $(\mathbf{R}, \rho, \dot{\mathbf{R}}, \dot{\rho}, \dot{\varphi})$. At this point we want to identify the leading terms in (49) with respect to ϵ after performing the gyroaverage. Note that any term with a single factor of ρ does not contribute after gyroaveraging, as it is periodic in φ .

Gyroaveraging the first term in (49) we obtain,

$$\left\langle \frac{m}{2} (\dot{\mathbf{R}} + \dot{\rho})^2 \right\rangle_\varphi = \frac{m}{2} \left(V_\parallel^2 + V_\perp^2 + \dot{\rho}^2 + \rho^2 \dot{\varphi}^2 + \frac{\rho^2}{2} (|\dot{\hat{\mathbf{e}}}_2|^2 + |\dot{\hat{\mathbf{e}}}_3|^2) + 2\rho^2 \dot{\varphi} \dot{\hat{\mathbf{e}}}_3 \cdot \hat{\mathbf{e}}_2 \right), \quad (52)$$

where $V_\parallel = \hat{\mathbf{b}}(\mathbf{R}) \cdot \dot{\mathbf{R}}$ and $V_\perp = |\dot{\mathbf{R}} - V_\parallel \hat{\mathbf{b}}(\mathbf{R})|$ and the unit vectors, $\hat{\mathbf{e}}_2$ and $\hat{\mathbf{e}}_3$, are evaluated at the guiding center position. The time derivatives of the unit vectors can be evaluated using $\dot{\hat{\mathbf{e}}}_{2,3} = \dot{\mathbf{R}} \cdot \nabla \hat{\mathbf{e}}_{2,3}$. Throughout we will use the notation $\nabla = \partial / \partial \mathbf{R}$. The quantity $\langle \dot{\rho} \cdot \dot{\rho} \rangle_\varphi$ is evaluated thanks to the identity

$$\dot{\rho} = (\dot{\rho} / \rho) \rho - \dot{\varphi} (\hat{\mathbf{b}} \times \rho) + (\dot{\mathbf{R}} \cdot \nabla) \rho. \quad (53)$$

From our set of assumptions, we can summarize the ordering in ϵ of terms in the following Table.

Terms	$\frac{m}{2} V_\parallel^2$	$\frac{m}{2} V_\perp^2$	$\frac{m}{2} \dot{\rho}^2$	$\frac{m}{2} \rho^2 \dot{\varphi}^2$	$\frac{m}{2} \frac{\rho^2}{2} (\dot{\hat{\mathbf{e}}}_2 ^2 + \dot{\hat{\mathbf{e}}}_3 ^2)$	$m\rho^2 \dot{\varphi} \dot{\hat{\mathbf{e}}}_2 \cdot \hat{\mathbf{e}}_3$
Order	$\sim m v_t^2$	$\sim \epsilon^2 m v_t^2$	$\sim \epsilon^2 m v_t^2$	$\sim m v_t^2$	$\sim \epsilon^2 m v_t^2$	$\sim \epsilon m v_t^2$

So we obtain

$$\left\langle \frac{m}{2} (\dot{\mathbf{R}} + \dot{\rho})^2 \right\rangle_\varphi = \frac{m}{2} (V_\parallel^2 + \rho^2 \dot{\varphi}^2) + \mathcal{O}(\epsilon m v_t^2). \quad (54)$$

To compute the gyroaverage of the second term in (49), we Taylor expand $\mathbf{A}(\mathbf{r})$ about \mathbf{R} ,

$$\mathbf{A}(\mathbf{R} + \rho) = \mathbf{A}(\mathbf{R}) + (\rho \cdot \nabla) \mathbf{A}(\mathbf{R}) + \mathcal{O}(\epsilon^2 \mathbf{A}(\mathbf{R})), \quad (55)$$

so by gyroaveraging we obtain

$$\begin{aligned} \left\langle q \mathbf{A}(\mathbf{R} + \rho) \cdot (\dot{\mathbf{R}} + \dot{\rho}) \right\rangle_\varphi &= \left\langle q (\mathbf{A}(\mathbf{R}) + (\rho \cdot \nabla) \mathbf{A}(\mathbf{R}) + \mathcal{O}(\epsilon^2 \mathbf{A}(\mathbf{R}))) \cdot (\dot{\mathbf{R}} + \dot{\rho}) \right\rangle_\varphi \\ &= q \mathbf{A}(\mathbf{R}) \cdot V_\parallel + q \mathbf{A}(\mathbf{R}) \cdot V_\perp + q \frac{\dot{\rho}}{\rho} \langle \rho \rho \rangle_\varphi : \nabla \mathbf{A}(\mathbf{R}) \\ &\quad - q \dot{\varphi} \left\langle (\hat{\mathbf{b}} \times \rho) \rho \right\rangle_\varphi : \nabla \mathbf{A}(\mathbf{R}) + q \langle (\dot{\mathbf{R}} \cdot \nabla) \rho \rho \rangle_\varphi : \nabla \mathbf{A}(\mathbf{R}) + \mathcal{O}(\epsilon^2 m v_t^2). \end{aligned} \quad (56)$$

Here (53) is used to express $\dot{\rho}$. The double-dot ($:$) indicates contraction between two tensors, $\overleftrightarrow{\mathbf{A}}$ and $\overleftrightarrow{\mathbf{B}}$, in the following way, $\overleftrightarrow{\mathbf{A}} : \overleftrightarrow{\mathbf{B}} = \sum_i \sum_j A_{ij} B_{ji}$. Again, from our set of assumptions, we can summarize the ordering in ϵ of terms in the following Table.

Terms	$q \mathbf{A} \cdot V_\parallel$	$q \mathbf{A} \cdot V_\perp$	$\frac{q \dot{\rho}}{\rho} \langle \rho \rho \rangle_\varphi : \nabla \mathbf{A}$	$q \dot{\varphi} \langle (\hat{\mathbf{b}} \times \rho) \rho \rangle_\varphi : \nabla \mathbf{A}$	$q \langle (\dot{\mathbf{R}} \cdot \nabla) \rho \rho \rangle_\varphi : \nabla \mathbf{A}$
Order	$\sim \epsilon^{-1} m v_t^2$	$\sim m v_t^2$	$\sim \epsilon m v_t^2$	$\sim m v_t^2$	$\sim \epsilon m v_t^2$

The fourth term can be evaluated using $\langle (\hat{\mathbf{b}} \times \boldsymbol{\rho}) \boldsymbol{\rho} \rangle_\varphi = (\rho^2/2) (\hat{\mathbf{e}}_3 \hat{\mathbf{e}}_2 - \hat{\mathbf{e}}_2 \hat{\mathbf{e}}_3) = (\rho^2/2) \hat{\mathbf{b}} \times \mathbb{I}$, where $\mathbb{I} = \hat{\mathbf{e}}_1 \hat{\mathbf{e}}_1 + \hat{\mathbf{e}}_2 \hat{\mathbf{e}}_2 + \hat{\mathbf{e}}_3 \hat{\mathbf{e}}_3$ is the identity tensor, and $\hat{\mathbf{b}} \times \mathbb{I} : \nabla \mathbf{A} = \hat{\mathbf{b}} \cdot \nabla \times \mathbf{A} = B$. So we obtain

$$\left\langle q\mathbf{A}(\mathbf{R} + \boldsymbol{\rho}) \cdot \left(\dot{\mathbf{R}} + \dot{\boldsymbol{\rho}} \right) \right\rangle_\varphi = q\mathbf{A}(\mathbf{R}) \cdot \dot{\mathbf{R}} - q \frac{\dot{\varphi} \rho^2}{2} B(\mathbf{R}) + \mathcal{O}(\epsilon m v_t^2). \quad (57)$$

We similarly expand $\Phi(\mathbf{r})$ about \mathbf{R} to evaluate the third term in (49),

$$\langle \Phi(\mathbf{R} + \boldsymbol{\rho}) \rangle_\varphi = \Phi(\mathbf{R}) + \mathcal{O}(\epsilon^2 \Phi(\mathbf{R})). \quad (58)$$

Inserting (54), (57), and (58) into (49), we thus obtain the following gyroaveraged Lagrangian to $\mathcal{O}(\epsilon m v_t^2)$,

$$\begin{aligned} \mathcal{L}(\mathbf{R}, \rho, \dot{\mathbf{R}}, \dot{\varphi}) := \langle L(\mathbf{R}, \boldsymbol{\rho}, \varphi, \dot{\mathbf{R}}, \dot{\boldsymbol{\rho}}, \dot{\varphi}) \rangle_\varphi &= \frac{m}{2} \left(\dot{\mathbf{R}} \cdot \hat{\mathbf{b}}(\mathbf{R}) + \rho^2 \dot{\varphi}^2 \right) + q\mathbf{A}(\mathbf{R}) \cdot \dot{\mathbf{R}} \\ &\quad - q \frac{\dot{\varphi} \rho^2}{2} B(\mathbf{R}) - q\Phi(\mathbf{R}). \end{aligned} \quad (59)$$

By construction, our gyroaveraged Lagrangian, \mathcal{L} , no longer depends on φ .

Further discussion of the gyroaveraged Lagrangian can be found in [69], Chapter 6 of [37], and [53].

5.2.1 Adiabatic invariant for gyromotion

An adiabatic invariant is an approximately conserved quantity associated with nearly periodic motion. We will obtain a conserved quantity consistent with the assumption of fast gyromotion, $\epsilon \ll 1$, by considering the Euler-Lagrange equations for \mathcal{L} .

We evaluate the Euler-Lagrange equation from (59) corresponding to the gyroradius, noting that $\partial \mathcal{L} / \partial \dot{\rho} = 0$,

$$\frac{\partial \mathcal{L}}{\partial \rho} = \frac{d}{dt} \left(\frac{\partial \mathcal{L}}{\partial \dot{\rho}} \right) \Rightarrow \dot{\varphi} = \frac{qB(\mathbf{R})}{m}. \quad (60)$$

We see that $\dot{\varphi}$ corresponds to the gyrofrequency Ω found in Section 5.1 but for a space dependent magnetic field $B(\mathbf{R})$, so we define $\Omega(\mathbf{R}) = qB(\mathbf{R})/m$.

Now we evaluate the Euler-Lagrange equation for the gyroangle, noting that $\partial \mathcal{L} / \partial \varphi = 0$,

$$\frac{\partial \mathcal{L}}{\partial \varphi} = \frac{d}{dt} \left(\frac{\partial \mathcal{L}}{\partial \dot{\varphi}} \right) \Rightarrow \frac{d}{dt} \left(m \rho^2 \dot{\varphi} - \frac{\rho^2 q B(\mathbf{R})}{2} \right) = 0. \quad (61)$$

This implies the conservation of the quantity $2m\rho^2\dot{\varphi} - \rho^2 q B(\mathbf{R}) = m\rho^2 \Omega(\mathbf{R})$ along trajectories. Any multiple of this quantity is conserved along trajectories, but the one that is most often used in the literature is defined in terms of the perpendicular velocity $v_\perp(\rho, \mathbf{R}) := \rho \Omega(\mathbf{R})$ as follows,

$$\mu = \frac{v_\perp^2(\rho, \mathbf{R})}{2B(\mathbf{R})}, \quad (62)$$

and is often referred to as the magnetic moment. Here v_\perp is the velocity associated with the gyromotion, as opposed to V_\perp which is associated with the guiding center motion.

5.2.2 Energy conservation

As we have made the assumption of time-independence of the fields ($\partial \Phi / \partial t = 0$, $\partial \mathbf{A} / \partial t = 0$), the Lagrangian does not depend explicitly on time. This results in a conserved quantity. Consider the total time derivative of \mathcal{L} ,

$$\frac{d\mathcal{L}}{dt} = \dot{\varphi} \frac{\partial \mathcal{L}}{\partial \varphi} + \dot{\rho} \frac{\partial \mathcal{L}}{\partial \rho} + \dot{\mathbf{R}} \cdot \frac{\partial \mathcal{L}}{\partial \mathbf{R}} + \ddot{\varphi} \frac{\partial \mathcal{L}}{\partial \dot{\varphi}} + \dot{\rho} \frac{\partial \mathcal{L}}{\partial \dot{\rho}} + \ddot{\mathbf{R}} \cdot \frac{\partial \mathcal{L}}{\partial \dot{\mathbf{R}}}. \quad (63)$$

Applying the Euler-Lagrange equations, we obtain

$$\frac{d\mathcal{L}}{dt} = \frac{d}{dt} \left(\dot{\varphi} \frac{\partial \mathcal{L}}{\partial \dot{\varphi}} + \dot{\rho} \frac{\partial \mathcal{L}}{\partial \dot{\rho}} + \dot{\mathbf{R}} \cdot \frac{\partial \mathcal{L}}{\partial \dot{\mathbf{R}}} \right). \quad (64)$$

If the fields are assumed to be time-independent, then \mathcal{L} has no explicit time dependence, and therefore the total time derivative of the following quantity vanishes,

$$E = \dot{\varphi} \frac{\partial \mathcal{L}}{\partial \dot{\varphi}} + \dot{\rho} \frac{\partial \mathcal{L}}{\partial \dot{\rho}} + \dot{\mathbf{R}} \cdot \frac{\partial \mathcal{L}}{\partial \dot{\mathbf{R}}} - \mathcal{L}. \quad (65)$$

Thus E is conserved along a trajectory if the fields are time-independent. From the gyroaveraged Lagrangian \mathcal{L} (59), we then obtain

$$E = \frac{m \left(v_{\perp}^2(\rho, \mathbf{R}) + V_{\parallel}^2(\dot{\mathbf{R}}, \mathbf{R}) \right)}{2} + q\Phi(\mathbf{R}), \quad (66)$$

where the parallel guiding center velocity is defined as $V_{\parallel}(\dot{\mathbf{R}}, \mathbf{R}) := \dot{\mathbf{R}} \cdot \hat{\mathbf{b}}(\mathbf{R})$ and the perpendicular velocity is $v_{\perp}(\rho, \mathbf{R}) = \rho\Omega(\mathbf{R})$. The conserved quantity E represents the total energy of a particle: the first term in (66) accounts for the kinetic energy, the energy due to the motion of the particle, while the second accounts for the potential energy, the energy due to the fields.

5.2.3 Particle trapping

Combining the expression of the adiabatic invariant (62) with the energy invariant (66), we obtain the following expression for the parallel velocity,

$$V_{\parallel}(\dot{\mathbf{R}}, \mathbf{R}) = \pm \sqrt{\frac{2(E - q\Phi(\mathbf{R}))}{m} - 2\mu B(\mathbf{R})}. \quad (67)$$

Since V_{\parallel} is a physical quantity, it must be real-valued. Often the electrostatic potential can be assumed to be constant in a given region. Therefore, only the second term in the above radical depends on space, and V_{\parallel} vanishes at points where $B(\mathbf{R}) = (E - q\Phi)/(\mu m) =: B_{\text{crit}}$. In particular, along a given trajectory, the values of the invariants $(E, \mu) \in \mathbb{R}^2$ are given so B_{crit} is fixed, and necessarily $B(\mathbf{R}) \leq B_{\text{crit}}$. Therefore the particle cannot access regions where $B(\mathbf{R}) > B_{\text{crit}}$.

The conservation of E and μ leads to the result that particles cannot access regions of sufficiently large magnetic field. This effect is known as mirroring, as a particle will be reflected away from high field regions. For a given magnetic field, particles with sufficiently large values of μ/E may become trapped in regions of low field strength, often referred to as trapped particles. Particles with sufficiently small values μ/E will not become trapped and are referred to as passing particles.

Although it will not be covered in detail in this document, particle trapping is an important concept for confinement. One of the first magnetic confinement devices, known as the mirror machine, relies on a strong magnetic field to confine a large fraction of particles. Trapped and passing particles tend to have very different confinement properties in magnetic confinement devices due to their distinct trajectories. See Section 8.9 in [26] for additional details.

5.3 Guiding center motion

In the absence of variation in the field, guiding centers exhibit a constant velocity along field lines (see Section 5.1). In the presence of a non-uniform magnetic field, guiding centers have an additional slow drift across field lines.

We will obtain these drifts by considering the Euler-Lagrange equation for the guiding center position from the gyroaveraged Lagrangian expression (59),

$$\begin{aligned} \frac{d}{dt} \left(m \left(\dot{\mathbf{R}} \cdot \hat{\mathbf{b}}(\mathbf{R}) \right) \hat{\mathbf{b}}(\mathbf{R}) + q\mathbf{A}(\mathbf{R}) \right) &= m \nabla \left(\dot{\mathbf{R}} \cdot \hat{\mathbf{b}}(\mathbf{R}) \right) \left(\dot{\mathbf{R}} \cdot \hat{\mathbf{b}} \right) \\ &+ q \nabla \left(\mathbf{A}(\mathbf{R}) \cdot \dot{\mathbf{R}} \right) - \frac{q\dot{\varphi}\rho^2}{2} \nabla B(\mathbf{R}) - q \nabla \Phi(\mathbf{R}). \end{aligned} \quad (68)$$

The time derivative on the left hand side can be written as $d/dt = \dot{\mathbf{R}} \cdot \nabla + \ddot{\mathbf{R}} \cdot \partial/\partial \dot{\mathbf{R}}$, as ρ and $\dot{\rho}$ do not appear and the Lagrangian does not have explicit time dependence.

Using the vector identity $\nabla(\mathbf{a} \cdot \mathbf{b}) = \mathbf{a} \times (\nabla \times \mathbf{b}) + \mathbf{b} \times (\nabla \times \mathbf{a}) + (\mathbf{a} \cdot \nabla)\mathbf{b} + (\mathbf{b} \cdot \nabla)\mathbf{a}$ as well as the definitions of the fields in terms of the vector and scalar potentials (20) we obtain

$$m \dot{V}_{\parallel} \hat{\mathbf{b}} + m V_{\parallel} \left(\dot{\mathbf{R}} \cdot \nabla \hat{\mathbf{b}}(\mathbf{R}) \right) = q \dot{\mathbf{R}} \times \mathbf{B}(\mathbf{R}) - \frac{q\dot{\varphi}\rho^2}{2} \nabla B(\mathbf{R}) + q\mathbf{E}(\mathbf{R}), \quad (69)$$

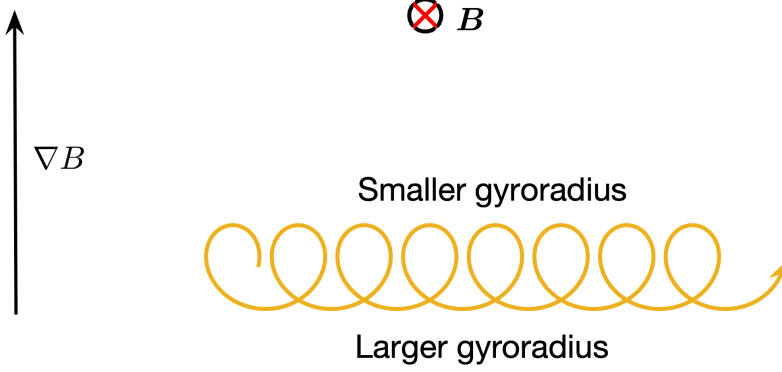


Figure 5: Consider a magnetic field pointing into the page with a gradient in the field strength pointing up. The trajectory of an ion is shown, with all motion projected into the plane perpendicular to \mathbf{B} . The ion will gyrate counter-clockwise, with a smaller gyroradius in the region of stronger field. This results in a grad- B drift to the right.

where the parallel guiding center velocity and acceleration are $V_{\parallel}(\dot{\mathbf{R}}, \mathbf{R}) = \dot{\mathbf{R}} \cdot \hat{\mathbf{b}}(\mathbf{R})$ and $\dot{V}_{\parallel}(\ddot{\mathbf{R}}, \mathbf{R}) = \ddot{\mathbf{R}} \cdot \hat{\mathbf{b}}(\mathbf{R})$, respectively.

We now can check that we have not introduced any terms of higher order in ϵ while computing the Euler-Lagrange equations. We can see that the term on the left hand side of (69) involving $\mathbf{V}_{\perp} = \dot{\mathbf{R}} - V_{\parallel} \hat{\mathbf{b}}$ are $\mathcal{O}(\epsilon \omega_B m v_t)$ while the other terms are $\mathcal{O}(\omega_B m v_t)$ or larger; thus we need only retain the component of these terms involving V_{\parallel} . The resulting expression can also be written in terms of the magnetic curvature, $\boldsymbol{\kappa} = \hat{\mathbf{b}} \cdot \nabla \hat{\mathbf{b}}$, and the magnetic moment (62),

$$m \dot{V}_{\parallel} \hat{\mathbf{b}}(\mathbf{R}) = -m V_{\parallel}^2 \boldsymbol{\kappa}(\mathbf{R}) + q \dot{\mathbf{R}}_{\perp} \times \mathbf{B}(\mathbf{R}) - m \mu \nabla B(\mathbf{R}) + q \mathbf{E}(\mathbf{R}). \quad (70)$$

5.3.1 Parallel guiding center motion

We can take the dot product of (70) with $\hat{\mathbf{b}}$ to obtain the parallel guiding center acceleration,

$$\dot{V}_{\parallel} = -\mu \hat{\mathbf{b}}(\mathbf{R}) \cdot \nabla B(\mathbf{R}) + \frac{q}{m} \mathbf{E}(\mathbf{R}) \cdot \hat{\mathbf{b}}(\mathbf{R}). \quad (71)$$

- The first term in the above expression expresses the fact that particles are repelled from regions of large field strength, as discussed in Section 5.2.3.
- The second term accounts for acceleration by electric fields parallel to the magnetic field.

5.3.2 Perpendicular guiding center motion

We now take the cross product of (70) with $\hat{\mathbf{b}}$ to obtain the following expression for the perpendicular guiding center acceleration,

$$\dot{\mathbf{R}}_{\perp} = \frac{V_{\parallel}^2(\dot{\mathbf{R}}, \mathbf{R})}{\Omega(\mathbf{R})} \hat{\mathbf{b}}(\mathbf{R}) \times \boldsymbol{\kappa}(\mathbf{R}) + \frac{\mu}{\Omega(\mathbf{R})} \hat{\mathbf{b}}(\mathbf{R}) \times \nabla B(\mathbf{R}) + \frac{\mathbf{E}(\mathbf{R}) \times \mathbf{B}(\mathbf{R})}{B(\mathbf{R})^2}. \quad (72)$$

- The first term is known as the curvature drift, resulting from curvature in the field lines. The sign of this drift is different for ions and electrons due to its dependence on Ω .
- The second term is the grad- B drift. This drift also depends on the sign of the charge. A physical picture for the grad- B drift can be found in Figure 5.
- The third term is the $\mathbf{E} \times \mathbf{B}$ drift. This charge does not depend on the charge or mass, so is the same for all species.

Further discussion of guiding center drifts can be found in Chapter 2 of [79], Section 2.4 of [34], Chapter 8 of [26], Chapter 6 of [37].

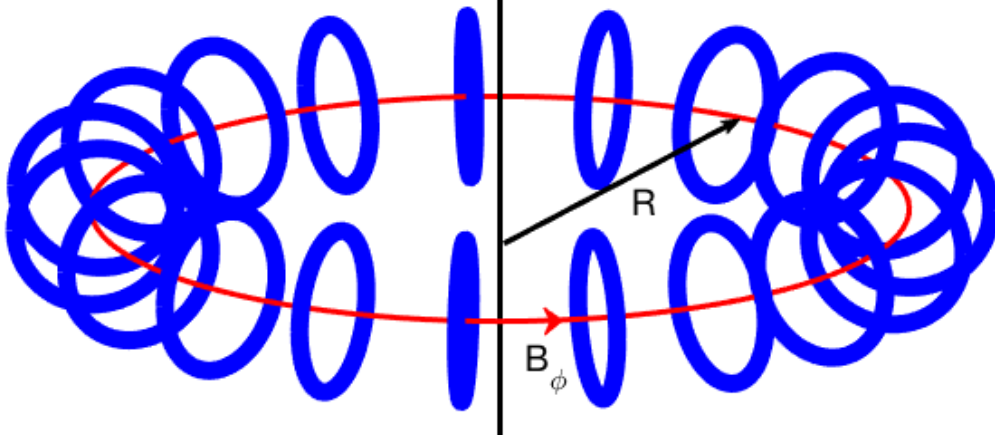


Figure 6: In a toroidal magnetic field, the magnitude of the toroidal field varies as $B_\phi \propto 1/R$ where R is the major radius, as can be seen by performing a line integral along the toroidal loop (red) which encloses coil current I , including contributions from the electro-magnetic coils (blue).

5.4 Introduction to toroidal confinement

In Section 5.1 we found that in a straight, uniform magnetic field, particles are confined in the direction perpendicular to the magnetic field lines but unconfined in the parallel direction. In order to avoid losses of particles along straight field lines, one can consider a modification of the field lines. A natural idea is to bend a set of straight field lines into closed field lines; this results in a toroidal shape. In this way the magnetic field points in the toroidal direction, the long way around the torus.

One could imagine generating a set of toroidally closed field lines by bending a long solenoid to join its two open ends, forming a circle. Nearly toroidal field lines can be generated thanks to several individual coils placed along a common circular axis (see Figure 6). This produces a magnetic field whose magnitude is nearly axisymmetric (does not depend on the toroidal angle about the axis of symmetry) and points in the toroidal direction.

To analyze such a configuration we will use the canonical cylindrical coordinates (R, ϕ, Z) , see Section 6.2 for a reminder. We will find that the magnitude of the toroidal field generated by such coils is a non-constant function of the position; the field is stronger inside (closer to the axis of symmetry) of the toroidal shape, where the coils are closer to each other, and decreases as a function of the major radius R . This can be seen by computing the current passing through a surface, S , lying in the $Z = 0$ plane whose boundary is a circle with major radius R . From Ampere's law (13) we find

$$I = \int_S \mathbf{J} \cdot \hat{\mathbf{n}} d^2x = \frac{1}{\mu_0} \oint_{\partial S} \mathbf{B} \cdot d\mathbf{l} = \frac{2\pi R B_\phi}{\mu_0}. \quad (73)$$

Here we have used ϕ to parameterize the line integral such that $\mathbf{B} \cdot d\mathbf{l} = R B_\phi d\phi$. Due to the assumption of axisymmetry, B_ϕ is constant along the line integral. If moreover the loop is taken to go through the electromagnetic coils that link the plasma poloidally, the total current enclosed by the loop is the sum of the currents in each coil. We furthermore assume that there are no other sources of current such that I does not depend on the radius R of the circle for any curve that encloses the coils (see Figure 6). Thus the toroidal field strength varies as $B_\phi \propto 1/R$ due to the toroidal geometry.

Because the toroidal field varies as $1/R$, it is impossible to have good confinement with only a toroidal field. As discussed in Section 5.1, in a straight, uniform field, particles exhibit gyromotion about field lines. If the magnetic field is non-uniform or curved or if an electric field is introduced, a particle will drift off of a field line on average, as discussed in Section 5.3.

Consider the grad-B drift of a particle, the second term in (72),

$$\mathbf{v}_{\nabla B} = \frac{v_\perp^2}{2\Omega} \frac{\mathbf{B} \times \nabla B}{B^2}. \quad (74)$$

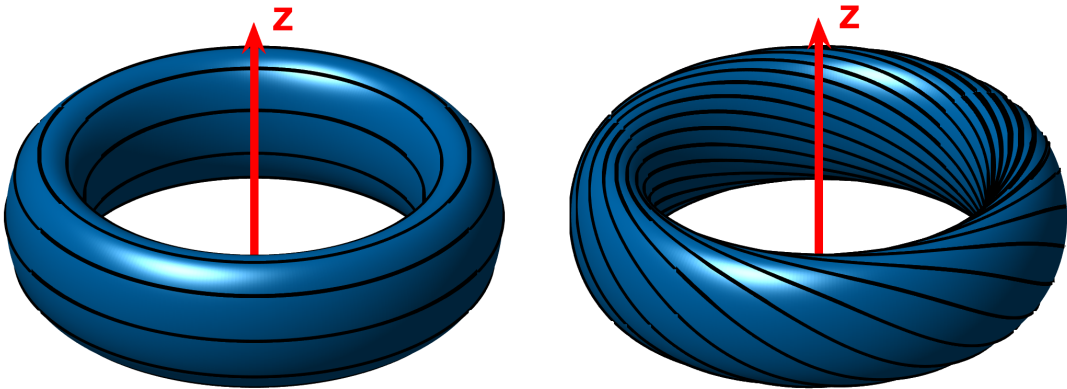


Figure 7: A purely toroidal field (left) cannot provide confinement due to the guiding center drifts. Therefore, we are interested in a magnetic field with both toroidal and poloidal components such that field lines twist to cover magnetic surfaces (right).

The gyrofrequency is $\Omega = qB/m$ and v_{\perp} is the magnitude of the velocity perpendicular to the magnetic field. The quantity $\mathbf{v}_{\nabla B}$ is the velocity at which guiding centers drift off of field lines in the presence of a gradient in the field strength. If the field is purely toroidal, a particle will drift in the $-q\hat{\phi} \times \hat{\mathbf{R}} = q\hat{\mathbf{Z}}$ direction, either up or down depending on the sign of q .

As ions and electrons move in opposite directions, an electric field will be set up in the $-\hat{\mathbf{Z}}$ direction to try to restore charge neutrality. This results in an additional $\mathbf{E} \times \mathbf{B}$ drift,

$$\mathbf{v}_E = \frac{\mathbf{E} \times \mathbf{B}}{B^2}. \quad (75)$$

We see that this drift is in the $-\hat{\mathbf{Z}} \times \hat{\phi} = \hat{\mathbf{R}}$ direction. As the direction of the $\mathbf{E} \times \mathbf{B}$ drift is the same for both electrons and ions, both species will drift radially out of the device. For this reason a purely toroidal field cannot provide sufficient confinement.

Thanks to a poloidal magnetic field, pointing the short way around the torus, these losses can be avoided. As we will discuss in Section 10.1, the existence of a poloidal magnetic field in axisymmetry ensures the existence of nested, toroidal magnetic surfaces. Consider field lines that twist to lie on a toroidal surface, having both a poloidal and toroidal component (see Figure 7). As particles move along field lines, they will move above and below the $Z = 0$ plane. When an electron is above the $Z = 0$ plane, it will grad- B drift in the $-\hat{\mathbf{Z}}$ direction away from a given surface, and when it is below the $Z = 0$ plane it will drift in the $-\hat{\mathbf{Z}}$ direction back toward the magnetic surface. In this way, on an average, charged particles stay close to a magnetic surface. The poloidal magnetic field is used for the magnetic confinement of tokamaks and stellarators. A more quantitative explanation for the necessity of a poloidal magnetic field is provided in Section 7.2.

An analogy can be made with the motion of honey on a rotating honey dipper. As gravity always pulls the fluid down, the honey will fall off the dipper if it is stationary. However, if the dipper is rotated, the honey will fall away from the dipper while it is on the bottom half and toward the dipper while it is on the upper half of the dipper. In this way, on average the honey will remain confined. In the same way, the twisting of the magnetic field lines allows particles to remain close to a given magnetic surface. The twisting of magnetic field lines is quantified by the rotational transform, which counts the number of poloidal turns per toroidal turn of a field line, see Section 7.5. Rotational transform is required for confinement in tokamak and stellarator magnetic confinement devices and will be discussed further in Section 7.6.

6 Coordinate systems

Toroidal geometry refers to a domain in \mathbb{R}^3 delimited by a genus one surface. The position in toroidal geometry can be conveniently described by several coordinate systems. In particular, for a given static magnetic field under specific assumptions, coordinates adapted to the shape of the magnetic field are useful to simplify the geometric representation.

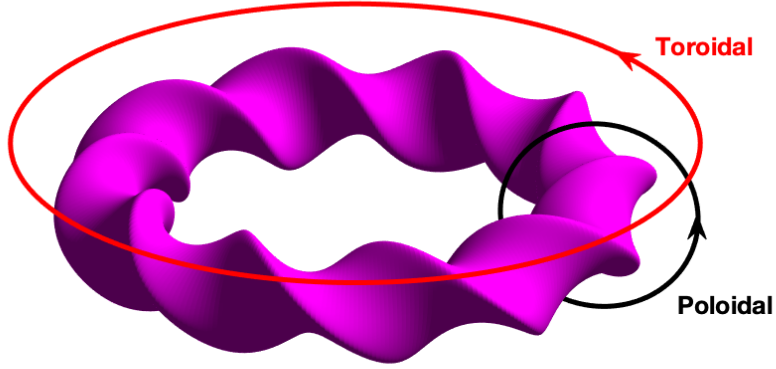


Figure 8: The position in a toroidal system is often described by two angles. A poloidal angle increases from 0 to 2π on any closed poloidal loop (black) about the magnetic axis, the short way around the torus. A toroidal angle increases from 0 to 2π on any closed toroidal loop (red) about the major axis of the coordinate system, the long way around the torus.

Section 6.1 presents a discussion of magnetic fields and toroidal magnetic surfaces, as a motivation. A reminder on the canonical cylindrical coordinate system, often used to describe toroidal systems, is proposed in Section 6.2. Section 6.3 focuses on flux surfaces and how they are labeled. These surfaces form the basis for flux coordinate systems, described in Section 6.4.

6.1 Magnetic field lines and flux surfaces

The magnetic field is a vector field, and flow lines of this vector field (field lines) are often used for visualization and interpretation of physical phenomena. Particle confinement is related to the geometry of magnetic field lines. As described in Section 5.1, in a straight magnetic field a particle will gyrate about field lines. When the field is curved or its magnitude varies in space, particles will exhibit a slow drift across field lines in addition to their motion along field lines, as described in Section 5.3. As particles are free to move in the direction parallel to the field, the temperature tends to equilibrate along field lines. In magnetic confinement fusion devices, it is necessary to maintain a hot core that is not in thermal contact with the material walls. Therefore, field lines should not connect the plasma core to the material wall or the cooler edge of the plasma. In particular, if field lines lie on a set of closed nested surfaces rather than filling the volume of the device, they do satisfy this property. Spherical surfaces will not suffice, as the hairy ball theorem states that a non-vanishing, continuous vector field cannot lie on a sphere in 3D. A flux surface is a smooth surface such that at every point on the surface $\mathbf{B} \cdot \hat{\mathbf{n}} = 0$, where $\hat{\mathbf{n}}$ is a normal vector to the surface. So, in particular, no magnetic field line crosses a magnetic surface. Additional motivation for magnetic surfaces is provided in Section 5.4, and justification for their existence is provided in Sections 10.1-10.2.

As our desired geometry consists of closed, nested, toroidal surfaces, it is useful to define a toroidal coordinate system. We will use the term toroidal to refer to the direction the long way around the torus, while the term poloidal refers to the direction the short way around the torus. See Figure 8 for a brief description of toroidal geometry.

In perfect axisymmetry, closed, nested flux surfaces are guaranteed if there is sufficient toroidal current in the plasma. This statement will be justified in Sections 10.1-10.2 by demonstrating that magnetic field line flow can be described by a Hamiltonian system which possesses a conserved quantity under the assumption of axisymmetry. However, in fully 3-dimensional geometry (such as in a stellarator or a tokamak with 3D perturbations), field lines may become chaotic (are not confined to a surface) or may form islands (toroidal surfaces that are not nested). In 3D geometry it may be possible to form nested flux surface in some regions of space. Refer to Figure 9 for a Poincaré plot of the magnetic field produced by the NCSX coils [101]. The plot is produced by following field lines around the device and placing a point wherever a field line passes through a surface at constant toroidal angle. Evidently there are regions where magnetic field lines lie on nested surfaces, form island structures, and do not form surfaces.

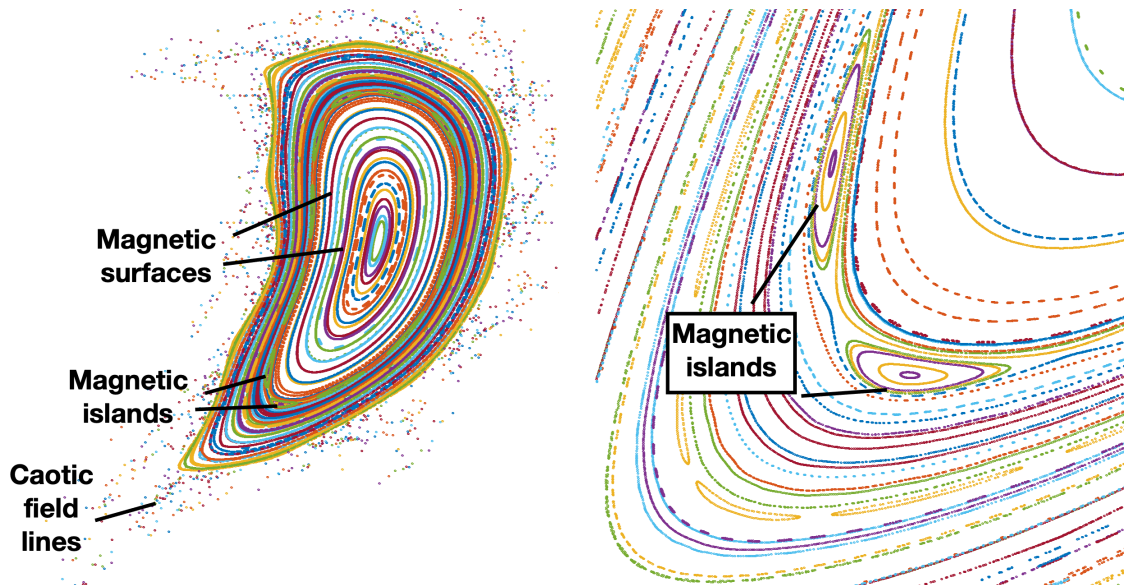


Figure 9: To produce this Figure, field lines are followed, and each time they hit a plane at constant toroidal angle, a point is marked on the plot with colors indicating a given field line. This is often referred to as a Poincaré plot. The magnetic field is generated by the coils of the NCSX stellarator [101]. Within the confinement region there are sets of magnetic surfaces as well as magnetic islands and chaotic field lines.

6.2 Canonical cylindrical coordinates

Toroidal geometry can be described by the classical cylindrical coordinates $(R, \phi, Z) \in \mathbb{R}^+ \times [0, 2\pi) \times \mathbb{R}$, see Figure 10. Given a reference axis \hat{Z} and a reference plane perpendicular to \hat{Z} , the plane can be parameterized by Cartesian coordinates X and Y , with $(\hat{X}, \hat{Y}) = (\nabla X, \nabla Y)$, unit vectors such that $\hat{X} \times \hat{Y} = \hat{Z}$. The toroidal angle ϕ is the standard cylindrical angle $\phi = \arctan(Y/X)$ while the major radius $R = \sqrt{X^2 + Y^2}$ measures the distance from the \hat{Z} axis. The unit vectors can be expressed in terms of gradients of the coordinates as $\hat{R} = \nabla R$, $\hat{\phi} = R\nabla\phi$, and $\hat{Z} = \nabla Z$. A poloidal plane is defined as a half plane at constant ϕ , so that (\hat{R}, \hat{Z}) is an orthonormal basis of the poloidal plane while $\hat{\phi}$ is orthogonal to the poloidal plane. It is convenient to apply this coordinate system to axisymmetric geometry, as ϕ is a symmetry direction (see Section 7.1).

This coordinate system is discussed in Section 4.6.1 of [20]. Note that it is independent of the magnetic field geometry: it can be constructed for non-symmetric systems and when magnetic surfaces do not exist. Cylindrical coordinates are also useful in practice as the coordinate singularity at $R = 0$ is typically outside the region of interest in toroidal systems.

6.3 Flux surfaces and flux functions

Assuming that a given magnetic field \mathbf{B} is such that the magnetic field lines lie on closed nested toroidal flux surfaces in a given domain, we can define flux functions in that domain as follows.

A flux function is any function which is constant on each flux surface. In practice particles are mostly confined to flux surfaces; therefore the temperature, density, and pressure are approximately flux functions.

A flux surface label, generally denoted ψ , is a smooth one-to-one real-valued function defined on the set of flux surfaces and often assumed to vanish on the magnetic axis, and might increase or decrease monotonically with distance from the axis. Each flux surface can be uniquely labeled by a value of ψ : a flux surface label is a flux function. We will discuss two examples of common flux labels: the poloidal and toroidal fluxes.

Suppose ϕ is an angle which increases by 2π upon a toroidal loop. The toroidal flux, Ψ_T , of a given flux surface, ψ , is the flux of magnetic field through a surface at constant ϕ bounded by the

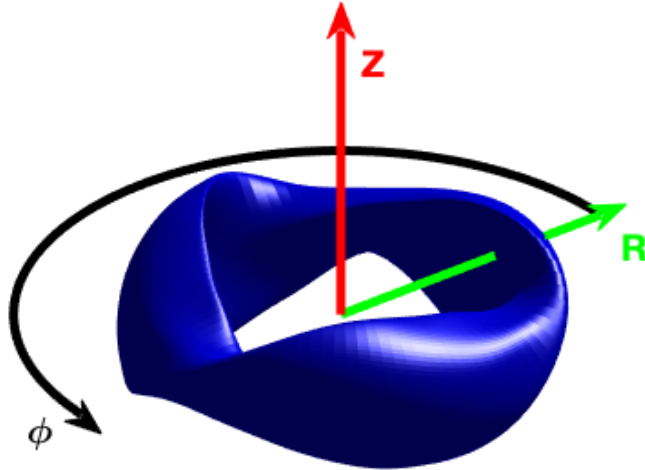


Figure 10: The standard cylindrical coordinate system: R measures distance from the \hat{Z} axis and ϕ is the standard angle of the cylindrical coordinate system such that $\hat{R} \times \hat{\phi} = \hat{Z}$.

constant ψ surface, which we call S_T (see Figure 11),

$$\Psi_T(\psi) = \int_{S_T} \mathbf{B} \cdot \hat{\mathbf{n}} d^2x, \quad (76)$$

where $\hat{\mathbf{n}}$ is an oriented unit normal and d^2x is the surface area element.

Suppose θ is an angle which increases by 2π upon a poloidal loop. The poloidal flux of a given flux surface, ψ , is the flux of the magnetic field through a surface at constant θ bounded between the magnetic axis and the constant ψ surface, which we call S_P (see Figure 12),

$$\Psi_P(\psi) = \int_{S_P} \mathbf{B} \cdot \hat{\mathbf{n}} d^2x. \quad (77)$$

The rotational transform, which quantifies the number of poloidal turns of a field line per toroidal turn (see Section 7.5), can be defined in terms of these fluxes,

$$\iota(\psi) = \frac{d\Psi_P(\psi)/d\psi}{d\Psi_T(\psi)/d\psi}. \quad (78)$$

This relation will become clear during the discussion of magnetic coordinates (Section 9).

Further discussion of flux functions can be found in Chapter 4 of [20].

6.4 Flux coordinates

If flux surfaces exist, coordinate systems can be constructed based on such surfaces. These are known as flux coordinate systems. The geometry of a set of toroidal surfaces nested along a closed curve, called the magnetic axis (see Figure 15) can be described by flux coordinates $(r, \theta, \phi) \in \mathbb{R}^+ \times [0, 2\pi) \times [0, 2\pi)$, where ϕ is an angle which increases by 2π upon a toroidal loop, θ is an angle which increases by 2π upon a poloidal loop, and r is a flux surface label. See Figure 13 for an example consisting of nested toroidal surfaces with circular cross-sections, which we call a cylindrical torus.

Flux coordinates are convenient to use in practice, as most quantities of interest are periodic in the poloidal and toroidal angles. Therefore, Fourier series can be used for both analytic study of physical systems and for efficient numerical discretization.

Using flux coordinates, the toroidal and poloidal fluxes can be expressed as,

$$\Psi_T(r) = \int_0^r \int_0^{2\pi} \frac{\mathbf{B} \cdot \nabla \phi}{\nabla r' \cdot \nabla \theta \times \nabla \phi} d\theta dr', \quad (79)$$

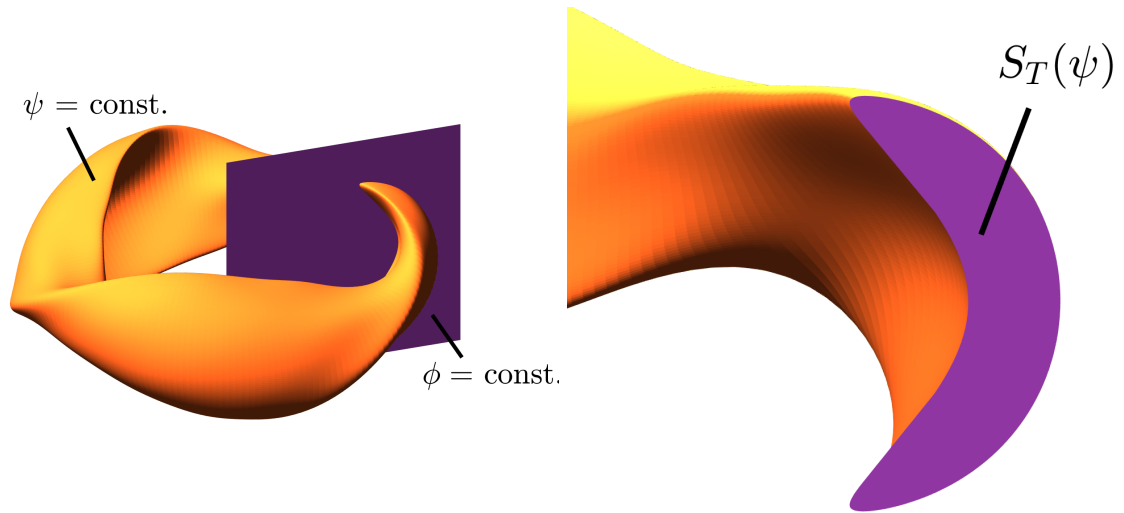


Figure 11: The toroidal flux, $\Psi_T(\psi)$, is the magnetic flux through a surface at constant ϕ bounded by the surface labeled by ψ .

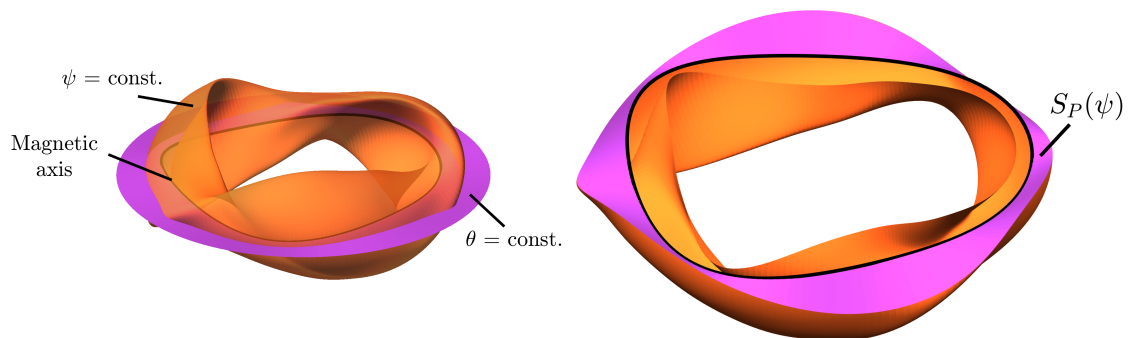


Figure 12: The poloidal flux, $\Psi_P(\psi)$, is the magnetic flux through a ribbon-like surface (pink) at constant θ bounded by the surface labeled by ψ (orange) and the magnetic axis (black).

where $\nabla\phi/|\nabla\phi|$ is a unit normal and $|\nabla\phi|(\nabla r' \cdot \nabla\theta \times \nabla\phi)^{-1}d\theta dr'$ is the surface area element for the surface at constant ϕ , and

$$\Psi_P(r) = \int_0^r \int_0^{2\pi} \frac{\mathbf{B} \cdot \nabla\theta}{\nabla r' \cdot \nabla\theta \times \nabla\phi} d\phi dr', \quad (80)$$

where $\nabla\theta/|\nabla\theta|$ is a unit normal and $|\nabla\theta|(\nabla r' \cdot \nabla\theta \times \nabla\phi)^{-1}d\phi dr'$ is the surface area element for the surface at constant θ .

For a cylindrical torus of major radius R and minor radius r , if the toroidal magnetic field $B_T = \mathbf{B} \cdot \nabla\phi/|\nabla\phi|$ is constant, then the toroidal flux is $\Psi_T = \pi r^2 B_T$; likewise if the poloidal magnetic field $B_P = \mathbf{B} \cdot \nabla\theta/|\nabla\theta|$ is constant, then the poloidal flux is $\Psi_P = 2\pi Rr B_P$. In practice B_T and B_P are not constant, but this provides a valid order of magnitude approximation. See Figure 13.

While flux coordinates can be used with any flux label, in this text we will use the toroidal flux function $\psi = \Psi_T/2\pi$ as our flux surface label. Another example in a cylindrical torus is r , which measure the distance to the magnetic axis within a poloidal plane. Other examples of flux functions are described in Section 6.3. Several examples of flux coordinate systems will be discussed in Section 9.

While the classical toroidal coordinates (see Section 6.2) form an orthogonal system, in general flux coordinates are non-orthogonal. In this case, physical vector fields, such as the magnetic field, can be expanded in the basis of the gradients of the coordinates,

$$\mathbf{B}(\psi, \theta, \phi) = B_\psi(\psi, \theta, \phi)\nabla\psi + B_\theta(\psi, \theta, \phi)\nabla\theta + B_\phi(\psi, \theta, \phi)\nabla\phi, \quad (81)$$

known as the covariant form, or in the basis of the derivatives of the position vector,

$$\mathbf{B}(\psi, \theta, \phi) = B^\theta(\psi, \theta, \phi)\frac{\partial\mathbf{r}(\psi, \theta, \phi)}{\partial\theta} + B^\phi(\psi, \theta, \phi)\frac{\partial\mathbf{r}(\psi, \theta, \phi)}{\partial\phi}, \quad (82)$$

known as the contravariant form. Note that $B^\psi = 0$ as the magnetic field lies in the constant ψ surfaces such that $\mathbf{B} \cdot \nabla\psi = 0$. A further discussion of non-orthogonal coordinates can be found in Chapter 2 of [20].

6.5 Cheat sheet for non-orthogonal coordinates

Below we include a summary of some useful formulae for non-orthogonal coordinate systems in 3D space. Considering a coordinate system (x_1, x_2, x_3) , two local bases can be defined at any point $\mathbf{r} \in \mathbb{R}^3$:

- the covariant basis $(\nabla x_1, \nabla x_2, \nabla x_3)$,
- the contravariant basis $(\partial\mathbf{r}/\partial x_1, \partial\mathbf{r}/\partial x_2, \partial\mathbf{r}/\partial x_3)$.

They are related by the following expression:

$$\frac{\partial\mathbf{r}}{\partial x_k} = \frac{\nabla x_i \times \nabla x_j}{\nabla x_i \times \nabla x_j \cdot \nabla x_k}. \quad (83)$$

The covariant and contravariant unit vectors satisfy the dual relation: $\nabla x_i \cdot \partial\mathbf{r}/\partial x_j = \delta_j^i$, for all indices $(i, j) \in \{1, 2, 3\}^2$.

In general these two bases are not orthogonal. However, for some coordinate systems, such as Cartesian or cylindrical coordinates, they are orthogonal at any point $\mathbf{r} \in \mathbb{R}^3$. Note that the contravariant and covariant bases can only be orthogonal simultaneously. In particular, it is a direct consequence of (83) that orthogonality of the covariant basis implies the orthogonality of the contravariant basis. In an orthogonal coordinate system, the covariant and contravariant basis vectors for each coordinate are parallel, that is to say that $\nabla x_i \parallel \partial\mathbf{r}/\partial x_i$ for all $i \in \{1, 2, 3\}$; this is another consequence of (83). This is related to the fact that in an orthogonal coordinate system, at any point $(y_1, y_2, y_3) \in \mathbb{R}^3$ any two surfaces of constant coordinates, like $\{(x_1, x_2, x_3) \in \mathbb{R}^3, x_i = y_i\}$ and $\{(x_1, x_2, x_3) \in \mathbb{R}^3, x_j = y_j\}$ for $i \neq j$, have orthogonal tangent planes along their intersection. As opposed to this, in a non-orthogonal coordinate system, covariant and contravariant basis vectors are not necessarily parallel, and surfaces of constant coordinates do not necessarily have orthogonal tangent planes.

Next we provide here some of the basic formulas for integrating and differentiating in such coordinates. Consider a vector field \mathbf{A} and a scalar function q . Here we assume that $(i, j, k) = (1, 2, 3)$ or one of its cyclic permutations.

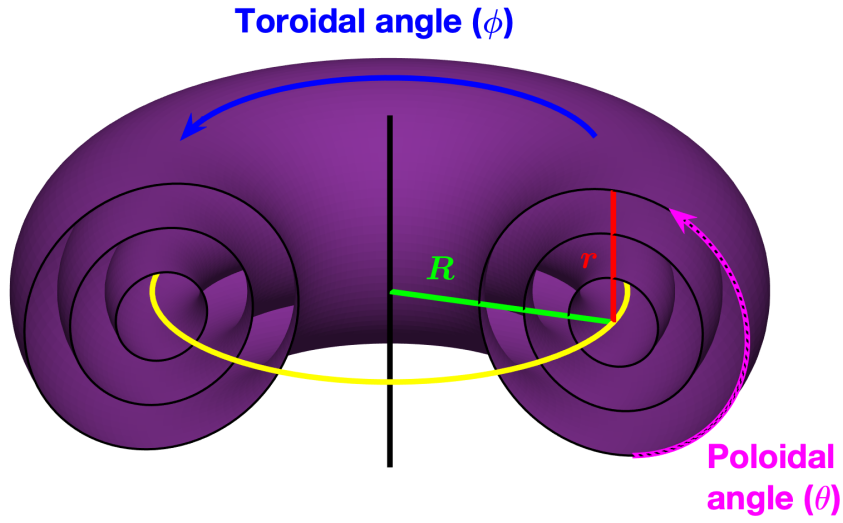


Figure 13: We consider a flux coordinate system consisting of tori with circular cross-Sections. Poloidal and toroidal angles describe the location on a magnetic surface. In the case of nested magnetic surfaces, the magnetic axis (yellow) is the line enclosed by all nested surfaces. The minor radius, r , is a measure of distance from the magnetic axis within a poloidal plane (half plane defined by $\phi = \text{const.}$). The major radius, R , measures distance from the axis of rotation of the toroidal coordinate system. Similar coordinates can be constructed for non-axisymmetric system, where r is a flux surface label.

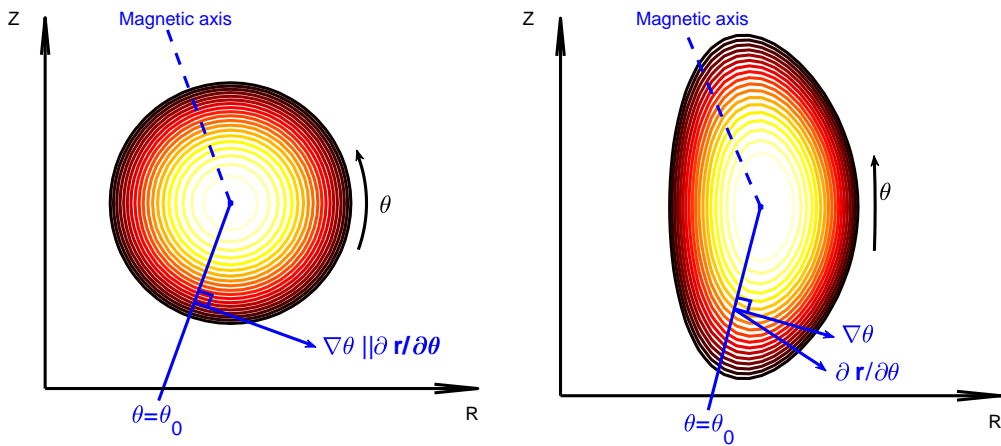


Figure 14: Comparison of orthogonal (left) and non-orthogonal (right) flux coordinate systems (ψ, θ, ϕ) in a plane of constant ϕ . Curves of constant coordinate ψ for orthogonal and non-orthogonal coordinates are shown. In an orthogonal system (left), the covariant and contravariant basis vectors for a given coordinate are parallel, while, in a non-orthogonal system (right), covariant and contravariant basis vectors are no longer parallel.

Covariant form	$\mathbf{A} = \sum_{i=1}^3 A_i \nabla x_i$ with $A_i = \mathbf{A} \cdot \partial \mathbf{r} / \partial x_i$
Contravariant form	$\mathbf{A} = \sum_{i=1}^3 A^i \frac{\partial \mathbf{r}}{\partial x_i}$ with $A^i = \mathbf{A} \cdot \nabla x_i$
Jacobian	$\sqrt{g} = \left(\frac{\partial \mathbf{r}}{\partial x_1} \times \frac{\partial \mathbf{r}}{\partial x_2} \right) \cdot \frac{\partial \mathbf{r}}{\partial x_3} = ((\nabla x_1 \times \nabla x_2) \cdot \nabla x_3)^{-1}$
Relation between basis vectors	$\frac{\partial \mathbf{r}}{\partial x_k} = \sqrt{g} (\nabla x_i \times \nabla x_j)$
Differential volume	$d^3 x = \sqrt{g} dx_1 dx_2 dx_3$
Differential surface area (constant x_k)	$d^2 x = \sqrt{g} \nabla x_k dx_i dx_j$
$\nabla \cdot \mathbf{A} = \sum_{i=1}^3 \frac{1}{\sqrt{g}} \frac{\partial}{\partial x_i} (\sqrt{g} A^i)$	$\nabla \times \mathbf{A} = \sum_{k=1}^3 \frac{1}{\sqrt{g}} \left(\frac{\partial A_j}{\partial x_i} - \frac{\partial A_i}{\partial x_j} \right) \frac{\partial \mathbf{r}}{\partial x_k}$
$\nabla q = \sum_{i=1}^3 \frac{\partial q}{\partial x_i} \nabla x_i$	$d\mathbf{r} = \sum_{i=1}^3 \frac{\partial \mathbf{r}}{\partial x_i} dx_i$

Table 2: Summary of formulas used to describe the geometry of a non-orthogonal coordinate system (x_1, x_2, x_3) . In the above, $\{i, j, k\}$ is a permutation of $\{1, 2, 3\}$.

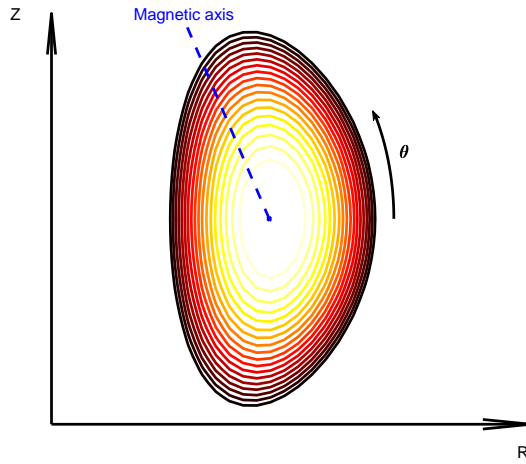


Figure 15: Poloidal angle θ and level curves of the flux label ψ in a poloidal half plane. In the poloidal plane, the magnetic axis is the point enclosed by all the flux surfaces.

7 Toroidal magnetic confinement

We can now discuss confinement of particles in magnetic confinement configurations. In this section we focus on two leading approaches: the tokamak and the stellarator. In Section 7.1 we propose a formal definition of axisymmetry, the fundamental property of the tokamak. In Section 7.2 we will see that axisymmetry leads to the conservation of a quantity, hence providing particle confinement. However, we will find that this confinement is associated with a major challenge: the necessity of a large current within the confinement region. We will revisit particle confinement without axisymmetry in Section 12.1. An overview of the tokamak and stellarator concepts is provided in Sections 7.3 and 7.4. Section 7.5 focuses on a concept important to toroidal confinement, the rotational transform. In Section 7.6 we discuss how rotational transform can be produced with and without the assumption of axisymmetry.

7.1 Axisymmetry

Axisymmetry is the symmetry of vector or scalar fields with respect to the azimuthal toroidal angle, ϕ , when expressed in canonical cylindrical coordinates (see Section 6.2).

Consider a vector field

$$\mathbf{F}(R, \phi, Z) = F_R(R, \phi, Z)\hat{\mathbf{R}}(\phi) + F_\phi(R, \phi, Z)\hat{\phi}(\phi) + F_Z(R, \phi, Z)\hat{\mathbf{Z}}. \quad (84)$$

Axisymmetry of \mathbf{F} implies that

$$\frac{\partial F_R(R, \phi, Z)}{\partial \phi} = \frac{\partial F_\phi(R, \phi, Z)}{\partial \phi} = \frac{\partial F_Z(R, \phi, Z)}{\partial \phi} = 0. \quad (85)$$

This furthermore implies that the magnitude, $F = |\mathbf{F}|$, satisfies

$$\frac{\partial F(R, \phi, Z)}{\partial \phi} = 0. \quad (86)$$

A vector field, \mathbf{F} , is said to be axisymmetric if it satisfies (85), and a scalar field, F , is said to be axisymmetric if it satisfies (86).

Some magnetic confinement devices, such as tokamaks, have axisymmetric magnetic fields, \mathbf{B} , according to the above definition. With a suitable choice for gauge, the corresponding vector potential, \mathbf{A} , is also axisymmetric according to (85). Similarly, the corresponding current density, \mathbf{J} , can be shown to be axisymmetric upon application of Ampere's law (13). Therefore, many physical quantities of interest are axisymmetric if the magnetic field is axisymmetric.

Axisymmetry can also be expressed in a flux coordinate system (r, θ, ϕ) (see Section 6.4) if the toroidal angle is chosen to be the canonical azimuthal angle. Consider a vector field expressed in its covariant and contravariant forms

$$\begin{aligned} \mathbf{F}(r, \theta, \phi) &= F_r(r, \theta, \phi)\nabla r + F_\theta(r, \theta, \phi)\nabla\theta + F_\phi(r, \theta, \phi)\nabla\phi \\ &= F^r(r, \theta, \phi)\frac{\partial\mathbf{r}(r, \theta, \phi)}{\partial r} + F^\theta(r, \theta, \phi)\frac{\partial\mathbf{r}(r, \theta, \phi)}{\partial\theta} + F^\phi(r, \theta, \phi)\frac{\partial\mathbf{r}(r, \theta, \phi)}{\partial\phi}. \end{aligned} \quad (87)$$

As flux coordinates are generally non-orthogonal, we need to consider the symmetry of both component forms. Axisymmetry implies that

$$\frac{\partial F_r(r, \theta, \phi)}{\partial \phi} = \frac{\partial F_\theta(r, \theta, \phi)}{\partial \phi} = \frac{\partial F_\phi(r, \theta, \phi)}{\partial \phi} = \frac{\partial F^r(r, \theta, \phi)}{\partial \phi} = \frac{\partial F^\theta(r, \theta, \phi)}{\partial \phi} = \frac{\partial F^\phi(r, \theta, \phi)}{\partial \phi} = 0. \quad (88)$$

We will consider several implications of axisymmetry in Sections 7.6 and 7.2.

7.2 Particle confinement in axisymmetry

Axisymmetry is desirable because it guarantees confinement of particles in the absence of collisions. This can be seen when considering the Lagrangian for the motion of a single particle with mass m and charge q in a magnetic field $\mathbf{B} = \nabla \times \mathbf{A}$ and an electric field $\mathbf{E} = -\nabla\Phi - \partial\mathbf{A}/\partial t$, as described

in Section 4.2. We will express the Lagrangian in a cylindrical coordinate system, (R, ϕ, Z) (see Section 6.2),

$$L(R, \phi, Z, \dot{R}, \dot{\phi}, \dot{Z}, t) = \frac{m}{2} \left(\dot{R}^2 + R^2 \dot{\phi}^2 + \dot{Z}^2 \right) + q \left(A_R(R, \phi, Z) \dot{R} + A_\phi(R, \phi, Z) R \dot{\phi} + A_Z(R, \phi, Z) \dot{Z} \right) - q\Phi(R, \phi, Z, t). \quad (89)$$

Here the scalar potential is decomposed in its components in cylindrical coordinates as $\mathbf{A} = A_R \hat{\mathbf{R}} + A_\phi \hat{\boldsymbol{\phi}} + A_Z \hat{\mathbf{Z}}$. Under the assumption of axisymmetry, each of the components of \mathbf{A} is independent of ϕ (see Section 7.1). Furthermore, Φ is assumed to be axisymmetric.

The equations of motion implied by the Lagrangian come from the Euler-Lagrange equations (25). The Euler-Lagrange equation for the toroidal angle is,

$$\frac{d}{dt} \left(\frac{\partial \mathcal{L}(R, \phi, Z, \dot{R}, \dot{\phi}, \dot{Z}, t)}{\partial \dot{\phi}} \right) = \frac{\partial \mathcal{L}(R, \phi, Z, \dot{R}, \dot{\phi}, \dot{Z}, t)}{\partial \phi}. \quad (90)$$

We will call $p_\phi := \partial \mathcal{L} / \partial \dot{\phi} = mR^2 \dot{\phi} + qRA_\phi$ the toroidal canonical momentum. We see that under the assumption of axisymmetry, the Lagrangian becomes independent of ϕ , and a constant of motion is implied,

$$\frac{dp_\phi(t)}{dt} = 0. \quad (91)$$

This is a consequence of Noether's theorem: a continuous symmetry (toroidal rotational symmetry) implies a conserved quantity (p_ϕ).

We will now estimate the size of each term in p_ϕ to gain additional insight. We can note from (95) that (RA_ϕ) can be related to the magnitude of the poloidal magnetic field as $B_P = (1/R)|\nabla(RA_\phi)|$. Assuming that the gradient length scale of (RA_ϕ) scales as $|(\nabla(RA_\phi))| \sim R^{-1}$, we can approximate $RA_\phi \sim R^2 B_P$. We can also approximate $R\dot{\phi} \sim v_t$, where $v_t = \sqrt{2T/m}$ is the thermal velocity. So we find the ratio of the two terms in p_ϕ to be,

$$\frac{mR^2 \dot{\phi}}{qRA_\phi} \sim \frac{mv_t}{qB_P R} \sim \frac{\omega_B}{\Omega_P}. \quad (92)$$

Here $\omega_B = v_t/L_B$ is the frequency associated with the time variation of the magnetic field as introduced in Section 5.2, the gradient length scale of the magnetic field is defined such that $L_B^{-1} = (1/B)|\nabla B|$, and $\Omega_P = qB_P/m$ is the poloidal gyrofrequency, the analogous gyrofrequency ($\Omega = qB/m$) associated with the poloidal magnetic field. We have made the assumption that $L_B \sim R$. If B_P is large enough, this ratio will be $\ll 1$. Therefore, we can make the approximation $p_\phi \approx qRA_\phi$.

We note that (RA_ϕ) is a flux function according to the discussion in Section 7.6. As p_ϕ is then approximately constant on a flux surface, a particle will be confined to within a small distance of a flux surface. This is another way to understand the need for a poloidal magnetic field for confinement in a tokamak. See [69] and Chapter 7 in [37] for more details.

In 3D geometry without a continuous symmetry, i.e. without axisymmetry, this result does not apply, so much more care must be taken in order to achieve good confinement. However, a 'hidden symmetry' can be exploited to obtain similar confinement properties in a stellarator, as will be explored in Section 12.1.

7.3 Tokamak

A tokamak is a toroidal confinement device with genus one topology. The magnetic fields of tokamaks are designed to be axisymmetric according to the definition provided in Section 7.1: thus many physical scalar quantities are independent of the toroidal angle, ϕ .

The poloidal magnetic field of a tokamak is produced by the toroidal plasma current. We will see in Section 7.6 that this plasma current is *required* to produce rotational transform in axisymmetry. While there is some self-generated plasma current, it is not sufficient for confinement, so current needs to be driven externally. Often this is done with a transformer through electro-magnetic induction. By varying the current through a central transformer coil (see Figure 16) an electric

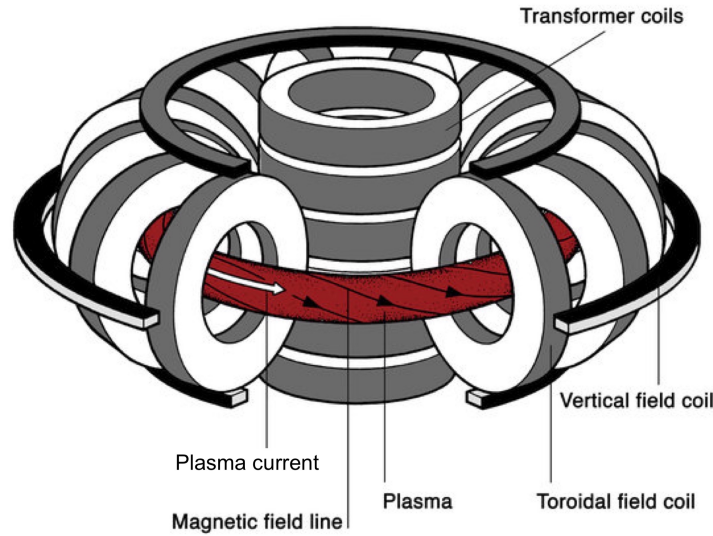


Figure 16: The poloidal magnetic field of a tokamak is produced by toroidal plasma current, which is inductively driven by transformer coils. The toroidal field is produced by electro-magnetic coils which are planar curves. Figure reproduced from [6].

field is induced in the plasma. As the current through the transformer coil cannot be increased or decreased indefinitely, this cannot be used as a steady-state approach. Driving current also requires a significant amount of energy, so some of the energy produced by fusion must be recirculated for current drive in a tokamak reactor. Many dangerous plasma instabilities are also driven by plasma current. The result of these instabilities is a sudden loss of confinement of the plasma, called a disruption.

Although the need for current has some disadvantages, the tokamak configuration is advantageous because of its simple geometry. The toroidal symmetry ensures that the collisionless particle orbits are confined when accounting for the drifts, as discussed in Section 7.2. The toroidal field coils of a tokamak are planar curves that are (relatively) easy to construct in contrast with those of a stellarator (see Figure 16).

7.4 Stellarator

A stellarator is a toroidal confinement device with genus one topology. Unlike a tokamak, it does not exhibit axisymmetry according to the definitions in Section 7.1.

Due to its lack of axisymmetry, plasma current is not required in order to produce rotational transform in a stellarator. The mechanisms by which rotational transform can be generated will be discussed in Section 7.6. These mechanisms require shaping of the magnetic field structure, which ultimately needs to be produced by external coils. Although stellarators generally do not have externally driven current, there is a small amount of self-driven current. As stellarator coils have to produce a carefully shaped magnetic field in order to have sufficient rotational transform, stellarator coils tend to be much more complex than tokamak coils (see Figure 17). This poses a major challenge for stellarator design. Because stellarators do not need driven current they can be run in a steady-state operation, as no inductive electric field is needed. Furthermore, stellarators tend to be more stable than tokamaks to current-driven instabilities.

7.5 Rotational transform

As described in Section 5.4, a poloidal magnetic field is required for confinement, resulting in field lines which twist about flux surfaces. The twist in the field lines is quantified by the rotational transform, ι , which indicates the number of poloidal turns of a field line around the magnetic axis for each toroidal turn around the \hat{Z} axis. The rotational transform can be defined in terms of the

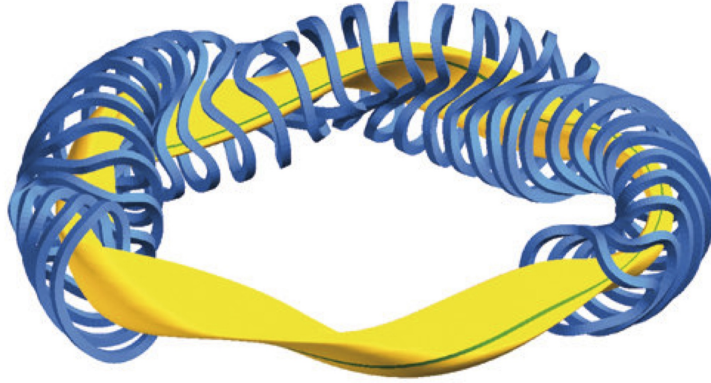


Figure 17: A stellarator confines hot plasma with magnetic fields that do not exhibit a continuous toroidal symmetry. The coils of the Wendelstein 7-X device are shown along with the outer magnetic surface (yellow) and a field line (blue). The twisting of the field line around the surface is produced by the rather complicated electro-magnetic coils. Figure reproduced from [5].

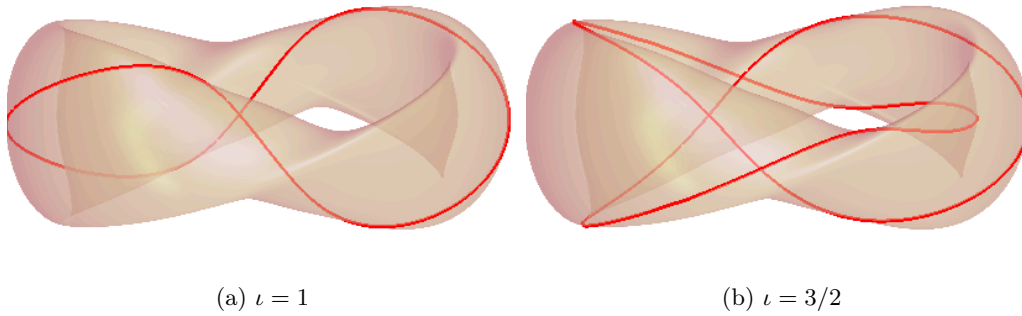


Figure 18: Two examples of field lines on a toroidal surface. An $\nu = 1$ field line (left) makes one poloidal turn for each toroidal turn, while an $\nu = 3/2$ field line (right) makes three poloidal turns for two toroidal turns. As both are rational field lines, they close on themselves after a finite number of toroidal turns.

change in poloidal angle, $(\Delta\theta)_k$, after the k^{th} toroidal turn along a field line,

$$\nu = \lim_{n \rightarrow \infty} \frac{\sum_{k=1}^n (\Delta\theta)_k}{2\pi n}. \quad (93)$$

Often in the tokamak literature the safety factor $q = 1/\nu$ is used rather than the rotational transform. If flux surfaces exist, the rotational transform can also be defined in terms of the fluxes as described in Section 6.3.

When the rotational transform is rational, $\nu = m/n$ for $m \in \mathbb{Z}$ and $n \in \mathbb{Z}$, a field line closes on itself after n toroidal turns, having completed m poloidal turns. Therefore, a given field line does not cover the entire surface (see Figure 18). Flux surfaces with rational values of ν are known as rational surfaces. When ν is irrational, a given field line comes arbitrarily close to every point on what is called an irrational surface. For details about the mechanisms by which rotational transform is produced, see Section 7.6.

7.6 Producing rotational transform

The rotational transform, ν , is the number of poloidal turns of a field line for every toroidal turn of a field line. As described in Section 5.4, this twist in the field lines is necessary for toroidal

confinement. We now explore how rotational transform can be produced with and without the assumption of axisymmetry.

7.6.1 With axisymmetry

The most straightforward way to produce rotational transform is with a toroidal plasma current, creating a poloidal magnetic field from Ampere's law (13). In fact, this is the *only* possibility under the assumption of axisymmetry. Throughout our discussion we will assume the existence of closed, nested flux surfaces. A further justification of this assumption is provided in Section 10.1.

To demonstrate this, we first express the magnetic field conveniently in terms of the poloidal flux. In the canonical cylindrical basis $(\hat{\mathbf{R}}, \hat{\phi}, \hat{\mathbf{Z}})$, see Section 6.2, the magnetic field reads

$$\mathbf{B} = B_R \hat{\mathbf{R}} + B_Z \hat{\mathbf{Z}} + B_\phi \hat{\phi}. \quad (94)$$

As $\nabla \cdot \mathbf{B} = 0$, the magnetic field can be written in terms of a vector potential \mathbf{A} as $\mathbf{B} = \nabla \times \mathbf{A}$. Under the assumption of axisymmetry the vector potential expressed in the canonical cylindrical coordinates satisfies $\partial A_Z / \partial \phi = 0$, $\partial A_R / \partial \phi = 0$, $\partial A_\phi / \partial \phi = 0$, so in particular the first two terms in (94), comprising the poloidal magnetic field, can be expressed in terms of the toroidal component of \mathbf{A} ,

$$\mathbf{B}_P(R, Z, \phi) = -\frac{\partial A_\phi(R, Z)}{\partial Z} \hat{\mathbf{R}}(\phi) + \frac{1}{R} \frac{\partial(RA_\phi(R, Z))}{\partial R} \hat{\mathbf{Z}}. \quad (95)$$

As a result, since $\mathbf{B} \cdot \nabla(RA_\phi) = 0$, the quantity (RA_ϕ) is a flux function.

More precisely, in order to relate RA_ϕ to the poloidal flux, consider a surface of constant RA_ϕ , whose intersection with the horizontal plane $Z = 0$ is made of two distinct curves. We denote by C_{ψ_P} the one standing further away from the $\hat{\mathbf{Z}}$ axis. Consider the surface S_P lying in the $Z = 0$ plane and bounded on one side by the magnetic axis, denoted C_0 , and on the other side by C_{ψ_P} . Both of these curves are circular under the assumption of axisymmetry. The setting is illustrated in Figure 12. The poloidal flux through S_P can be computed thanks to Stokes' theorem as

$$2\pi\psi_P = \int_{S_P} \mathbf{B} \cdot \hat{\mathbf{n}} d^2x = \int_{C_{\psi_P}} \mathbf{A} \cdot d\mathbf{l} - \int_{C_0} \mathbf{A} \cdot d\mathbf{l}.$$

The two curves can be parameterized by ϕ so that in both integrals $\mathbf{A} \cdot d\mathbf{l} = RA_\phi d\phi$,

$$2\pi\psi_P = 2\pi \left((RA_\phi)|_{C_{\psi_P}} - (RA_\phi)|_{C_0} \right). \quad (96)$$

As a result (RA_ϕ) is the poloidal flux function ψ_P up to an additive constant $(RA_\phi)|_{C_0}$, and therefore the poloidal magnetic field can be expressed in terms of ψ_P ,

$$\mathbf{B} = -\nabla\phi \times \nabla\psi_P + B_\phi \hat{\phi}, \quad (97)$$

by expressing (95) in terms of ψ_P and noting that $\nabla\phi = (1/R)\hat{\phi}$.

We now consider the implications of the above expression. We compute the toroidal current through a surface $S_T(\psi_P)$ at constant ϕ bounded by a surface at constant ψ_P . This surface integral can be computed using Ampere's law (13),

$$I_T(\psi_P) = \int_{S_T(\psi_P)} \mathbf{J} \cdot \hat{\mathbf{n}} d^2x = \frac{1}{\mu_0} \oint_{\partial S_T(\psi_P)} \mathbf{B} \cdot d\mathbf{l}. \quad (98)$$

The line integral is explained in more detail in Section 9.2. We define a coordinate $l(R, Z)$ to parameterize the length along $\partial S_T(\psi_P)$.

The integrand of the above is computed to be,

$$\mathbf{B} \cdot d\mathbf{l} = \mathbf{B} \cdot \frac{\partial \mathbf{r}}{\partial l} dl = \left(-\frac{1}{R} \frac{\partial \psi_P}{\partial Z} \frac{\partial l}{\partial R} + \frac{1}{R} \frac{\partial \psi_P}{\partial R} \frac{\partial l}{\partial Z} \right) dl = (\nabla l \times \nabla \psi_P \cdot \nabla \phi) dl. \quad (99)$$

By construction, the quantity $\nabla l \times \nabla \psi_P \cdot \nabla \phi$ does not vanish within the integrand, as ∇l points along the contour while $\nabla \psi_P$ is perpendicular to the contour within the surface of constant ϕ . Thus the toroidal current $I_T(\psi_P)$ is non-zero from (98).

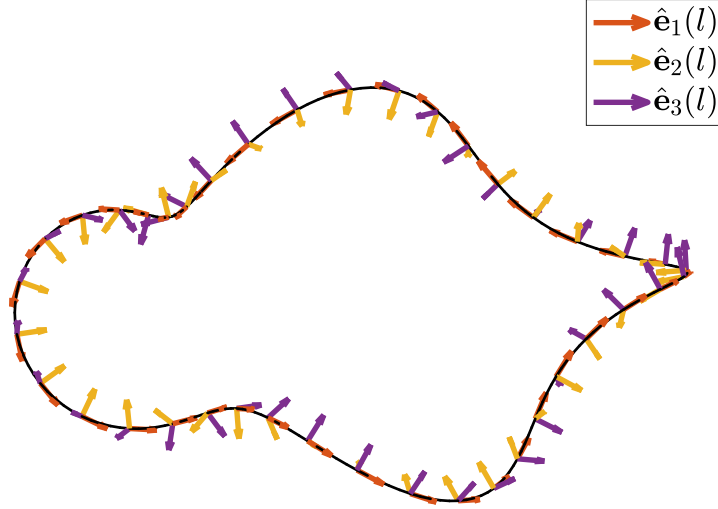


Figure 19: The magnetic axis of the TJ-II stellarator (black) is displayed with the orthonormal Frenet-Serret unit vectors.

We conclude that, under the assumption of axisymmetry, closed nested flux surfaces can only exist if there is a non-zero toroidal current in the confinement region. Moreover, ψ_P cannot be constant within a volume, as this implies that the poloidal magnetic field vanishes from (97) but a purely toroidal field was ruled out for toroidal confinement in Section 5.4.

Finally, if the rotational transform (78) $\iota = d\Psi_P(\Psi_T)/d\Psi_T$ is non-zero in a volume then ψ_P is non-constant in that volume and the toroidal current I_T is non-zero from (98). Therefore, in order to produce rotational transform in an axisymmetric system with flux surfaces, a toroidal current is necessary. Thus tokamaks require current in the confinement region. The consequences are discussed further in Section 7.3.

7.6.2 Without axisymmetry

Surprisingly, rotational transform can also be produced without current in the confinement region. A classic result of Mercier [73, 36], using an asymptotic expansion of the magnetic field near the magnetic axis demonstrates the mechanisms by which rotational transform can be generated.

We will use a Frenet-Serret coordinate system to discuss this result. We define orthonormal unit vectors, at any point $P \in \mathbb{R}^3$:

- $\hat{e}_1^P = \hat{\mathbf{b}}(P)$, the unit tangent vector in the direction of the magnetic field;
- $\hat{e}_2^P = \frac{\boldsymbol{\kappa}(P)}{|\boldsymbol{\kappa}(P)|}$, the unit vector in the direction of the magnetic curvature $\boldsymbol{\kappa}(P) = (\hat{\mathbf{b}}(P) \cdot \nabla) \hat{\mathbf{b}}(P)$;
- $\hat{e}_3^P = \hat{e}_1^P \times \hat{e}_2^P$.

The magnetic axis can be defined by a line $\mathbf{r}_0(l)$, where l is a parameter which measures distance along the curve. Consider the Frenet-Serret basis defined along the magnetic axis ($\hat{e}_1(l)$, $\hat{e}_2(l)$, $\hat{e}_3(l)$). The basis vectors \hat{e}_2 and \hat{e}_3 define a plane perpendicular to the magnetic axis. These vectors are related in the following way,

$$\frac{d\hat{e}_3(l)}{dl} = -\tau(l)\hat{e}_2(l), \quad (100)$$

where τ is the torsion of the magnetic axis. The torsion of a planar curve vanishes at all points, and τ can be thought of as a measure of the non-planarity of the magnetic axis. The Frenet-Serret unit vectors on the magnetic axis of the TJ-II stellarator are shown in Figure 19.

As a result of the calculation which is discussed in detail in Section 10.4, we find that the cross-sections of the flux surfaces in the $\hat{e}_2 - \hat{e}_3$ plane form ellipses. The angle of the major axis of the ellipse with respect to \hat{e}_2 is denoted by $\delta(l)$. In order to have non-zero rotational transform in the absence of plasma current, either a non-zero value of $\delta'(l)$ or $\tau(l)$ are required

(the functional dependence of the rotational transform on $\tau(l)$ and $\delta'(l)$ is given in (215)). Both of these mechanisms require breaking of toroidal symmetry as defined in Section 7.1.

This idea was the basis for the first stellarator designed by Spitzer [89], which featured a magnetic axis shaped as a Figure-eight to produce torsion of the magnetic axis. Most stellarators use both torsion and ellipticity to produce rotational transform.

8 Coupling of particles and electro-magnetic fields: MHD models

Magnetohydrodynamics (MHD) is a one-fluid model of plasma: it couples Maxwell's equations with a fluid model for the particles. It describes the plasma by a mass density ρ , center of mass fluid velocity \mathbf{u} , species-summed pressure p , and current density \mathbf{J} . Although many MHD models exist, in this document we will focus our attention on the ideal MHD model, as it provides a relatively simple, computationally tractable set of equations. This will be discussed in Section 8.1. Section 8.2 describes how the magnetic topology is preserved by ideal MHD. Our ultimate goal is to understand the ideal equilibrium limit of these equations, see Section 8.3, such that the fluid flow and time dependence vanish. The axisymmetric MHD equilibrium is presented in Section 8.4, before a more detailed discussion of 3D MHD models presented in Sections 10 and 11.

8.1 Ideal MHD

We now outline the equations satisfied by the fluid mass density ρ , current density \mathbf{J} , and flow velocity \mathbf{u} under the ideal MHD model. Mass conservation is ensured by the continuity equation,

$$\frac{\partial \rho}{\partial t} + \nabla \cdot (\rho \mathbf{u}) = 0. \quad (101)$$

Momentum density obeys a similar conservation equation,

$$\rho \left(\frac{\partial}{\partial t} + \mathbf{u} \cdot \nabla \right) \mathbf{u} = \mathbf{J} \times \mathbf{B} - \nabla p, \quad (102)$$

and the energy conservation equation is,

$$\left(\frac{\partial}{\partial t} + \mathbf{u} \cdot \nabla \right) \left(\frac{p}{\rho^\gamma} \right) = 0. \quad (103)$$

Here γ is the ratio of specific heats ($\gamma = 5/3$ for a monatomic gas system).

The fields, \mathbf{E} and \mathbf{B} , obey Maxwell's equations (see Section 3). Here the displacement current term, $(\partial \mathbf{E} / \partial t)$ can be dropped for non-relativistic plasmas,

$$\nabla \times \mathbf{B} = \mu_0 \mathbf{J} \quad (104a)$$

$$\nabla \times \mathbf{E} = -\frac{\partial \mathbf{B}}{\partial t} \quad (104b)$$

$$\nabla \cdot \mathbf{B} = 0. \quad (104c)$$

In ideal MHD, we furthermore make the approximation that the electric field in a frame moving with the fluid is zero,

$$\mathbf{E} + \mathbf{u} \times \mathbf{B} = 0. \quad (105)$$

This comes from the assumption that the plasma is perfectly conducting. Non-ideal MHD models include additional effects, such as resistivity which results from friction between electrons and ions. Resistive effects are needed to allow for changes in the magnetic topology, known as magnetic reconnection. In Section 6.3 we will discuss the result that ideal MHD does not allow for changes in topology.

The MHD equations can be considered to be a set of PDEs for ρ , \mathbf{u} , p , and \mathbf{B} , while \mathbf{E} is determined from \mathbf{u} and \mathbf{B} , and \mathbf{J} is determined from \mathbf{B} . This model is derived under a series of assumptions, which are explained more completely in many references [79, 25, 29]. Specifically, the MHD equations can be obtained from kinetic or fluid models under certain limits.

- Collisions are very strong, such that the electron and ion temperature have equilibrated.
- The gyroradius is small compared to wavelengths of interest.
- The system is non-relativistic, such that the displacement current can be dropped from Ampere's law.
- Frequencies faster than the electron plasma frequency, $\omega_{pe} = \sqrt{n_e e^2 / (\mu_0 m_e)}$, are not included.

These assumptions have the following consequences.

- Since the displacement current is dropped from Ampere's law, MHD does not include light waves.
- As this is a fluid model, it does not account for velocity space effects such as particle trapping.
- As high frequency and small wavelengths are neglected, MHD describes the macroscopic, low-frequency behavior of plasmas.
- An important result of ideal MHD is the frozen-in theorem, which states that the magnetic field is frozen into the fluid and must move with it. This will be discussed in Section 8.2.

8.2 Flux freezing

An important consequence of the ideal MHD equations is Alfvén's flux freezing theorem. This states that the magnetic flux through an open surface moving with an ideal MHD plasma does not change in time. Stated another way, magnetic field lines move with an ideal MHD plasma. As we will see, a consequence is that ideal MHD does not allow for changes in magnetic topology.

Consider the magnetic flux through a surface, S ,

$$\Phi_S = \int_S \mathbf{B} \cdot \hat{\mathbf{n}} d^2x. \quad (106)$$

We will compute the change in Φ_S as the surface moves with the plasma and the field evolves according to Maxwell's equations,

$$\frac{d\Phi_S}{dt} = \int_{S(t)} \frac{\partial \mathbf{B}}{\partial t} \cdot \hat{\mathbf{n}} d^2x - \oint_{\partial S(t)} \mathbf{u} \times \mathbf{B} \cdot d\mathbf{l}. \quad (107)$$

The first term corresponds to the change in magnetic field at fixed position, while the second corresponds to the motion of the surface with velocity \mathbf{u} . For a proof of the above, we reference to Appendix C in [25] and Chapter 4 in [29]. Applying (105) and Stokes' theorem we obtain

$$\frac{d\Phi_S}{dt} = \int_{S(t)} \hat{\mathbf{n}} \cdot \left(\frac{\partial \mathbf{B}}{\partial t} + \nabla \times \mathbf{E} \right) d^2x. \quad (108)$$

Thus from (104b) we obtain $d\Phi_S/dt = 0$: the magnetic flux is conserved in the frame moving with the plasma.

Consider a flux tube, a volume such that magnetic field lines lie tangent to its boundary surface. Consider two non-intersecting surfaces S_1 and S_2 cutting through the flux tube, as represented in Figure 20, and the volume V of the flux tube delimited by S_1 and S_2 . We now demonstrate that the flux through a surface slicing through the flux tube, Φ_S , is independent of the choice of surface. Since $\nabla \cdot \mathbf{B} = 0$ from (104c), then Gauss's law yields

$$0 = \int_V \nabla \cdot \mathbf{B} d^3x = \int_{S_1} \mathbf{B} \cdot \hat{\mathbf{n}} d^2x - \int_{S_2} \mathbf{B} \cdot \hat{\mathbf{n}} d^2x, \quad (109)$$

where the unit normals, $\hat{\mathbf{n}}$ are chosen to be oriented in the same direction for both surface integrals. There is no contribution from the sides of the flux tube, as the field lines are tangent to this surface. As it holds for any choice of bounding surfaces, then for a given flux tube we conclude that Φ_S across a surface S cutting through the flux tube is independent of the choice of surface.

Furthermore, the flux-freezing theorem implies that the flux through a given flux tube, Φ_S , does not change with time. This leads to the well-known result that ideal MHD plasmas do not

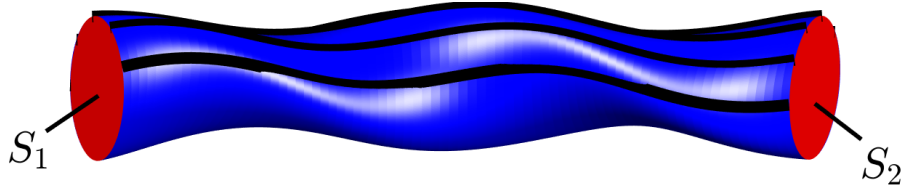
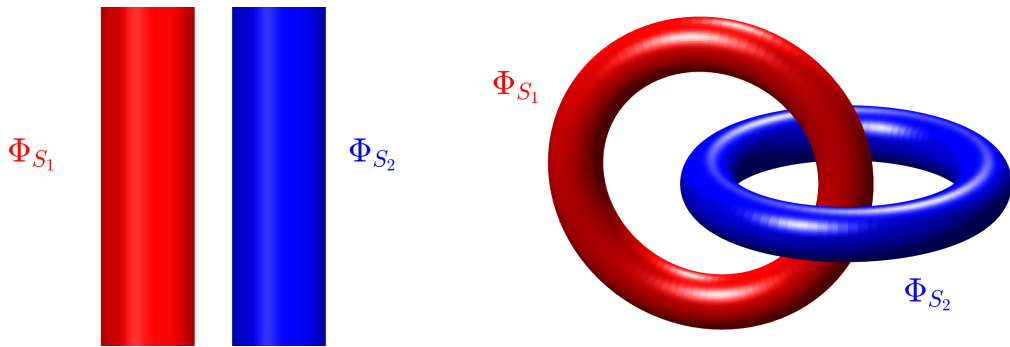


Figure 20: A flux tube is shown (blue) on which field lines lie (black). The magnetic flux through the flux tube can be computed with any any surface as shown in (109).



(a) Two flux tubes which are initially adjacent cannot merge under ideal MHD evolution, as their fluxes, Φ_{S_1} and Φ_{S_2} , must be preserved. (b) Two flux tubes which are initially linked cannot break under ideal MHD evolution, as their fluxes, Φ_{S_1} and Φ_{S_2} , must be preserved.

allow changes in topology. A first example consists of two neighboring flux tubes with fluxes Φ_1 and Φ_2 : under ideal MHD evolution, it is impossible for these two flux tubes to merge into one, as this would result in a single flux tube with flux $\Phi_1 + \Phi_2$ (see Figure 21a). A second example consists of two flux tubes that are initially linked to each other: as the flux through each tube must be preserved, the tubes cannot break and must remain linked (see Figure 21b). This can apply to the topology of a field line itself: we can imagine shrinking a flux tube down to a single field line, then the number of times this field line links another field line cannot change under ideal MHD evolution. It is in this sense that the topology of magnetic field lines is fixed under ideal MHD evolution. These considerations will be discussed in the application to 3D equilibrium models in Section 11.

8.3 Ideal MHD equilibrium

We now consider the ideal MHD equations under the assumption of static ($\mathbf{u} = 0$) equilibrium ($\partial/\partial t = 0$). This limit is of interest when considering time scales longer than MHD time scales and when typical flow velocities, $|\mathbf{u}|$, are expected to be smaller than the sound speed, $c_s = \sqrt{\gamma p/\rho}$.

The conservation of momentum density (102) shows that the plasma pressure gradient balances electro-magnetic forces,

$$\mathbf{J} \times \mathbf{B} = \nabla p. \quad (110)$$

The equilibrium fields must also satisfy,

$$\nabla \times \mathbf{B} = \mu_0 \mathbf{J} \quad (111a)$$

$$\nabla \cdot \mathbf{B} = 0. \quad (111b)$$

For magnetic confinement fusion, the resulting non-linear system of PDEs (110)-(111) is often solved in a toroidal domain Ω .

The force balance condition (110) is often considered under the assumption that $p(\psi)$, where ψ is a flux surface label (see Section 6.3). Under these assumptions, (110) implies that $\mathbf{J} \cdot \nabla \psi = 0$, such that streamlines of both the current density and magnetic field line on surfaces of constant ψ .

The resulting equations in axisymmetry are described in the following Section 8.4, and further details about computing 3D MHD equilibria will be discussed in Sections 10 and 11.

8.4 MHD equilibrium in a tokamak: Grad-Shafranov

We now consider the MHD equilibrium equations under the assumption of axisymmetry (see Section 7.3). We will find that (110)-(111) can be reduced to a two-dimensional, non-linear PDE.

We begin with a convenient expression for the magnetic field in terms of the poloidal flux function ψ_P , discussed in Section 7.6.1,

$$\mathbf{B} = -\nabla\phi \times \nabla\psi_P + B_\phi \hat{\phi}, \quad (112)$$

and the current can be computed using Ampere's law (111a),

$$\mu_0 \mathbf{J} = -R\nabla \cdot \left(\frac{\nabla\psi_P}{R^2} \right) \hat{\phi} + \nabla(RB_\phi) \times \nabla\phi. \quad (113)$$

Here the vector identity $\nabla \cdot (\mathbf{a} \times \mathbf{b}) = \mathbf{b} \cdot \nabla \times \mathbf{a} - \mathbf{a} \cdot \nabla \times \mathbf{b}$ is used to compute the toroidal component of \mathbf{J} . We next note that the toroidal component of the magnetic field can be expressed in terms of the poloidal current, $I_P(\psi_P)$. Here $2\pi I_P(\psi_P)$ is the current through a surface, $S_P(\psi_P)$, lying in the plane $Z = 0$ and bounded by the ψ_P surface,

$$\begin{aligned} 2\pi I_P(\psi_P) &= \int_{S_P(\psi_P)} \mathbf{J} \cdot \hat{\mathbf{n}} \, d^2x \\ &= \int_0^{2\pi} \int_0^{R(\psi_P)} R \mathbf{J} \cdot \hat{\mathbf{Z}} \, dR d\phi \\ &= 2\pi R B_\phi. \end{aligned} \quad (114)$$

The surface $S_P(\psi_P)$ used to compute the poloidal current is described in Figure 23. Therefore, in a tokamak, the vector unknowns, \mathbf{B} and \mathbf{J} , can be expressed in terms of the scalar unknown, $\psi_P(R, Z)$,

$$\mathbf{B} = -\nabla\phi \times \nabla\psi_P + I_P(\psi_P) \nabla\phi \quad (115a)$$

$$\mathbf{J} = \frac{1}{\mu_0} \left(-R\nabla \cdot \left(\frac{\nabla\psi_P}{R^2} \right) \hat{\phi} - \nabla\phi \times \nabla I_P(\psi_P) \right). \quad (115b)$$

Given this form for \mathbf{B} and \mathbf{J} , dotting $\nabla\psi_P$ into the MHD equilibrium force balance equation (110) results in the Grad-Shafranov equation,

$$R^2 \nabla \cdot \left(\frac{\nabla\psi_P}{R^2} \right) = -\mu_0 R^2 \frac{dp(\psi_P)}{d\psi_P} - I_P(\psi_P) \frac{dI_P(\psi_P)}{d\psi_P}. \quad (116)$$

Often the notation $\Delta^* \psi_P = R^2 \nabla \cdot (R^{-2} \nabla \psi_P)$ is used. The Grad-Shafranov equation (116) is solved in a toroidal domain $\Omega \subset \mathbb{R}^3$, bounded by a flux surface with poloidal flux function $\psi_{P0} \in \mathbb{R}$. By prescribing the constant Dirichlet boundary condition $\psi_P = \psi_{P0}$ on $\partial\Omega$, we fix the boundary to be the flux surface of label ψ_{P0} . This is a non-linear elliptic PDE for $\psi_P(R, Z)$, since ψ_P is independent of ϕ . Thus solving (116) provides the shape of the flux surfaces $\psi_P(R, Z)$ bounded by the ψ_{P0} surface. Generally, the flux functions $p(\psi_P)$ and $I_P(\psi_P)$ are given. In other words, given the shape of the outer boundary, we want to find the shape of the inner flux surfaces with specified pressure and current profiles. Once ψ_P is determined, the magnetic field is known from (115a).

For more details about the Grad-Shafranov equation, see Chapter 7 of [37] and Chapter 6 of [25]. For a discussion of computational methods for the Grad-Shafranov equation, see Chapter 4 in [51].

8.5 Summary

Under various sets of hypotheses, the ideal MHD equations can be reduced to simpler models. Common reduced models are gathered in the following Table.

	Ideal MHD	MHD Equilibrium	Grad-Shafranov
Hyp.	$\partial \mathbf{E} / \partial t = 0$ Low frequency/long wavelength 3D	$\mathbf{u} = 0$ $\partial / \partial t = 0$ 3D	MHD equilibrium $\partial / \partial \phi = 0$ 2D (R, Z)
PDE model	$\frac{\partial \rho}{\partial t} + \nabla \cdot (\rho \mathbf{u}) = 0$ $\rho \left(\frac{\partial}{\partial t} + \mathbf{u} \cdot \nabla \right) \mathbf{u} = \mathbf{J} \times \mathbf{B} - \nabla p$ $\left(\frac{\partial}{\partial t} + \mathbf{u} \cdot \nabla \right) \left(\frac{p}{\rho^\gamma} \right) = 0$ $\nabla \times \mathbf{B} = \mu_0 \mathbf{J}$ $\nabla \times \mathbf{E} = -\frac{\partial \mathbf{B}}{\partial t}$ $\nabla \cdot \mathbf{B} = 0$ $\mathbf{E} + \mathbf{u} \times \mathbf{B} = 0$	$\mathbf{J} \times \mathbf{B} = \nabla p$ $\nabla \times \mathbf{B} = \mu_0 \mathbf{J}$ $\nabla \cdot \mathbf{B} = 0$	Given $I_P(\psi_P)$ and $p(\psi_P)$, $\nabla \cdot \left(\frac{\nabla \psi_P}{R^2} \right) = -\mu_0 p'(\psi_P)$ $-\frac{I_P(\psi_P)}{R^2} I_P'(\psi_P)$
Unkn.	$\rho, \mathbf{u}, p, \mathbf{B}$	\mathbf{B}, p	$\psi_P(R, Z)$
with	\mathbf{E} function of \mathbf{B}, \mathbf{u} \mathbf{J} function of \mathbf{B}	\mathbf{J} function of \mathbf{B}	$\mathbf{B} = I_P(\psi_P) \nabla \phi - \nabla \phi \times \nabla \psi_P$ $\mathbf{J} = -\frac{1}{\mu_0} \left(\nabla \phi \times \nabla I_P(\psi_P) \right. \\ \left. + R^2 \nabla \cdot \left(\frac{\nabla \psi_P}{R^2} \right) \nabla \phi \right)$

9 Magnetic coordinates

As magnetic coordinates are a specific form of flux coordinates, see Section 6.4, we assume again the existence of flux surfaces. To construct magnetic coordinates, it is also assumed that $\nabla \cdot \mathbf{B} = 0$, which holds for any physical magnetic field. A special property of magnetic coordinates with poloidal angle ϑ and toroidal angle φ is that field lines appear straight in the ϑ - φ plane. The slope of the field lines is given by the rotational transform,

$$\iota = \frac{\mathbf{B} \cdot \nabla \vartheta}{\mathbf{B} \cdot \nabla \varphi} = \frac{d\vartheta}{d\varphi} \Big|_{\text{along field line}}. \quad (117)$$

Magnetic coordinates are constructed from general flux coordinates in Section 9.1, leading to the desired contravariant form. The covariant representation is simplified under the assumption of MHD equilibrium in Section 9.2. A special form of magnetic coordinates, called Boozer coordinates, is introduced in Section 9.3.

9.1 Contravariant form

Magnetic coordinates can be constructed from a general flux coordinate system (ψ, θ, ϕ) where $\psi = \Psi_T / 2\pi$ is the toroidal flux label (see Section 6.3), θ is any poloidal angle, and ϕ is any toroidal angle, as follows. As $\mathbf{B} \cdot \nabla \psi = 0$, the magnetic field can be written in the contravariant form as:

$$\mathbf{B} = B^\phi \frac{\partial \mathbf{r}}{\partial \phi} + B^\theta \frac{\partial \mathbf{r}}{\partial \theta}, \quad (118)$$

(B^ϕ, B^θ) being the toroidal and poloidal contravariant components of the field. Requiring that $\nabla \cdot \mathbf{B} = 0$, the following condition must hold,

$$0 = \frac{1}{\sqrt{g}} \left(\frac{\partial(B^\phi \sqrt{g})}{\partial \phi} + \frac{\partial(B^\theta \sqrt{g})}{\partial \theta} \right), \quad (119)$$

where $\sqrt{g} = (\nabla \psi \times \nabla \theta \cdot \nabla \phi)^{-1}$. Here $B^\theta \sqrt{g}$ and $B^\phi \sqrt{g}$ can be written in terms of some functions $A(\psi, \theta, \phi)$, $C(\psi, \theta, \phi)$, $j(\psi)$, and $h(\psi)$ such that,

$$B^\phi \sqrt{g} = A(\psi, \theta, \phi) + j(\psi), \quad (120a)$$

$$B^\theta \sqrt{g} = C(\psi, \theta, \phi) + h(\psi). \quad (120b)$$

As each of the contravariant components and the Jacobian must be periodic in θ and ϕ , so must $A(\psi, \theta, \phi)$ and $C(\psi, \theta, \phi)$. Defining the function λ as,

$$\lambda(\psi, \theta, \phi) = - \int_0^\phi C(\psi, \theta, \phi') d\phi', \quad (121)$$

then from (119), we must have that

$$A(\psi, \theta, \phi) = \frac{\partial \lambda(\psi, \theta, \phi)}{\partial \theta} \quad (122a)$$

$$C(\psi, \theta, \phi) = - \frac{\partial \lambda(\psi, \theta, \phi)}{\partial \phi}. \quad (122b)$$

So \mathbf{B} can be written as,

$$\mathbf{B} = \nabla \psi \times \nabla (j(\psi)\theta - h(\psi)\phi + \lambda(\psi, \theta, \phi)), \quad (123)$$

using the relation between basis vectors (Table 2) and noting that $\nabla q = (\partial q / \partial \theta) \nabla \theta + (\partial q / \partial \phi) \nabla \phi + (\partial q / \partial \psi) \nabla \psi$ for any q . As we noted that $C(\psi, \theta, \phi)$ and $A(\psi, \theta, \phi)$ are periodic in the two angle, so must $\lambda(\psi, \theta, \phi)$.

We can now compute the toroidal flux using (79) and (123),

$$\Psi_T = 2\pi \int_0^\psi j(\psi') d\psi', \quad (124)$$

so $j(\psi) = 1$, since by definition of the toroidal flux label we have $\psi = \Psi_T / 2\pi$. Similarly for the poloidal flux defined in (80) we obtain

$$\Psi_P = 2\pi \int_0^\psi h(\psi') d\psi', \quad (125)$$

so from the definition of ι (78) we see that $h(\psi) = \iota(\psi)$. We can now define the new magnetic coordinates: let $\vartheta = \theta + \lambda$ and $\varphi = \phi$, then it is clear that

$$\mathbf{B} = \nabla \psi \times \nabla \vartheta - \iota(\psi) \nabla \psi \times \nabla \varphi, \quad (126)$$

and therefore we obtain the defining characteristic of magnetic coordinates (117): $\iota(\psi) = \mathbf{B} \cdot \nabla \vartheta / \mathbf{B} \cdot \nabla \varphi$, and so the field lines are straight in the coordinates $(\psi, \vartheta, \varphi)$.

9.2 Covariant form

The magnetic field can also be written in the basis of the gradients of the magnetic coordinates $(\psi, \vartheta, \varphi)$, the covariant form,

$$\mathbf{B} = B_\psi \nabla \psi + B_\vartheta \nabla \vartheta + B_\varphi \nabla \varphi. \quad (127)$$

To find the expressions for B_ϑ , B_φ , and B_ψ , we substitute (127) into Ampere's law (13),

$$\mu_0 \mathbf{J} = \nabla B_\vartheta \times \nabla \vartheta + \nabla B_\varphi \times \nabla \varphi + \nabla B_\psi \times \nabla \psi. \quad (128)$$

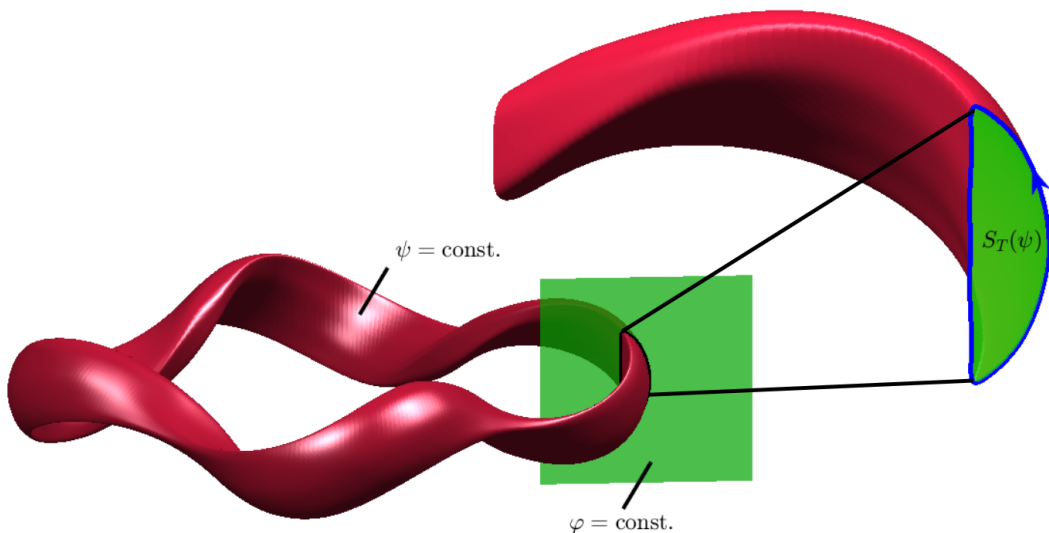


Figure 22: The integration curve at $\varphi = \text{const.}$ and $\psi = \text{const.}$ (black) encloses the surface $S_T(\psi)$ (green) through which the toroidal current is integrated.

Assuming an MHD equilibrium with $p(\psi)$ (110) so that $\mathbf{J} \cdot \nabla\psi = 0$ and taking the dot product of \mathbf{J} with $\nabla\psi$ it follows that,

$$\mu_0 \sqrt{g} \mathbf{J} \cdot \nabla\psi = \frac{\partial B_\varphi}{\partial \vartheta} - \frac{\partial B_\vartheta}{\partial \varphi} = 0. \quad (129)$$

Consider a curve at constant φ and ψ . The surface enclosed by this curve is denoted by $S_T(\psi)$, shown in Figure 22. From Ampere's law (13),

$$\mu_0 I_T(\psi) = \mu_0 \int_{S_T(\psi)} \mathbf{J} \cdot \hat{\mathbf{n}} d^2x = \oint_{\partial S_T(\psi)} \mathbf{B} \cdot d\mathbf{l} = \int_0^{2\pi} B_\vartheta d\vartheta, \quad (130)$$

where we have used $d\mathbf{l} = (\partial\mathbf{r}/\partial\vartheta) d\vartheta$. The requirement that I_T be a flux function comes from integration of (129) with respect to ϑ , noting that B_φ must be periodic with respect to ϑ .

Now consider a curve at constant ϑ and ψ . The surface enclosed by this curve is denoted by $S_P(\psi)$, shown in in Figure 23. The current passing through this surface is computed from Ampere's law,

$$\mu_0 I_P(\psi) = \mu_0 \int_{S_P(\psi)} \mathbf{J} \cdot \hat{\mathbf{n}} d^2x = \oint_{\partial S_P(\psi)} \mathbf{B} \cdot d\mathbf{l} = \int_0^{2\pi} B_\varphi d\varphi, \quad (131)$$

where we have used $d\mathbf{l} = (\partial\mathbf{r}/\partial\varphi) d\varphi$.

Here I_P is the poloidal current outside the $\vartheta = \text{const.}$ surface, including contributions from the plasma current outside the ψ surface and any coil current that passes through the center of the torus. The requirement that I_P be a flux function comes from integration of (129) with respect to φ , noting that B_ϑ must be periodic with respect to φ . In general, we can write B_φ and B_ϑ in terms of the flux functions, $I_T(\psi)$ and $I_P(\psi)$,

$$B_\vartheta = \frac{\mu_0 I_T(\psi)}{2\pi} + H_1(\psi, \vartheta, \varphi) \quad (132a)$$

$$B_\varphi = \frac{\mu_0 I_P(\psi)}{2\pi} + H_2(\psi, \vartheta, \varphi), \quad (132b)$$

Here we have separated out the components of B_ϑ and B_φ that are averaged over the angles (from (130) and (131)) from the components that depend on the angles.

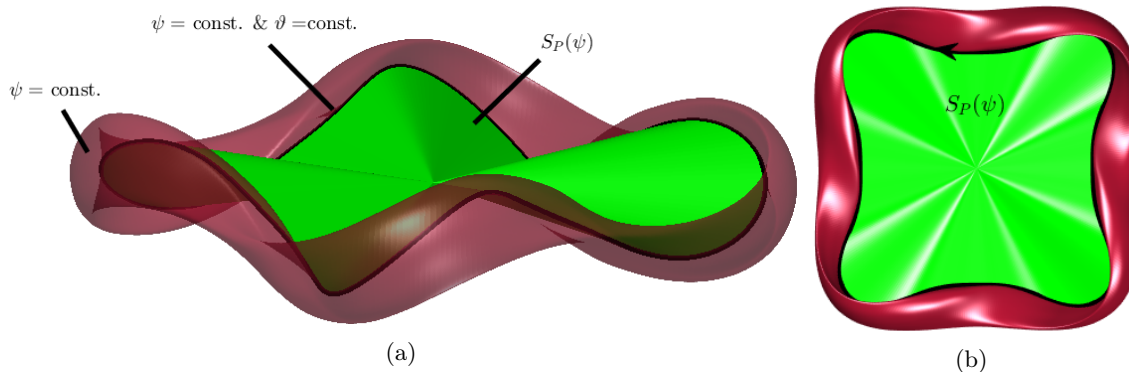


Figure 23: The integration curve at $\vartheta = \text{const.}$ and $\psi = \text{const.}$ (black) encloses the surface $S_P(\psi)$ (green) through which the poloidal current is integrated.

According to (129), we must have

$$H_1(\psi, \vartheta, \varphi) = \frac{\partial H(\psi, \vartheta, \varphi)}{\partial \vartheta} \quad (133a)$$

$$H_2(\psi, \vartheta, \varphi) = \frac{\partial H(\psi, \vartheta, \varphi)}{\partial \varphi}. \quad (133b)$$

where

$$H(\psi, \vartheta, \varphi) = \int_0^{\vartheta} H_1(\psi, \vartheta', \varphi) d\vartheta'. \quad (134)$$

We can furthermore define $K(\psi, \vartheta, \varphi)$ in the following way,

$$B_\psi = K(\psi, \vartheta, \varphi) + \frac{\partial H(\psi, \vartheta, \varphi)}{\partial \psi}. \quad (135)$$

So, the covariant form of an equilibrium magnetic field is

$$\mathbf{B} = I(\psi)\nabla\vartheta + G(\psi)\nabla\varphi + K(\psi, \vartheta, \psi)\nabla\psi + \nabla H(\psi, \vartheta, \varphi), \quad (136)$$

where $G(\psi) = \mu_0 I_P(\psi)/2\pi$ and $I(\psi) = \mu_0 I_T(\psi)/2\pi$. Additional details regarding magnetic coordinates can be found in Chapter 6 of [20] and Section 2 of [36].

9.3 Boozer coordinates

Boozer coordinates are magnetic coordinates; thus flux surfaces are assumed to exist and the condition (104c) is assumed. In addition, the MHD equilibrium force balance condition (110) is assumed to hold. Boozer coordinates are constructed such that the magnetic field has a simple form when expanded in the basis of the gradients of the coordinates, ∇x_i for $x_i = \{\psi, \vartheta_B, \varphi_B\}$, the covariant form. This specific choice of magnetic coordinates are especially useful for some applications, as will be discussed further in Section 12.1. The angles ϑ_B and φ_B are chosen such that the magnetic field can be written in the following way,

$$\mathbf{B} = I(\psi)\nabla\vartheta_B + G(\psi)\nabla\varphi_B + K(\psi, \vartheta_B, \varphi_B)\nabla\psi. \quad (137)$$

Comparing with the general covariant form for magnetic coordinates of equilibrium fields (136), we see that the Boozer angles must be chosen such that H vanishes.

We can also write the field in the contravariant form, expanded in the basis of the partial derivatives of the position vector with respect to the coordinates, $\partial\mathbf{r}/\partial x_i$

$$\mathbf{B} = \sqrt{g}^{-1} \iota \frac{\partial\mathbf{r}(\psi, \vartheta_B, \varphi_B)}{\partial\vartheta_B} + \sqrt{g}^{-1} \frac{\partial\mathbf{r}(\psi, \vartheta_B, \varphi_B)}{\partial\varphi_B}, \quad (138)$$

which follows from the expression for magnetic coordinates (126). The expression for the Jacobian, $\sqrt{g} = (\nabla\psi \times \nabla\vartheta_B \cdot \nabla\varphi_B)^{-1}$, can be obtained by dotting (137) with (138),

$$\sqrt{g}(\psi, \vartheta_B, \varphi_B) = \frac{G(\psi) + \iota(\psi)I(\psi)}{B^2}. \quad (139)$$

Thus, all components of the magnetic field are described by five scalar quantities: $I(\psi)$, $G(\psi)$, $\iota(\psi)$, $K(\psi, \vartheta_B, \varphi_B)$, and $B(\psi, \vartheta_B, \varphi_B)$.

Note that an assumption implied by writing the magnetic field in Boozer coordinates is that the radial current, $\mathbf{J} \cdot \nabla\psi$, vanishes. This can also be seen by applying Ampere's law to the covariant form (137). This is one of the conditions implied by the MHD equilibrium force balance equation (110) assuming $p(\psi)$. The other equations of MHD equilibrium (111) were also used in arriving at these results.

Boozer coordinates are especially useful for stellarators, as quasisymmetric magnetic fields exhibit a symmetry in this coordinate system. This results from the fact that Boozer coordinates have a particularly simple covariant form such that B_{φ_B} and B_{ϑ_B} are flux functions, and the Jacobian only varies on a surface due to the field strength. Therefore, confinement properties can be seen by simply considering the symmetry of the field strength.

Boozer coordinates are discussed in Section 6.6 of [20] and Section 2.5 of [36].

9.3.1 Radial covariant component

We now obtain an expression for the radial covariant component, K , by applying the MHD equilibrium force balance condition.

Consider the MHD equilibrium condition with flux surfaces for a given pressure profile $p(\psi)$,

$$(\nabla \times \mathbf{B}) \times \mathbf{B} = \mu_0 \nabla p(\psi). \quad (140)$$

Using the covariant form of \mathbf{B} to evaluate the curl, and its contravariant form when taking the cross product, we get,

$$\left(\frac{dI}{d\psi} \nabla\psi \times \nabla\vartheta_B + \frac{dG}{d\psi} \nabla\psi \times \nabla\varphi_B + \nabla K \times \nabla\psi \right) \times \left(\nabla\psi \times \nabla\vartheta_B - \iota(\psi) \nabla\psi \times \nabla\varphi_B \right) = \mu_0 \frac{dp}{d\psi} \nabla\psi. \quad (141)$$

From the vector identity $(\mathbf{A} \times \mathbf{B}) \times (\mathbf{C} \times \mathbf{D}) = \mathbf{C}(\mathbf{A} \times \mathbf{B} \cdot \mathbf{D}) - \mathbf{D}(\mathbf{A} \times \mathbf{B} \cdot \mathbf{C})$ and multiplying through by the Jacobian, \sqrt{g} , we find,

$$\iota(\psi) \frac{\partial K}{\partial \vartheta_B}(\psi, \vartheta_B, \varphi_B) + \frac{\partial K}{\partial \varphi_B}(\psi, \vartheta_B, \varphi_B) = \sqrt{g}(\psi, \vartheta_B, \varphi_B) \mu_0 \frac{dp}{d\psi}(\psi) + \frac{dG}{d\psi}(\psi) + \iota(\psi) \frac{dI}{d\psi}(\psi). \quad (142)$$

We now seek the solution K of this partial differential equation (142) in terms of a Fourier series in (ϑ_B, φ_B) . For well-posedness, we require that the average of the right hand side of (142) over ϑ_B and φ_B vanishes,

$$\frac{G(\psi) + \iota(\psi)I(\psi)}{B_0^2} \mu_0 \frac{dp}{d\psi}(\psi) + \frac{dG}{d\psi}(\psi) + \iota(\psi) \frac{dI}{d\psi}(\psi) = 0, \quad (143)$$

where $B_0^{-2}(\psi) = (2\pi)^{-2} \int_0^{2\pi} \int_0^{2\pi} B^{-2}(\psi, \vartheta_B, \varphi_B) d\vartheta_B d\varphi_B$.

On the right hand side of (142), for fixed ψ , only \sqrt{g} is a function of ϑ_B and φ_B . Moreover, since $\sqrt{g}(\psi, \vartheta_B, \varphi_B) = (G(\psi) + \iota(\psi)I(\psi))/B^2(\psi, \vartheta_B, \varphi_B)$ and B must be bounded and periodic in both angles, we can write B^{-2} as a Fourier series such that,

$$B^{-2}(\psi, \vartheta_B, \varphi_B) = B_0^{-2}(\psi) + \sum_{m,n,mn \neq 0} b_{m,n} e^{i(m\vartheta_B - n\varphi_B)}, \quad (144)$$

where the coefficients $\{b_{m,n}\}_{(m,n) \in \mathbb{Z}^2, mn \neq 0}$ are complex numbers.

We write the Fourier expansion of K as

$$K(\psi, \vartheta_B, \varphi_B) = \mathcal{K}(\psi) + \sum_{m,n,mn \neq 0} a_{m,n} e^{i(m\vartheta_B - n\varphi_B)}, \quad (145)$$

and from (142)-(143) the Fourier coefficients satisfy

$$\forall(m, n) \in \mathbb{Z}^2 \text{ such that } mn \neq 0, a_{m,n} i(\iota(\psi)m - n) = \mu_0(G(\psi) + \iota(\psi)I(\psi)) \frac{dp}{d\psi}(\psi) b_{m,n}. \quad (146)$$

When $\iota(\psi)$ is irrational, (146) uniquely defines the coefficients $\{a_{m,n}\}_{(m,n) \in \mathbb{Z}^2, mn \neq 0}$, whereas when $\iota(\psi) = n_0/m_0$ is rational the corresponding Fourier coefficient a_{m_0, n_0} is free while (146) imposes an extra constraint on the right hand side, namely $(dp(\psi)/d\psi)b_{m_0, n_0} = 0$ ($G + \iota I$ can never vanish, as this implies that $\sqrt{g} = 0$). In both cases, the solution K to (142) can now be written as :

$$K(\psi, \vartheta_B, \varphi_B) = \mathcal{K}(\psi) + \sum_{m,n, mn \neq 0} \left(i\mu_0 \frac{dp}{d\psi} \frac{G + \iota I}{n - \iota m} b_{m,n} + \Delta_{mn} \delta(n - \iota m) \right) e^{i(m\vartheta_B - n\varphi_B)}, \quad (147)$$

where δ is the Dirac delta function and the Δ_{mn} are arbitrary constants. When $\iota(\psi)$ is irrational, $\delta(n - \iota m) = 0$ so K is independent of the Δ_{mn} 's. On the other hand, when $\iota(\psi) = n_0/m_0 \in \mathbb{Q}$, K depends on the additional free parameter Δ_{m_0, n_0} . Moreover, since the denominator, $n - \iota m$, vanishes when $\iota(\psi) = m_0/n_0$, there exists a $1/x$ type singularity unless we also require $(dp(\psi)/d\psi)b_{m_0, n_0} = 0$. These singularities will be discussed further in Section 10.3.

9.4 Summary

Below we include a Table which summarizes the important properties of magnetic and Boozer coordinate systems.

	Magnetic	Boozer
Assumptions	$\nabla \cdot \mathbf{B} = 0$	$\nabla \cdot \mathbf{B} = 0$ $\mathbf{J} \cdot \nabla \psi = 0$
Contravariant	$\mathbf{B} = \nabla \psi \times \nabla \vartheta - \iota(\psi) \nabla \psi \times \nabla \varphi$	$\mathbf{B} = \nabla \psi \times \nabla \vartheta_B - \iota(\psi) \nabla \psi \times \nabla \varphi_B$
Covariant	$\mathbf{B} = B_\vartheta(\psi, \vartheta, \varphi) \nabla \vartheta + B_\varphi(\psi, \vartheta, \varphi) \nabla \varphi$ $+ B_\psi(\psi, \vartheta, \varphi) \nabla \psi$	$\mathbf{B} = I(\psi) \nabla \vartheta_B + G(\psi) \nabla \varphi_B$ $+ K(\psi, \vartheta_B, \varphi_B) \nabla \psi$ $G(\psi) = \mu_0 I_P(\psi) / 2\pi$ $I(\psi) = \mu_0 I_T(\psi) / 2\pi$
Jacobian	$\sqrt{g} = \frac{B_\varphi(\psi, \vartheta, \varphi) + \iota(\psi) B_\vartheta(\psi, \vartheta, \varphi)}{B^2}$	$\sqrt{g} = \frac{G(\psi) + \iota(\psi) I(\psi)}{B^2}$

10 Challenges associated with 3D equilibrium fields

Under the assumption of axisymmetry, there are only two non-trivial spacial variables. Without this assumption, a physical system is therefore said to be 3D. As we will see, the resulting loss of a conserved quantity has important implications, namely that the existence of continuously nested equilibrium flux surfaces is no longer guaranteed. This is particularly important for devices such as stellarators which rely on equilibrium magnetic fields that lie on closed nested surfaces.

Sections 10.1-10.2 consider questions related to the existence of surfaces in 2D and 3D. The equations of motion which follow magnetic field line trajectories in a toroidal system can be cast as a Hamiltonian system. Using the concept of integrability, the existence of flux surfaces arises as a fundamental consequence of the Hamiltonian nature of the system under specific assumptions. Finally, Section 10.3 describes the implications, and potential complications, which can arise from presuming the existence of continuously nested magnetic surfaces in the calculation of 3D MHD equilibria. In spite of these challenges, Section 10.4 demonstrates the existence of 3D equilibrium solutions with magnetic surfaces by considering an asymptotic expansion near the magnetic axis.

10.1 From existence to non-existence of magnetic surfaces

In axisymmetric geometry, we will find that the equations describing the position of field lines possess a conserved quantity which implies that the field lines lie on surfaces. When axisymmetry

is broken, however, the conserved quantity may be lost leading to the possibility of non-existence of surfaces.

10.1.1 Analysis of the vector potential

To begin the discussion on the existence of surfaces, we will analyze the vector potential with and without the assumption of axisymmetry. Consider a coordinate system (r, θ, ϕ) , where θ is a poloidal angle, ϕ is a toroidal angle, and r labels toroidal nested surfaces, not necessarily flux surfaces. The vector potential is not uniquely defined since the addition of a curl-free component, the gradient of any scalar function, does not affect the value of $\mathbf{B} = \nabla \times \mathbf{A}$. The standard by which \mathbf{A} is chosen is called the gauge. The vector potential \mathbf{A} can generally be expressed in the (r, θ, ϕ) coordinate system as

$$\mathbf{A}(r, \theta, \phi) = \psi_1(r, \theta, \phi) \nabla \theta - \psi_2(r, \theta, \phi) \nabla \phi + \nabla g(r, \theta, \phi), \quad (148)$$

and we choose the scalar function g so that $\nabla g(r, \theta, \phi) = 0$, which yields the magnetic field,

$$\mathbf{B} = \nabla \psi_1 \times \nabla \theta - \nabla \psi_2 \times \nabla \phi. \quad (149)$$

The form of (149) is similar to that of magnetic coordinates except that surfaces of constant ψ_1 do not overlap with those of constant ψ_2 . This form for the magnetic field can be applied with or without the assumptions of surfaces. If we assume that surfaces of ψ_1 form closed, nested toroidal surfaces, then $2\pi\psi_1$ will denote the toroidal flux enclosed by a surface of constant ψ_1 . This can be seen by computing the toroidal flux using (79) with the flux coordinate system (ψ_1, θ, ϕ) ,

$$2\pi\psi_1 = \int_0^{\psi_1} \int_0^{2\pi} \frac{\mathbf{B} \cdot \nabla \phi}{\nabla \psi_1' \times \nabla \theta \cdot \nabla \phi} d\theta d\psi_1'. \quad (150)$$

Thus we will denote ψ_1 by ψ_T in analogy with (126). Similarly, we can denote ψ_2 by ψ_P , noting that $2\pi\psi_2$ is the poloidal flux enclosed by a surface of constant ψ_2 under the assumption of flux surfaces. This can be seen by computing the poloidal flux using (80) with the flux coordinate system (ψ_2, θ, ϕ) ,

$$2\pi\psi_2 = \int_0^{\psi_2} \int_0^{2\pi} \frac{\mathbf{B} \cdot \nabla \theta}{\nabla \psi_2' \times \nabla \theta \cdot \nabla \phi} d\phi d\psi_2'. \quad (151)$$

With $\psi_1 = \psi_T$ and $\psi_2 = \psi_P$ and the gauge defined above, the vector potential can now be expressed in the (ψ_T, θ, ϕ) system as,

$$\mathbf{A}(\psi_T, \theta, \phi) = \psi_T \nabla \theta - \psi_P(\psi_T, \theta, \phi) \nabla \phi. \quad (152)$$

In using this coordinate system, we have made the assumption that $\nabla \psi_T \times \nabla \theta \cdot \nabla \phi \neq 0$ in the domain of interest. This is equivalent to the assumption that $\mathbf{B} \cdot \nabla \phi \neq 0$ from (149).

In what follows, we will not be assuming that flux surfaces exist, but we will simply use the form of the vector potential given in (152) assuming that $\nabla \psi_T \times \nabla \theta \cdot \nabla \phi \neq 0$; in that case surfaces of constant ψ_T and ψ_P may not overlap to form a set of closed, nested, toroidal surfaces. However, for axisymmetry, each of the vector components of the vector potential must be independent of the toroidal angle, implying that $\partial \psi_P / \partial \phi = 0$. If this condition holds, then it follows from (149) that $\mathbf{B} \cdot \nabla \psi_P = \nabla \psi_T \times \nabla \theta \cdot \nabla \phi (\partial \psi_P / \partial \phi) = 0$. Under the assumption that ψ_P is differentiable, the level sets of ψ_P form surfaces except for at critical points where $\nabla \psi_P = 0$. We are not interested in solutions for which ψ_P is constant throughout a volume, as this implies that the poloidal component of the field, the second term in (149), vanishes. Thus the level sets of ψ_P form surfaces except at isolated points or lines. One example of such a line is the magnetic axis when it exists. We conclude that the magnetic field is tangent to surfaces of constant ψ_P . Under the assumption that the isosurfaces of ψ_P are closed and compact, the Poincaré-Hopf theorem implies that their topology is toroidal (see ch. 4 in [21]). Thus we conclude that a set of toroidal magnetic surfaces exists; these are the flux surfaces.

10.1.2 Variational principle for field line flow

While we have seen that axisymmetry implies the existence of surfaces by simply analyzing the vector potential in toroidal coordinates, as we will now see, this property turns out to be a consequence of the Hamiltonian nature of field line flow. Thus we will arrive at the same conclusion by considering the equations of field line flow as a Hamiltonian system.

We begin by showing that field lines obey equations of motion which can be derived from a variational principle analogous to Hamilton's principle in classical mechanics. The equation of motion describing the position of a field line, \mathbf{r} , parameterized by distance along a field line, l , is given by,

$$\hat{\mathbf{b}}(l) = \frac{d\mathbf{r}(l)}{dl}. \quad (153)$$

We will show that this equation of motion can be obtained from a variational principle involving the following functional,

$$W[\mathbf{r}] := \int \mathbf{A}(\mathbf{r}(l)) \cdot \frac{d\mathbf{r}(l)}{dl} dl, \quad (154)$$

where \mathbf{A} is the vector potential (8). The first variation of $W[\mathbf{r}]$ reads,

$$\begin{aligned} \delta W[\mathbf{r}; \delta \mathbf{r}] &= \int \mathbf{A}(\delta \mathbf{r}(l)) \cdot \frac{d\mathbf{r}(l)}{dl} + \mathbf{A}(\mathbf{r}(l)) \cdot \frac{d\delta \mathbf{r}(l)}{dl} dl \\ &= \int \delta \mathbf{r}(l) \cdot \left(\nabla \mathbf{A} \cdot \frac{d\mathbf{r}(l)}{dl} - \frac{d\mathbf{r}(l)}{dl} \cdot \nabla \mathbf{A} \right) dl, \end{aligned} \quad (155)$$

where the second line is obtained by integration by parts, using the boundary condition $\mathbf{A} \cdot \delta \mathbf{r} = 0$ at the endpoints of the trajectory and applying the notation $\nabla = \partial/\partial \mathbf{r}$. We use the vector identity $(\nabla \times \mathbf{A}) \times \mathbf{B} = (\mathbf{B} \cdot \nabla) \mathbf{A} - (\nabla \mathbf{A}) \cdot \mathbf{B}$ to obtain the following condition,

$$(\nabla \times \mathbf{A}) \times \frac{d\mathbf{r}(l)}{dl} = 0, \quad (156)$$

which implies that $d\mathbf{r}/dl$ is parallel to $\hat{\mathbf{b}}$ since $\mathbf{B} = \nabla \times \mathbf{A}$. Furthermore, $d\mathbf{r}(l)/dl$ is a unit vector by definition, thus we recover the equation of motion describing a field line (153).

10.1.3 Relation to Hamiltonian dynamics

We now demonstrate explicitly the connection between Hamiltonian mechanics and the variational principle for field line flow by casting the latter as a Hamiltonian system.

We express the functional W defined by (153) along a trajectory \mathbf{r} , expressed in toroidal coordinates (ψ_T, θ, ϕ) and parametrized by l , as follows:

$$W[\mathbf{r}] = \int \left(\mathbf{A}(\mathbf{r}(l)) \cdot \frac{\partial \mathbf{r}(\theta(l))}{\partial \theta} \frac{d\theta(l)}{dl} + \mathbf{A}(\mathbf{r}(l)) \cdot \frac{\partial \mathbf{r}(\phi(l))}{\partial \phi} \frac{d\phi(l)}{dl} \right) dl. \quad (157)$$

From the assumption that (ψ_T, θ, ϕ) is a coordinate system, then $\mathbf{B} \cdot \nabla \phi \neq 0$ so field lines can be parametrized by ϕ . Hence $(d\theta/dl)dl = (d\theta/d\phi)d\phi$ and $(d\phi/dl)dl = d\phi$. With the expression of the vector potential (152) we can then write

$$W[\psi_T, \theta] = \int \left(\psi_T(\phi) \frac{d\theta(\phi)}{d\phi} - \psi_P(\psi_T(\phi), \theta(\phi), \phi) \right) d\phi. \quad (158)$$

This is analogous to (30) where (θ, ψ_T, ϕ) correspond to $(\mathbf{q}, \mathbf{p}, t)$, and ψ_P corresponds to H .

The resulting Euler-Lagrange equations are given by,

$$\frac{d\theta(\phi)}{d\phi} = \frac{\partial \psi_P(\theta(\phi), \psi_T(\phi), \phi)}{\partial \psi_T} \quad (159a)$$

$$\frac{d\psi_T(\phi)}{d\phi} = - \frac{\partial \psi_P(\theta(\phi), \psi_T(\phi), \phi)}{\partial \theta}. \quad (159b)$$

Thus, by analogy with (33), if ψ_P does not depend explicitly on ϕ , meaning the system is axisymmetric, then ψ_P is a constant of the motion from (34),

$$\frac{d\psi_P(\theta(\phi), \psi_T(\phi), \phi)}{d\phi} = 0. \quad (160)$$

In an axisymmetric system, field lines are therefore confined to surfaces of constant ψ_P . Thus magnetic surfaces exist. Further discussion of the Hamiltonian nature of field line flow can be found in many references [16, 13, 23, 36].

10.2 Integrability of a Hamiltonian system

We have seen that the behavior of magnetic field lines can be described by a Hamiltonian system, and we will now employ the framework of Hamiltonian dynamics to understand the fundamental challenges associated with the behavior of magnetic field lines in 3D, that is, without the assumption of axisymmetry. The properties, which follow from the Hamiltonian nature of the system, have important implications for stellarator physics and the existence of continuously nested flux surfaces. This is particularly relevant for finding MHD equilibria in 3D, as the assumption of the existence of surfaces leads to several consequences which will be discussed in Section 10.3.

10.2.1 Defining integrability

If a system is not integrable, some trajectories of the Hamiltonian are ergodic, meaning they may eventually fill out a finite volume of phase space rather than being confined to surfaces. In the context of field line flow, this implies that in a non-integrable system, some field lines do not lie on toroidal surfaces. We will define the concept of integrability in a generic way before considering the application to magnetic fields in 3D.

To begin, we define precisely a Hamiltonian system as follows. We consider coordinates and momenta $\mathbf{q} \in \mathbb{R}^N$, $\mathbf{p} \in \mathbb{R}^N$; the space $\mathbb{R}^N \times \mathbb{R}^N$ is referred to as the phase space. The space spanned by $(\mathbf{q}(t), \mathbf{p}(t))$ satisfying Hamilton's equations (33) is denoted by $M \in \mathbb{R}^N \times \mathbb{R}^N$. Let the Hamiltonian $H(\mathbf{q}, \mathbf{p}, t)$ be a real scalar function. A trajectory is defined as a solution $t \mapsto (\mathbf{q}(t), \mathbf{p}(t))$ to Hamilton's equations.

Consider any scalar function F of $(\mathbf{q}, \mathbf{p}, t)$. The time derivative of this function along the trajectory $(\mathbf{q}(t), \mathbf{p}(t))$ is given by,

$$\frac{dF(\mathbf{q}(t), \mathbf{p}(t), t)}{dt} = \{F(\mathbf{q}(t), \mathbf{p}(t), t), H\} + \frac{\partial F(\mathbf{q}(t), \mathbf{p}(t), t)}{\partial t}, \quad (161)$$

where $\{f, g\}$ is the Poisson bracket which will be defined subsequently in a local coordinate system. This is obtained by simply applying the chain rule and Hamilton's equations.

In a small neighbourhood of any point of M there are local coordinates $q_1 \dots q_N$ and $p_1 \dots p_N$ such that,

$$\{f, g\} = \sum_{i=1}^N \left(\frac{\partial f}{\partial q_i} \frac{\partial g}{\partial p_i} - \frac{\partial f}{\partial p_i} \frac{\partial g}{\partial q_i} \right), \quad (162)$$

where q_i and p_i , which we call respectively the canonical coordinate and canonical momentum. The Poisson bracket satisfies several algebraic properties which are discussed in detail in [58].

For $i = 1, \dots, N$, each conjugate pair (q_i, p_i) corresponds to one degree of freedom (dof). A $2N$ dimensional system has N conjugate pairs and can thus be described by an N -dof Hamiltonian.

A quantity, $I(\mathbf{q}(t), \mathbf{p}(t), t)$, is said to be a constant of the motion if $dI/dt = 0$: I is a conserved quantity along any trajectory. Two functions f and g are said to be in involution if,

$$\{f, g\} = 0, \quad (163)$$

meaning that they commute. An autonomous Hamiltonian system (where H does not depend explicitly on time) with N -degrees of freedom is then said to be integrable if there exist N independent, smooth constants of the motion, $\{I_i\}_{1 \leq i \leq N}$, which are in involution. This implies that the constants of motion are independent in the sense that none of the I_i can be expressed as a function of the other $(N - 1)$. An integrable Hamiltonian system means that solutions can be found by evaluating integrals of known functions from a given set of initial conditions. Integrable systems exhibit regular motion meaning that trajectories are confined to N different surfaces of

dimension $2N - 1$ in a $2N$ dimensional phase space, defined by the constants of motion. It can be shown that these surfaces are N -tori under the assumption that the phase space M is compact and connected [9]; thus they are often referred to as invariant tori. In the context of axisymmetric field line flow, which is an integrable 1-dof Hamiltonian (159), only one constant of the motion is required to guarantee integrability. As the Hamiltonian, ψ_P , is one such constant, it is sufficient, and magnetic field lines are thus confined to lie on invariant tori.

Integrability can be similarly defined for non-autonomous Hamiltonian systems (H depends explicitly on time). The procedure involves extending the non-autonomous Hamiltonian to a higher dimensional autonomous one for which integrability can be defined as above [8, 67]. A non-autonomous Hamiltonian system with N -dof can also be shown to be integrable if there exist N , possibly time-dependent, constants of the motion [14].

In the following Sections, we limit our attention to the Hamiltonian associated with field line flow. With the correspondence (θ, ψ_T, ϕ) to $(\mathbf{q}, \mathbf{p}, t)$, and ψ_P to H , we have seen that, with axisymmetry, the magnetic field line flow corresponds to a 1-dof Hamiltonian system. In 3D, since $d\psi_p/d\phi \neq 0$, the field line flow Hamiltonian becomes non-autonomous. In the literature, this is sometimes referred to as a 1.5-dof Hamiltonian. Therefore, as we will see, in 3D systems, integrability of the field line flow is no longer guaranteed, as the Hamiltonian is not a constant of the motion.

10.2.2 Hamilton-Jacobi method

As we are interested in the 1-dof field line flow Hamiltonian, for the remaining discussion, we limit our consideration to 1-dof autonomous and non-autonomous Hamiltonian systems. However the subsequent discussion regarding non-integrability can be generalized to higher dimensional systems.

One approach to solving the equations of motion (33), known as the Hamilton-Jacobi method [58, 76, 30], involves the use of canonical transformations to find ignorable coordinates, meaning that the Hamiltonian is independent of this coordinate. Stated precisely, a canonical transformation is a diffeomorphism, $\varphi : (q, p) \in M \rightarrow (Q(q, p), P(q, p)) \in M$ which preserves the Poisson bracket such that $\{f(q, p), g(q, p)\} = \{\tilde{f}(Q, P), \tilde{g}(Q, P)\}$ where $\tilde{f}(Q(q, p), P(q, p)) = f(q, p)$ and similarly for \tilde{g} . In particular, both the mapping and its inverse are smooth and differentiable, ensuring it is possible to transform from one set of phase space coordinates to another.

Our goal is to choose a transformed coordinate system in which the motion becomes very simple.

We start by assuming that a generating function $S(q, P, t) : \mathbb{R}^3 \rightarrow \mathbb{R}$ and a coordinate transformation $(q, p) \rightarrow (Q, P)$ satisfy,

$$p(t) = \frac{\partial S(q(t), P(t), t)}{\partial q} \quad (164a)$$

$$Q(t) = \frac{\partial S(q(t), P(t), t)}{\partial P}. \quad (164b)$$

Hamilton's equations (33) can then be expressed in the transformed coordinates

$$\frac{dP(t)}{dt} = -\frac{\partial K(Q(t), P(t), t)}{\partial Q} \quad (165a)$$

$$\frac{dQ(t)}{dt} = \frac{\partial K(Q(t), P(t), t)}{\partial P}, \quad (165b)$$

where the new Hamiltonian is

$$K(Q, P, t) := H(q(Q, P, t), p(Q, P, t), t) + \frac{\partial S(q(Q, P, t), P, t)}{\partial t}. \quad (166)$$

It can be shown that (165) is equivalent to (33).

In order to find such a generating function $S(q, P, t)$, for a desired new Hamiltonian K , we consider (166) as the non-linear Hamilton-Jacobi equation in S ,

$$H\left(q, \frac{\partial S(q, P, t)}{\partial q}, t\right) + \frac{\partial S(q, P, t)}{\partial t} = K\left(\frac{\partial S(q, P, t)}{\partial P}, P, t\right). \quad (167)$$

This is a first order PDE for $S(q, P, t)$ in q , P , and t .

We make a particular choice of canonical transformation under the assumption of an autonomous system which exhibits periodic motion, either p is periodic in q or both p and q are periodic in time with the same frequency. This transformation, known as action-angle variables, has a particularly simple form: the momentum becomes constant in time while the position coordinate grows linearly. Moreover, the new Hamiltonian becomes independent of Q . We will first discuss the action-angle variables, in order to apply them to the field line flow system under the assumption of axisymmetry, as the momentum ψ_T is periodic in the coordinate θ .

From the assumption that the new momentum is constant, $\dot{P} = 0$, we conclude that K is independent of Q from (165b). Under the assumption that \dot{Q} is a constant of the motion, we can conclude from (165a) that $\partial K/\partial P$ is only a function of P , which is itself a constant of the motion. As any function of only t can be added to K without consequence to Hamilton's equations (165), we therefore seek a new Hamiltonian which depends on only the new momentum, $K(P)$. Furthermore, we note that for an autonomous system the Hamiltonian is a constant of the motion, so it can be expressed as a function of P alone which we denote $E(P)$. From (167) we find the generating function satisfies

$$\frac{\partial S(q, P, t)}{\partial t} = K(P) - E(P). \quad (168)$$

We are free to choose the generating function such that $E(P) = K(P)$; thus we can express it in the functional form $S(q, P, t) = W(q, P)$.

We will now define a choice for P such that the Hamiltonian becomes a function of P alone. The new momentum, often called the action variable, is defined as,

$$P = \frac{1}{2\pi} \oint p dq = \frac{1}{2\pi} \oint p(t) \frac{dq(t)}{dt} dt. \quad (169)$$

The integral is computed along a trajectory $(p(t), q(t))$ for a single period of the motion. Hence P is constant along a trajectory as it only depends on $H(q(t), p(t)) = E$, a constant of the motion for an autonomous system. The action-angle coordinate transformation is obtained from the following generating function,

$$S(q, P, t) = \int_0^q p(q', P) dq', \quad (170)$$

where the integral is computed at constant P along a trajectory. Hamilton's equations in the canonical coordinates (165) therefore become,

$$\frac{dP}{dt} = 0 \quad (171a)$$

$$\frac{dQ}{dt} = \frac{\partial K(P)}{\partial P} = \omega(P), \quad (171b)$$

where $\omega(P)$ can be interpreted as a constant angular frequency. Solving the ODE to obtain an explicit expression for Q , it is apparent that the new coordinate changes linearly with time,

$$Q(t) = Q_0 + \omega(P)t, \quad (172)$$

where Q_0 is a constant of integration associated with the initial condition of the trajectory. We can note that Q can be interpreted as an angle by computing the change in this coordinate, ΔQ , during one period of the motion,

$$\Delta Q = \oint \frac{\partial Q}{\partial q} dq = \frac{\partial}{\partial P} \oint \frac{\partial S(q, P, t)}{\partial q} dq = \frac{\partial}{\partial P} \oint p dq = 2\pi. \quad (173)$$

Therefore we expect many physical properties to be 2π periodic in Q .

The field line flow Hamiltonian system is integrable under the assumption of axisymmetry, as it is an autonomous system with 1-dof and there exists one constant of the motion, (160). Furthermore, the momentum, ψ_T , is periodic in the coordinate, θ . Thus there exists a transformation into action-angle coordinates for this system. The action integral for the field line flow Hamiltonian system is given by,

$$P = \frac{1}{2\pi} \int_0^{2\pi} \psi_T(\psi_P, \theta) d\theta = \frac{1}{2\pi} \oint \mathbf{A}(\mathbf{r}) \cdot d\mathbf{r}. \quad (174)$$

The integration is performed at constant ψ_P along a closed poloidal loop. Here we have used (152) such that $\psi_T = \mathbf{A} \cdot \partial \mathbf{r} / \partial \theta$. Upon application of Stokes' theorem, we see that P is related to the magnetic flux through S_T , a surface enclosed by the isosurface of ψ_P at constant toroidal angle,

$$P = \frac{1}{2\pi} \int_{S_T} \mathbf{B} \cdot \hat{\mathbf{n}} d^2x. \quad (175)$$

Therefore $P = (1/2\pi)\Psi_T$, the toroidal flux function. By a similar argument we note that $\psi_P = (1/2\pi)\Psi_P$, the poloidal flux function.

The action-angle transformation allows us to write the Hamiltonian as a function of P alone, which we denote $\overline{\psi}_P(P)$. Since the angle satisfies $dQ/t = \partial \overline{\psi}_P(P) / \partial P$, the equation of motion for the canonical coordinate is given by (165b),

$$\frac{dQ}{dt} = \frac{\partial \overline{\psi}_P(P)}{\partial P} = \frac{d\psi_P(\psi_T)}{d\psi_T} = \iota(\psi_T), \quad (176)$$

where $\iota(\psi_T)$ is the rotational transform (78), a constant of the motion. Thus the canonical coordinate, Q , increases linearly with the toroidal angle,

$$Q(\phi) = Q_0 + \iota(\psi_T)\phi. \quad (177)$$

We note that Q can be interpreted as a poloidal angle, as the quantity $(\theta - \iota\phi)$ is constant along a field line. Thus Q_0 is a constant which labels a field line.

The contours of ψ_P , the conserved quantity, define invariant tori in the system's phase space on which all motion is confined. The magnetic field line trajectories thus lie on concentric tori, yielding the continuously nested flux surfaces.

10.2.3 Perturbations about integrability

Many Hamiltonian systems are, in fact, non-integrable. In the absence of axisymmetry the Hamiltonian of the field line flow system, ψ_P , is no longer independent of ϕ and thus non-autonomous. In particular, there may not exist a solution by the Hamilton-Jacobi method such that $\dot{\mathbf{P}} = 0$ as required for action-angle coordinates, since this implies that there exist N independent constants of the motion and therefore the Hamiltonian is integrable.

Although many physical systems are not integrable, the need for analytic tractability led historically to the development of a perturbation theory approach [58, 24]. A Hamiltonian is described as nearly integrable if it can be constructed as a perturbation series about an autonomous integrable Hamiltonian, $H_0(q, p)$, for which there exists a canonical transformation to the action-angle coordinates (Q_0, P_0) . The corresponding generating function is then denoted $S^*(q, P_0)$ and the transformed Hamiltonian $H_0(P_0)$. We seek a canonical transformation from (Q_0, P_0) to (Q, P) , as in (167), for the perturbed Hamiltonian such that

$$H \left(Q_0(Q, P, t), \frac{\partial S(Q_0(Q, P, t), P, t)}{\partial Q_0}, t \right) + \frac{\partial S(Q_0(Q, P, t), P, t)}{\partial t} = K(Q, P, t). \quad (178)$$

Formally, the perturbed Hamiltonian and generating function expressed in the unperturbed action-angle coordinates are expanded with respect to $\epsilon \ll 1$ as follows,

$$H(Q_0, P_0, t) = H_0(P_0) + \sum_{i=1}^{\infty} \epsilon^i H_i(Q_0, P_0, t) \quad (179a)$$

$$S(Q_0, P, t) = \sum_{i=0}^{\infty} \epsilon^i S_i(Q_0, P, t). \quad (179b)$$

Assuming that H can be written as (179a), if there exists S_i for all $i \geq 1$, satisfying (178), such that the perturbation series (179b) for S converges, then the perturbed Hamiltonian H is nearly integrable and the corresponding nearly integrable system has a solution. Our goal is to obtain conditions under which the motion remains periodic although there is a perturbation away from integrability.

Recall that, for the canonical transformation associated with action-angle coordinates, the generating function is chosen such that $\dot{P} = 0$ and $\dot{Q} = \omega(P)$: the momentum is constant while

the coordinates change linearly with time. As we saw, this transformation provided insight into periodic motion. While the action-angle transformation assumes an autonomous Hamiltonian, this assumption is not satisfied for the field line flow Hamiltonian without axisymmetry.

We now aim to obtain a different coordinate transformation under which the motion becomes very simple: we seek a generating function, $S(Q_0, P, t)$ such that both \dot{Q} and \dot{P} vanish. The constant coordinate and momentum can be determined from the initial conditions of the problem. Thus the generating function (164) provides a mapping from the initial conditions and time to the old coordinates. Together $\dot{Q} = 0$ and $\dot{P} = 0$ imply that both $\partial K/\partial Q$ and $\partial K/\partial P$ vanish. Such a transformation implies $K(Q, P, t)$ depends only on t . Observing that the equations of motion remain invariant under the addition of any function of only t to $K(Q, P, t)$, we seek a transformation such that $K = 0$. The lowest orders of the perturbation series obtained from the Hamiltonian-Jacobi equation (178) combined with (179) read,

$$H_0 \left(\frac{\partial S_0(Q_0, P, t)}{\partial Q_0} \right) + \frac{\partial S_0(Q_0, P, t)}{\partial t} + \epsilon \frac{\partial H_0(P_0)}{\partial P_0} \frac{\partial S_1(Q_0, P, t)}{\partial Q_0} + \epsilon H_1 \left(Q_0, \frac{\partial S_0(Q_0, P, t)}{\partial Q_0}, t \right) + \epsilon \frac{\partial S_1(Q_0, P, t)}{\partial t} + \mathcal{O}(\epsilon^2) = 0. \quad (180)$$

The $\mathcal{O}(\epsilon^0)$ terms provide the following equation for S_0 ,

$$H_0 \left(\frac{\partial S_0(Q_0, P, t)}{\partial Q_0} \right) + \frac{\partial S_0(Q_0, P, t)}{\partial t} = 0. \quad (181)$$

In other words, $S_0(Q_0, P, t)$ provides a coordinate transformation from (Q_0, P_0) to (Q, P) such that the new Hamiltonian is zero; therefore Q and P are invariants with respect to H_0 as in (161).

The $\mathcal{O}(\epsilon^1)$ terms provide an equation for S_1 given S_0 and H_1 ,

$$\omega_0 \frac{\partial S_1(Q_0, P, t)}{\partial Q_0} + H_1 \left(Q_0, \frac{\partial S_0(Q_0, P, t)}{\partial Q_0}, t \right) + \frac{\partial S_1(Q_0, P, t)}{\partial t} = 0, \quad (182)$$

since $\partial H_0(P_0)/\partial P_0 = \dot{Q}_0 = \omega_0$, which is the canonical unperturbed frequency.

We consider a perturbed Hamiltonian that is periodic in Q_0 , the unperturbed angle, and in time,

$$H_1(Q_0, P, t) = \sum_{m,n} H_1^{m,n}(P) e^{i(mQ_0 - nt)}. \quad (183)$$

This assumption is justified for the field line flow Hamiltonian, as we note that Q_0 and time (ϕ) are poloidal and toroidal angles, respectively from (177). The Hamiltonian for this system, ψ_P , is one of the covariant components of the vector potential (152). Thus any physically relevant Hamiltonian is doubly periodic in t and Q_0 .

We now attempt to construct a solution by expressing $S_1(Q_0, P, t)$ as a Fourier series in (Q_0, t) :

$$S_1(Q_0, P, t) = \sum_{m,n} S_1^{m,n}(P) e^{i(mQ_0 - nt)}. \quad (184)$$

Inserting these expressions into (182) we obtain

$$S_1(Q_0, P, t) = i \sum_{m,n} \left(\frac{H_1^{m,n}(P)}{m\omega_0 - n} + \Delta_{m,n} \delta(m - \omega_0 n) \right) e^{i(mQ_0 - nt)}. \quad (185)$$

As long as $\omega_0 \notin \mathbb{Q}$, then this solution is unique since the δ term is always zero. If $\omega_0 \in \mathbb{Q}$ then there exists an infinite set of solutions parameterized by the $\Delta_{m,n}$, and a series solution S_1 can only be expressed in the above form if $H_1^{m,n}(P) = 0$ for all $(m, n) \in \mathbb{Z}^2$ such that $\omega_0 = n/m$. In fact, the series (185) may diverge, even for $\omega_0 \in \mathbb{R} \setminus \mathbb{Q}$, if ω_0 is sufficiently well approximated by a rational number. We discuss some implications in the following Section. This is known as the problem of small divisors in classical mechanics perturbation theory and has been recognized since the time of Poincaré [58, 99]. In the context of the field line flow Hamiltonian, recall that $\omega_0 = \iota(\psi_P)$. The preceding results demonstrate that the magnetic field may not be integrable in the neighborhood of rational values of the rotational transform and thus these flux surfaces may not exist.

In order to construct a solution as a perturbation series, the $\mathcal{O}(\epsilon^n)$ terms provide equations for the corresponding S_n . In general, we do not expect a non-integrable system to be close enough to an integrable system to be represented as such a convergent perturbation series in ϵ . The following Section will discuss conditions under which a perturbative solution exists.

10.2.4 Persistence of some flux surfaces: KAM theory

In Section 10.2.1 we have seen that the non-existence of continuously nested flux surfaces in 3D MHD is a consequence of fundamental properties of the associated Hamiltonian system. That is not to say, however, that an infinitesimal deviation away from axisymmetry results in a complete loss of all flux surfaces. In this Section, we briefly describe the persistence of some surfaces, even in the presence of perturbations away from axisymmetry, which follows the results of Kolmogorov [55], Arnold [9], and Moser [77], known as KAM theory. We refer to several other sources [82, 30, 47].

We continue our discussion from Section 10.2.3, considering bounded, periodic motion of an integrable Hamiltonian with canonical frequency ω_0 . KAM theory addresses the question of which invariant surfaces persist as a perturbation is applied, quantified by non-zero values of ϵ in the expansion of H (179a). In the context of magnetic field line flow in a torus, the result identifies some conditions under which flux surfaces persist in the presence of perturbations away from integrability, or axisymmetry.

An invariant surface associated with frequency ω_0 is said to persist if it can be transformed continuously with ϵ into an invariant surface of the perturbed system for a frequency $\omega(\epsilon)$. While the perturbation may deform the invariant surface in phase space, the surfaces must be deformed continuously from the unperturbed invariant surfaces.

Assuming perturbations are sufficiently small ($\epsilon \ll 1$), for an invariant surface to persist, it is sufficient for the unperturbed frequency ω_0 to satisfy the Diophantine condition,

$$\exists(r, k) \in \mathbb{R}^+ \times \mathbb{N}, k \geq 2, \text{ s.t. } \forall(m, n) \in \mathbb{Z}^* \times \mathbb{Z}, \left| \omega_0 - \frac{n}{m} \right| > \frac{r}{m^k}. \quad (186)$$

This condition excludes regions surrounding each rational value of the frequency $\omega_0 = n/m$. For magnetic field lines, where ω_0 is ι , the condition (186) means that the rotational transform must be sufficiently irrational. Another sufficient condition is that the frequencies of the unperturbed Hamiltonian are non-degenerate,

$$\left| \frac{\partial \omega_0(P)}{\partial P} \right| > 0, \quad (187)$$

implying that there does not exist multiple unperturbed periodic orbits with the same frequency. In the context of magnetic field line flow, the magnetic shear, $d\iota(\psi_T)/d\psi_T$, cannot vanish at any point. As there are applications in which this assumption cannot be made, for example stellarators sometimes are designed to have small magnetic shear, a similar theory has been developed for degenerate systems [17, 76].

An important result of measure theory is that the set of frequencies satisfying the Diophantine condition (186) is of finite measure in \mathbb{R} , in the sense of Lebesgue. KAM theory implies that for a Hamiltonian system sufficiently close to integrability satisfying (187), a non-zero Lebesgue measure of the tori of the unperturbed Hamiltonian system survive. For non-axisymmetric magnetic fields satisfying the above conditions, this means that these invariant tori (i.e. flux surfaces) occupy a non-zero volume in phase space.

As the perturbation from integrability, ϵ , increases, invariant surfaces may break up. The trajectories of field lines may no longer lie on nested toroidal surfaces but instead fill an area on the Poincaré surface of Section or form magnetic island structures.

We will demonstrate by considering a model magnetic field given by,

$$\mathbf{B}(r, \theta, \phi) = \nabla r \times \nabla \theta - \nabla \chi(r, \theta, \phi) \times \nabla \phi, \quad (188)$$

where $\chi(r, \theta, \phi) = r^2/2(1 + \epsilon \cos(\theta - \phi))$. Here, considering the fixed curve defined by ($R_0 = 5$, $Z_0 = 0$), r is a radial coordinate measuring distance from the fixed curve within the poloidal plane, $\theta = \arctan((R - R_0)/(Z - Z_0))$ is a poloidal angle, and ϕ is the standard azimuthal angle. When $\epsilon = 0$, this magnetic field is integrable, lying on surfaces of constant r with rotational transform $\iota(r) = r$. When ϵ is non-zero, a non-axisymmetric perturbation is added that causes an island to form. When the perturbation is small, a large volume of magnetic surfaces remain. For larger values of ϵ , a large magnetic island near the $\iota = 1$ surface begins to develop. Poincaré surfaces of Section are shown in Figure 24 for several values of ϵ .

An important practical consequence of these results is that confinement is not completely destroyed upon an infinitesimal deviation away from axisymmetry, as necessarily occurs in all real tokamak and stellarator fusion devices. In closing we note that the existence of some flux surfaces

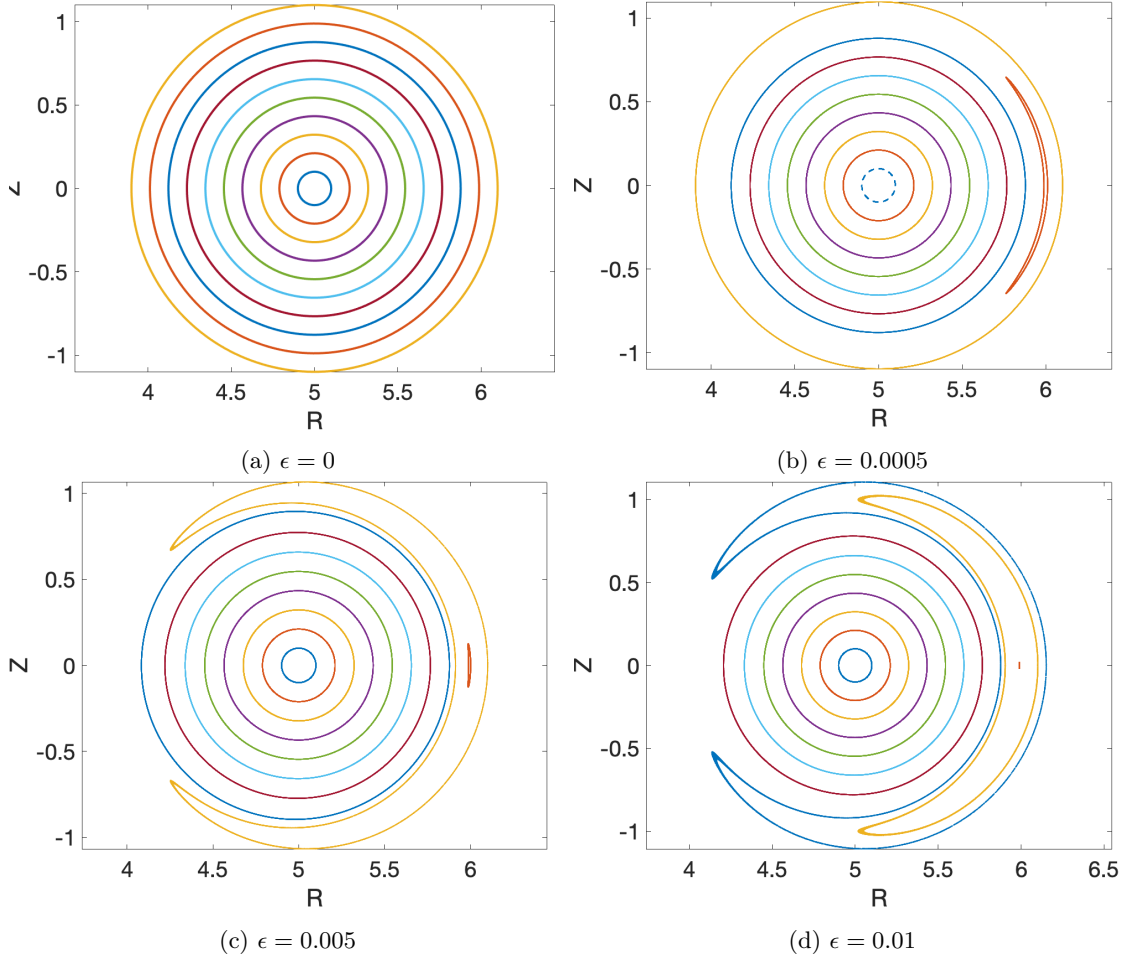


Figure 24: Poincaré surfaces of Section are shown for the model magnetic field (188) with several values of ϵ . Here magnetic field lines are followed in the model field, and when a field line hits a plane at constant toroidal angle ϕ , a mark is made with color indicating the field line.

(as shown above) is distinct from the existence of continuously nested flux surfaces (as occurs in axisymmetric magnetic fields). This behavior is a consequence of the Hamiltonian nature of the flow of static magnetic field lines, and is thus independent of choice of physical model used to describe the plasma itself. In seeking to use and develop models for plasma physics, it is therefore important to note the compatibility of imposed properties of the magnetic field with assumptions of the model. Next we discuss some implications in the context of 3D MHD equilibria.

10.3 Singularities and surface currents in 3D MHD

As we saw in Section 10.2, the existence or otherwise of magnetic surfaces in 3D ideal MHD is a direct consequence of the Hamiltonian nature of the system. In general 3D magnetic fields may not be integrable. Nonetheless, for computational tractability, the existence of magnetic surfaces is often assumed in 3D equilibrium calculations in order to apply a variational principle (see Sections 11.1 and 11.2). This assumption is also physically motivated, as 3D systems without magnetic surfaces do not have good confinement properties as described in Section 6.1; thus we are typically interested in configurations that possess a region with good flux surfaces.

Assuming the existence of continuously nested flux surfaces in 3D ideal MHD equilibria gives rise to two types of current density singularities, only one of which is eliminated upon integration to compute the physically observed quantity, the plasma current. That there remains a singularity in the current is unphysical. This is a fundamental challenge associated with constructing 3D MHD equilibria and has led to questions about the existence of smooth solutions to the 3D MHD, which remain unresolved [32]. The challenges described below will motivate the search for *non-smooth* pressure profiles as discussed in Section 11.5, which may circumvent the problem of unphysical

currents in 3D.

The manifestation of singular current densities at rational surfaces in 3D equilibria can be seen by evaluating the expression for the parallel current, $\mu_0 \mathbf{J} \cdot \mathbf{B} = (\nabla \times \mathbf{B}) \cdot \mathbf{B}$, using the Boozer covariant form (137) to evaluate the field,

$$\begin{aligned} \mu_0 \mathbf{J} \cdot \mathbf{B} &= (\nabla G \times \nabla \varphi_B + \nabla I \times \nabla \vartheta_B + \nabla K \times \nabla \psi) \cdot (G(\psi) \nabla \varphi_B + I(\psi) \nabla \vartheta_B + K(\psi, \vartheta_B, \varphi_B) \nabla \psi) \\ &= \sqrt{g}^{-1} \left(-G'(\psi) I(\psi) + I'(\psi) G(\psi) + \frac{\partial K(\psi, \vartheta_B, \varphi_B)}{\partial \varphi_B} I(\psi) - \frac{\partial K(\psi, \vartheta_B, \varphi_B)}{\partial \vartheta_B} G(\psi) \right). \end{aligned} \quad (189)$$

We now use the solution for the radial covariant component, K , obtained in Section 9.3.1 from the force balance condition, namely

$$K(\psi, \vartheta_B, \varphi_B) = \mathcal{K}(\psi) + \sum_{m,n,mn \neq 0} \left(i \mu_0 \frac{dp}{d\psi} \frac{G + \iota I}{n - \iota m} b_{m,n} + \Delta_{mn} \delta(n - \iota m) \right) e^{i(m\vartheta_B - n\varphi_B)}, \quad (190)$$

where $\mathcal{K}(\psi)$ and Δ_{mn} are constants on a surface ψ . Inserting this into (189), with $\sqrt{g}(\psi, \vartheta_B, \varphi_B) = (G(\psi) + \iota(\psi)I(\psi))/B^2(\psi, \vartheta_B, \varphi_B)$, we obtain

$$\begin{aligned} \mu_0 \mathbf{J} \cdot \mathbf{B} &= B^2 \left(\frac{I'(\psi)G(\psi) - G'(\psi)I(\psi)}{G + \iota I} \right) \\ &+ \sum_{m,n,mn \neq 0} \left(\mu_0 \frac{dp}{d\psi} \frac{B^2}{n - \iota m} b_{m,n} - i \frac{\Delta_{mn} \delta(n - \iota m)}{\sqrt{g}} \right) e^{i(m\vartheta_B - n\varphi_B)} (nI(\psi) + mG(\psi)). \end{aligned} \quad (191)$$

Defining $x = \iota(\psi) - n/m$ we can identify two singularities in the coefficient of the resonant Fourier harmonics, the n and m such that $x = 0$. These correspond to a $1/x$ and $\delta(x)$ -function singularity. The former gives rise to what is known as the Pfirsch-Schlüter current [36].

The current is the integral surface integral of the current density, \mathbf{J} , given by:

$$I = \int_S \mathbf{J} \cdot \hat{\mathbf{n}} d^2x. \quad (192)$$

Notice that the $1/x$ singularity associated with the Pfirsch-Schlüter current is still present in I : there remains after integration a logarithmic singularity in the current at $x = 0$ which is unphysical because this implies an infinite amount of charge moving through the surface per unit time. To avoid such unphysical currents, we can require that the coefficients associated with the $1/x$ term vanish. The quantity $n/mI(\psi) + G(\psi) = B^2(\psi, \vartheta_B, \varphi_B) \sqrt{g}(\psi, \vartheta_B, \varphi_B)$ cannot vanish, as this would imply that \sqrt{g} vanishes. So instead, we therefore can require that the product $b_{m,n} dp/d\psi$ vanishes.

One approach to obtaining 3D equilibria without these unphysical infinite currents is thus to avoid pressure gradients at rational surfaces. In this case, in analogy with the convergence of the Fourier series in Section 10.2.3, pressure gradients are thus prohibited not only exactly at rational surfaces, but also in nearby neighborhoods, at irrationals which recurrently approximate close to rationals, to avoid singularities in the sum (191), see [32]. Such a pressure profile, if it could be constructed, would therefore necessitate seemingly unnatural pressure gradients. We are not interested in configurations with uniform pressure, as confining a hot plasma surrounded by a vacuum region requires a pressure gradient. The challenges associated with constructing 3D MHD equilibria with continuously nested flux surfaces thus motivates alternative models which assume the existence of only some flux surfaces leading to discontinuous but globally non-uniform pressure profiles, see Sections 11.4 and 11.5.

Alternatively, in place of such seemingly unnatural profile, it has been shown that the $1/x$ singularity can be avoided by careful construction of the magnetic geometry such that the resonant $b_{m,n}$ terms vanish on rational surfaces [96, 100, 97]. While this approach is advantageous as it does not require flattening of the pressure profile, restricts the class of allowed boundaries of the MHD equilibria. It also requires a rotational transform close to a rational value and low shear (the rotational transform stays close to this rational value).

The $1/x$ current singularity is a manifestation of solving a magnetic differential equation (MDE) of the form

$$\mathbf{B} \cdot \nabla f = S, \quad (193)$$

for a prescribed source S and unknown periodic function f . The parallel current satisfies the following MDE, noting that $\nabla \cdot \mathbf{J} = 0$ and $\mathbf{J} = (J_{\parallel}/B)\mathbf{B} + \mathbf{J}_{\perp}$,

$$\mathbf{B} \cdot \nabla \left(\frac{J_{\parallel}}{B} \right) = -\nabla \cdot \mathbf{J}_{\perp}. \quad (194)$$

In order for the MDE to have a solution, we must have that the following integral vanish on all closed field lines,

$$\oint \frac{S}{B} dl = 0, \quad (195)$$

where l measures length along a field line. We cannot expect this condition to be satisfied for an arbitrary source S . Source functions which respect this constraint do not exhibit a $1/x$ singularity [20], and methods of correction of the source function have been proposed to enable solubility [46].

In addition to the Pfirsch-Schlüter current, recall the $\delta(x)$ -function singularity which, when integrated, produces a current sheet, a non-zero current supported on a surface. Since, on integration, the $\delta(x)$ -function current density yields a physically well-behaved, though discontinuous, current, the existence of current sheets in the equilibrium solutions is not generally considered to be problematic. Their existence near rational surfaces has been verified numerically in 3D equilibrium codes [65, 70].

The ideal MHD approximation yields a comparatively simple and tractable set of equations. Although in many applications this is sufficient as a first approximation to describe macroscopic, global behaviors, an important implication is that magnetic field lines are ‘frozen-in’ meaning that no topological changes of the field are permitted, see Section 8.2. The appearance of the singular currents is a direct consequence of the non-dissipative nature of ideal MHD. While 3D *ideal* MHD equilibria with surfaces are known to have possible current singularities, it should be noted that other MHD models do not suffer from such pathologies. For example, it is thought that a time-dependent MHD model which includes resistivity such that (105) is replaced by

$$\mathbf{E} + \mathbf{u} \times \mathbf{B} = \eta \mathbf{J}, \quad (196)$$

where η is the resistivity, could regularize the singular currents [88, 48]. Resistive MHD models are implemented in the M3D-C1 [52] and NIMROD codes [87].

Although ideal MHD is associated with the difficulties discussed in this Section, it remains the primary tool for determining stellarator equilibrium magnetic fields. In the following Section we will discuss a 3D equilibrium solution with magnetic surfaces obtained by analytic construction. In Section 11 we provide an overview of several 3D equilibrium models applied in numerical calculation.

10.4 Constructing 3D MHD equilibria near the magnetic axis

While computing general 3D MHD equilibria with surfaces is associated with difficulties, we will demonstrate a technique by which a class of solutions can be obtained for the vacuum field equations with surfaces near the magnetic axis. The calculation will be performed by asymptotic expansion. As a result, we obtain the expression for the rotational transform on the magnetic axis discussed in Section 7.6.

The magnetic axis \mathbf{r}_0 is parameterized by the length, l . The corresponding Frenet-Serret orthonormal basis introduced in Section 7.6 is denoted by $(\hat{\mathbf{e}}_1(l), \hat{\mathbf{e}}_2(l), \hat{\mathbf{e}}_3(l))$, and $(\rho, \vartheta) \in \mathbb{R}^+ \times [0, 2\pi)$ denote polar coordinates in the $\hat{\mathbf{e}}_2$ - $\hat{\mathbf{e}}_3$ plane. The position \mathbf{r} can then be expressed as:

$$\mathbf{r}(\rho, \vartheta, l) = \mathbf{r}_0(l) + \rho \cos(\vartheta) \hat{\mathbf{e}}_2(l) + \rho \sin(\vartheta) \hat{\mathbf{e}}_3(l). \quad (197)$$

In order to construct an orthogonal system, consider the angle $\omega = \vartheta + \int_0^l \tau(l') dl'$, where τ is the torsion of the magnetic axis (100). In the coordinate system (ρ, ω, l) the Jacobian is given by $\sqrt{g}(\rho, \omega, l) = \rho \left(1 - \kappa(l) \rho \cos \left(\omega - \int_0^l \tau(l') dl' \right) \right)$ where $\kappa(l) = |\hat{\mathbf{e}}_1(l) \cdot \nabla \hat{\mathbf{e}}_1(l)|$ is the magnitude of the curvature.

We seek a vacuum field solution (see Section 3.4) so \mathbf{B} is both divergence and curl free. From the curl-free condition we can represent the field by a scalar potential, $\mathbf{B} = \nabla \Phi(\mathbf{r})$. From the divergence-free condition the potential must satisfy Laplace’s equation, following Section 3.4,

$\Delta\Phi(\mathbf{r}) = 0$. Under the assumption that a field with continuously nested flux surfaces exists, the magnetic field can be described in terms of flux coordinates by a toroidal flux label ψ and a function which labels field lines, α , satisfying

$$\nabla\Phi(\mathbf{r}) = \nabla\psi(\mathbf{r}) \times \nabla\alpha(\mathbf{r}), \quad (198)$$

as described in Section 9, see (123). In order to build the vacuum magnetic field with surfaces, we now seek the unknown scalar functions Φ , ψ , and α . There is obviously no unique solution to this problem for two reasons: (1) each unknown can be defined up to an additive constant without altering (198), and (2) the right-hand side being bilinear in (ψ, α) , each of these two unknowns can be multiplied respectively by a constant and its inverse without altering the equation. This second point will be addressed through the constant μ defined below, by imposing that $\psi(\mathbf{r})$ be the toroidal flux label. The functions $\Phi(\mathbf{r})$ and $\alpha(\mathbf{r})$ need not be periodic functions of l and ω , while $\psi(\mathbf{r})$ must be periodic as it is related to the magnetic flux.

Expressed in our orthogonal coordinate system (ρ, ω, l) , (198) is equivalent to the following set of equations

$$\frac{1}{\rho} \left(\frac{\partial\psi}{\partial\rho} \frac{\partial\alpha}{\partial\omega} - \frac{\partial\psi}{\partial\omega} \frac{\partial\alpha}{\partial\rho} \right) = \frac{1}{h} \frac{\partial\Phi}{\partial l} \quad (199a)$$

$$\frac{1}{\rho h} \left(\frac{\partial\psi}{\partial\omega} \frac{\partial\alpha}{\partial l} - \frac{\partial\alpha}{\partial\omega} \frac{\partial\psi}{\partial l} \right) = \frac{\partial\Phi}{\partial\rho} \quad (199b)$$

$$\frac{1}{h} \left(\frac{\partial\psi}{\partial l} \frac{\partial\alpha}{\partial\rho} - \frac{\partial\alpha}{\partial l} \frac{\partial\psi}{\partial\rho} \right) = \frac{1}{\rho} \frac{\partial\Phi}{\partial\omega}, \quad (199c)$$

and Laplace's equation is expressed as

$$\frac{1}{h\rho} \frac{\partial}{\partial\rho} \left(h\rho \frac{\partial\Phi}{\partial\rho} \right) + \frac{1}{h\rho^2} \frac{\partial}{\partial\omega} \left(h \frac{\partial\Phi}{\partial\omega} \right) + \frac{1}{h} \frac{\partial}{\partial l} \left(\frac{1}{h} \frac{\partial\Phi}{\partial l} \right) = 0, \quad (200)$$

where $h(\rho, \omega, l) = 1 - \kappa(l)\rho \cos\left(\omega - \int_0^l \tau(l') dl'\right)$.

Rather than search for a general solution to (199)-(200), we focus on a local solution near the magnetic axis. To this end, we consider the following asymptotic series expansions in ρ ,

$$\Phi(\rho, \omega, l) = \Phi_{[0]}(\omega, l) + \Phi_{[1]}(\omega, l)\rho + \Phi_{[2]}(\omega, l)\rho^2 + \mathcal{O}(\rho^3) \quad (201a)$$

$$\psi(\rho, \omega, l) = \psi_{[2]}(\omega, l)\rho^2 + \mathcal{O}(\rho^3) \quad (201b)$$

$$\alpha(\rho, \omega, l) = \alpha_{[0]}(\omega, l) + \alpha_{[1]}(\omega, l)\rho + \mathcal{O}(\rho^2), \quad (201c)$$

where $\psi_{[0]} = 0$ as the magnetic flux vanishes on the magnetic axis, and $\psi_{[1]} = 0$ since we require that $\nabla\psi$ vanish on axis as it is a coordinate singularity.

The $\mathcal{O}(\rho^{-1})$ expression of (199c) gives

$$\frac{\partial\Phi_{[0]}}{\partial\omega} = 0. \quad (202)$$

Thus $\Phi_{[0]}$ is an unknown function of l only: $\Phi_{[0]}(l)$. From (198), this implies that the $\mathcal{O}(\rho^0)$ magnetic field strength on axis is $B_{[0]}(l) = \Phi'_{[0]}(l)$. The expression of (199b) to $\mathcal{O}(1)$ is

$$\Phi_{[1]} = 0. \quad (203)$$

The expression of (200) to $\mathcal{O}(1)$ is

$$4\Phi_{[2]} + \frac{\partial^2\Phi_{[2]}}{\partial\omega^2} + \frac{\partial^2\Phi_{[0]}}{\partial l^2} = 0, \quad (204)$$

then $\Phi_{[2]}$ can be expressed in terms of $\Phi_{[0]}$ as

$$\Phi_{[2]}(\omega, l) = -\frac{\Phi''_{[0]}(l)}{4} + \Phi_c(l) \cos(2u(\omega, l)) + \Phi_s(l) \sin(2u(\omega, l)), \quad (205)$$

where $u(\omega, l) = \omega - \int_0^l \tau(l') dl' + \delta(l)$ and $\delta(l)$, $\Phi_c(l)$, and $\Phi_s(l)$ are integration constants with respect to ω .

The expressions of (199c) to $\mathcal{O}(\rho)$ and (199a) to $\mathcal{O}(1)$ give

$$\frac{\partial \alpha_{[0]}}{\partial l} = -\frac{\partial \Phi_{[2]}}{\partial \omega} \frac{1}{2\psi_{[2]}} \quad (206a)$$

$$\frac{\partial \alpha_{[0]}}{\partial \omega} = \frac{\partial \Phi_{[0]}}{\partial l} \frac{1}{\psi_{[2]}}. \quad (206b)$$

By requiring that the mixed partial derivatives of $\alpha_{[0]}$ commute, we arrive at a PDE for $1/\psi_{[2]}$,

$$\frac{\partial}{\partial \omega} \left(\frac{\partial \Phi_{[2]}}{\partial \omega} \frac{1}{\psi_{[2]}} \right) + \frac{\partial}{\partial l} \left(\frac{\partial \Phi_{[0]}}{\partial l} \frac{1}{\psi_{[2]}} \right) = 0. \quad (207)$$

Expressed as a linear PDE for $\psi_{[2]}$ in terms of $\Phi_{[2]}$ and $\Phi_{[0]}$, subject to boundary conditions of periodicity in ω and l , a solution can be written

$$\psi_{[2]}(\omega, l) = \Phi'_{[0]}(l) \mu \left(e^{\eta(l)} \cos^2 u(\omega, l) + e^{-\eta(l)} \sin^2 u(\omega, l) \right), \quad (208)$$

for constants of integration $\eta(l)$ and μ .

Equation (207) also implies the following forms for $\Phi_s(l)$ and $\Phi_c(l)$,

$$\Phi_s(l) = \frac{\Phi'_{[0]}(l)(\delta'(l) - \tau(l))}{2} \tanh(\eta(l)) \quad (209a)$$

$$\Phi_c(l) = -\frac{\Phi'_{[0]}(l)\eta'(l)}{4}. \quad (209b)$$

Thanks to the expression of $\Phi_{[2]}$ (205) with the integration constants Φ_s (209a) and Φ_c (209b), together with the expression of $\psi_{[2]}$ (208), $\alpha_{[0]}$ can be computed from (206a) as

$$\alpha_{[0]}(\omega, l) = \bar{\alpha} + \frac{1}{2\mu} \arctan \left(e^{-\eta(l)} \tan u(\omega, l) \right) - \frac{1}{2\mu} \int_0^l \frac{\delta'(l') - \tau(l')}{\cosh(\eta(l'))} dl', \quad (210)$$

where $\bar{\alpha}$ is a constant of integration.

We can now fix the constant of integration, μ . We define, $\Psi_{[2]} = \rho^2 \psi_{[2]}$, the lowest order approximation of the toroidal flux label ψ . We use the flux coordinate system $(\Psi_{[2]}, \vartheta, l)$ to compute the toroidal flux from (79) using the lowest order magnetic field, $\nabla \Psi_{[2]} \times \nabla \alpha_{[0]}$,

$$\begin{aligned} 2\pi \Psi_{[2]} &= \int_0^{\Psi_{[2]}} \int_0^{2\pi} \frac{\nabla \Psi'_{[2]} \times \nabla \alpha_{[0]} \cdot \nabla l}{\nabla \Psi'_{[2]} \times \nabla \vartheta \cdot \nabla l} d\vartheta d\Psi'_{[2]} = \int_0^{\Psi_{[2]}} \int_0^{2\pi} \frac{\partial \alpha_{[0]}}{\partial \vartheta} \Big|_l d\vartheta d\Psi'_{[2]} \\ &= \frac{\Psi_{[2]}}{2\mu} \int_0^{2\pi} \frac{d\vartheta}{\cosh(\eta(l)) + \sinh(\eta(l)) \cos(2(\vartheta + \delta(l)))} = \frac{\pi \Psi_{[2]}}{\mu}. \end{aligned} \quad (211)$$

Thus we find $\mu = 1/2$. In the above expression, we have used (210) to compute $\partial \alpha_{[0]}/\partial \vartheta$ by expressing $\omega(\vartheta, l) = \vartheta + \int_0^l \tau(l') dl'$.

In consideration of (208), we see that at fixed l , the boundary of $\psi_{[2]}$ describes an ellipse, with major axis a and minor axis b satisfying,

$$a(\omega, l) = \sqrt{\frac{\Phi'_{[0]}(l)}{2}} e^{\eta(l)/2} \cos u(\omega, l) \quad (212a)$$

$$b(\omega, l) = \sqrt{\frac{\Phi'_{[0]}(l)}{2}} e^{-\eta(l)/2} \sin u(\omega, l). \quad (212b)$$

The quantity u measures the angle from the a axis, the area of the ellipse is $\pi \Phi'_{[0]}(l)/2$, and $e^{\eta(l)}$ is a measure of the ellipticity of the cross-sections of surfaces of constant flux. The quantity $\Phi'_{[0]}(l)$ is non-negative, as it is the $\mathcal{O}(\rho^0)$ magnetic field strength $B_{[0]}(l)$. As the angle with respect to the major axis is given by $u = \vartheta + \delta(l)$ and ϑ denotes an angle in the poloidal plane with respect to the curvature vector, $\delta(l)$ can be interpreted as the angle between the major axis of the ellipse and the curvature vector. The coordinate system is shown in Figure 25.

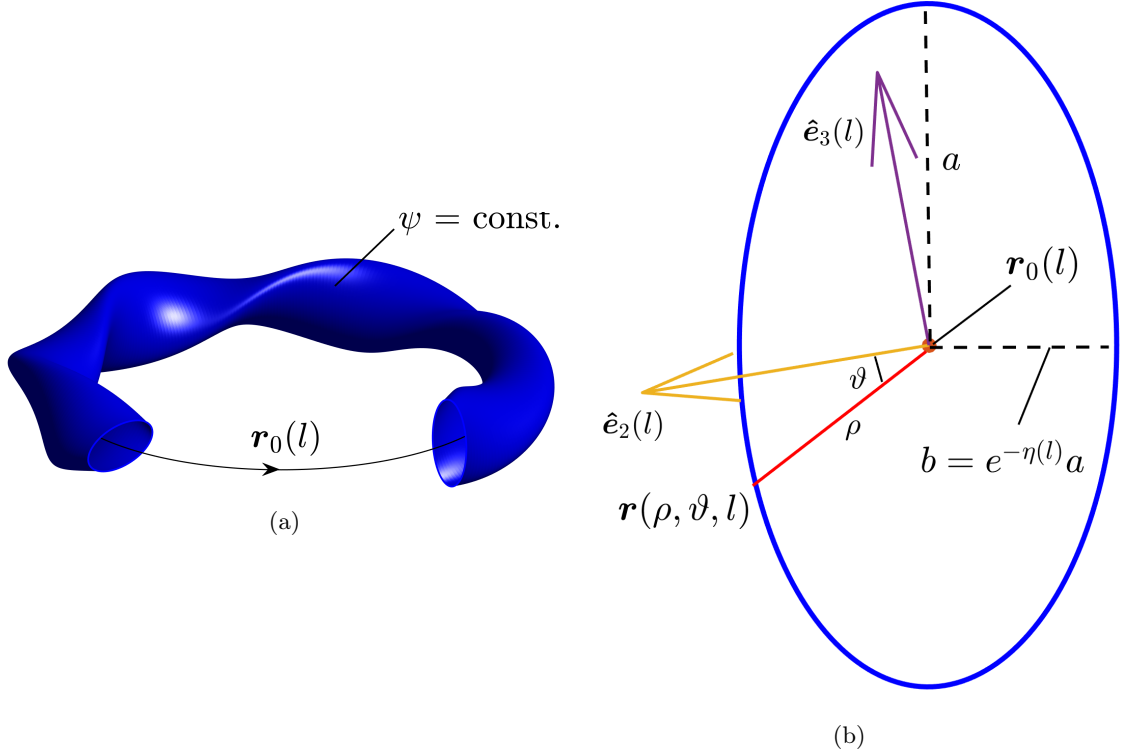


Figure 25: We consider a surface of constant ψ near the magnetic axis, $\mathbf{r}_0(l)$ (a). The cross-section of such a surface in the plane spanned by $\hat{\mathbf{e}}_1(l)$ and $\hat{\mathbf{e}}_2(l)$ is shown in (b). A point in this plane is given in the (ρ, ϑ, l) coordinate system by (197). Near the axis, the magnetic surfaces take the form of an ellipse with major axis a and minor axis b .

As discussed in Section 5.4, rotational transform is important for toroidal confinement, and we will now compute the rotational transform generated by the lowest order terms in the expansions (201), corresponding to the rotational transform on the axis. Through this calculation we will demonstrate the geometric dependence of the rotational transform on the axis shape and flux surface shapes near the axis. Importantly, we will find that this class of equilibrium solutions allows for non-zero rotational transform.

To do so, we express the $\mathcal{O}(\rho^0)$ magnetic field, $\mathbf{B}_{[0]} = \nabla\Psi_{[2]} \times \nabla\alpha_{[0]}$, in flux coordinates $(\Psi_{[2]}, \vartheta, \zeta)$, where $\zeta := 2\pi l/L$ defines a toroidal angle increasing by 2π upon a toroidal loop. Following the discussion in Section 9, the field line label $\alpha_{[0]}$ can be identified in (123) as:

$$\alpha_{[0]}(\psi_{[0]}, \vartheta, \zeta) = \vartheta - \iota_{[0]}\zeta + \tilde{\lambda}(\psi_{[0]}, \vartheta, \zeta), \quad (213)$$

where $\iota_{[0]}$ is the $\mathcal{O}(\rho^0)$ rotational transform of interest, while the function $\tilde{\lambda}$ is 2π periodic in ζ . The rotational transform to $\mathcal{O}(\rho^0)$ is then computed by integration with respect to ζ :

$$2\pi\iota_{[0]}(\psi_{[2]}) = -\alpha_{[0]}(\psi_{[2]}, \vartheta = 0, l = L) + \alpha_{[0]}(\psi_{[2]}, \vartheta = 0, l = 0). \quad (214)$$

We now apply expression (210) for $\alpha_{[0]}$, noting that $\delta(L) - \delta(0) = m\pi$ for $m \in \mathbb{Z}$, as the elliptical cross-sections must make a half integer number of rotations in one toroidal turn, to get:

$$\begin{aligned} \iota_{[0]}(\psi_{[2]}) &= \frac{1}{2\pi} \left(-\arctan\left(e^{-\eta(l)} \tan(\delta(l))\right) \Big|_0^L + \int_0^L \frac{\delta'(l) - \tau(l)}{\cosh(\eta(l))} dl \right) \\ &= \frac{1}{2\pi} \left(-\delta(L) + \delta(0) + \int_0^L \frac{\delta'(l) - \tau(l)}{\cosh(\eta(l))} dl \right). \end{aligned} \quad (215)$$

As a consequence, under the assumption of vacuum field, i.e. in the absence of current in the plasma, rotational transform can be produced due to torsion $\tau(l)$ of the magnetic axis and ellipticity

$\delta'(l)$ of the flux surfaces. That is, if the magnetic axis is non-planar or the flux surfaces are ellipses which twist as one moves toroidally, there may be a non-zero rotational transform. While tokamaks use only current to produce rotational transform ι , the plasma current in stellarators is very small. However, stellarators can still generate a non-zero rotational transform due to torsion and rotating ellipticity, which may be present in 3D geometry.

In conclusion, we have constructed 3D equilibrium solutions with magnetic surfaces valid locally in a neighborhood of the magnetic axis with a possibly non-zero rotational transform.

This classical result of Mercier is also discussed in [86, 36, 84, 54]. There has continued to be an effort to understand 3D equilibria with near-axis expansions [28, 63, 64].

11 Models of 3D equilibrium magnetic fields

There are many situations in which it is desirable to study the steady-state behavior of a magnetic confinement device. As described in Section 5, charged particle motion depends on the geometry of the magnetic fields. For computing particle trajectories, as well as other figures of merit such as stability and transport, the equilibrium magnetic field must be determined. Here we will focus our attention on ideal MHD equilibrium models as introduced in Section 8.3. Ideal MHD equilibrium provides a relatively simple set of equations and is computationally tractable.

We will consider several levels of approximation. Pressure gradients and currents in the plasma can be included, as in Sections 11.2 and 11.3. An important subset of MHD models is the force-free model, presented in Section 11.4, where all currents are parallel to the magnetic field while the pressure is constant throughout the domain of interest. An extension of the force-free model is provided by MRxMHD (section 11.5), which allows for annular regions each with a force free magnetic field. In the vacuum model, presented in Section 11.6, currents and pressure gradients are not included in the equilibrium model, i.e. the pressure is constant while the current is zero. Thus some models include a feedback of the plasma on the magnetic field however the vacuum model does not.

There is also a distinction between models based on the assumption of surfaces. As discussed in Section 10, the existence of flux surfaces cannot generally be assumed in 3D. However, models based on the assumption of closed nested surfaces are often applied because of their computational efficiency. These are discussed in Sections 11.1 and 11.2. An alternative model assumes the existence of only some surfaces, see Section 11.5, and others rely on the existence of only one surface which serves as the boundary of the computational domain, see Sections 11.4 and 11.6. Models not assuming the existence of any surfaces are presented in Sections 11.3 and 11.6.

We will discuss the benefits and related challenges of the various 3D equilibrium models since they can each be useful in different applications.

11.1 Variational principle for MHD equilibria

In this Section we will discuss the variational principle for MHD equilibria with surfaces. Physically, this follows from the intuition that the plasma will tend towards a state which minimizes the energy. As we will see, equilibria are found by using techniques of variational calculus to extremize the plasma energy, subject to a set of constraints. These constraints include the existence of a set of closed, nested flux surfaces. This is not to say, however, that the variational principle provides any information on the *evolution to* an equilibrium state. The idea of finding ideal MHD equilibria via energy minimization was first studied over 60 years ago [60], but remains widely used today.

We will now show that MHD force balance,

$$\mathbf{J} \times \mathbf{B} = \nabla p(\psi), \quad (216)$$

is equivalent to finding stationary points of W ,

$$W[\mathbf{B}, p] = \int_{\Omega} \left(\frac{B^2(\mathbf{r})}{2\mu_0} - p(\mathbf{r}) \right) d^3x, \quad (217)$$

with respect to perturbations of \mathbf{B} and p , subject to several constraints:

1. There exists a set of flux surfaces such that $\mathbf{B} \cdot \nabla \psi = 0$, labeled by a toroidal flux label ψ ;
2. $\nabla \cdot \mathbf{B} = 0$;

3. the pressure as a function of flux is fixed $\delta p(\psi) = 0$;
4. the rotational transform as a function of flux is fixed, $\delta \iota(\psi) = 0$;
5. the total toroidal flux enclosed by the toroidal domain is fixed, $\delta \psi = 0$ on $\partial \Omega$.

Constraints 1 and 4 correspond to constraints of ideal MHD and preclude changes to the magnetic field topology (see Section 8.2). Constraint 3 follows as a consequence of assuming the plasma evolves adiabatically. Working directly with the assumption of adiabatic evolution, however, leads to minor differences in the energy functional. For simplicity, here we begin directly from the assumption that $\delta p(\psi) = 0$. Constraint 5 arises under the assumption that the plasma is surrounded by a perfectly conducting boundary such that the magnetic field lines must lie tangent to this surface. Although we assume that flux surfaces exist, their shapes are not fixed and will be determined from the variational principle.

We will start by deriving a convenient expression for the field \mathbf{B} . We choose a flux coordinate system (ψ, θ, ϕ) , where the position of surfaces of constant $\psi = \Psi_T/2\pi$ are not yet determined, while θ and ϕ are the poloidal and toroidal angles that are given functions of space. As shown in Section 9 (see (123)), the magnetic field in a toroidal system under assumptions 1 and 2 can generally be expressed as

$$\mathbf{B} = \nabla \psi \times \nabla (\theta - \iota(\psi)\phi + \lambda(\psi, \theta, \phi)). \quad (218)$$

Therefore, we will consider variations of $\{\lambda, \psi\}$ rather than \mathbf{B} , as the angles θ and ϕ and the rotational transform $\iota(\psi)$ are held fixed.

The linear perturbation to the magnetic field can be expressed as

$$\begin{aligned} \delta \mathbf{B}[\lambda, \psi; \delta \lambda, \delta \psi] &= \nabla \delta \psi \times \nabla (\theta - \iota(\psi)\phi + \lambda(\psi, \theta, \phi)) \\ &\quad + \nabla \psi \times \nabla \left(\theta - \iota'(\psi)\delta \psi \phi + \delta \lambda(\psi, \theta, \phi) + \frac{\partial \lambda(\psi, \theta, \phi)}{\partial \psi} \delta \psi \right). \end{aligned} \quad (219)$$

We see that λ varies due to its dependence on ψ and also through explicit variations. Moreover, constraint 3 is enforced by expressing the perturbation to the pressure at a given position in terms of the perturbation to the flux label,

$$\delta p(\mathbf{r}) = p'(\psi)\delta \psi, \quad (220)$$

in particular it is independent of λ .

The first variation of W with respect to λ is now computed,

$$\begin{aligned} \delta W[\lambda, \psi; \delta \lambda] &= \int_{\Omega} \frac{\mathbf{B} \times \nabla \psi \cdot \nabla \delta \lambda(\psi, \theta, \phi)}{\mu_0} d^3 x \\ &= - \int_{\Omega} \delta \lambda(\psi, \theta, \phi) \mathbf{J} \cdot \nabla \psi d^3 x, \end{aligned} \quad (221)$$

where we have integrated by parts, noting that $\partial \Omega$ is a flux surface such that the boundary term vanishes. Thus we obtain a condition that stationary points of W satisfy

$$\mathbf{J} \cdot \nabla \psi = 0. \quad (222)$$

We note that this condition is equivalent to applying $\mathbf{B} \times \nabla \psi \cdot (\dots)$ to (216); thus we recover one component of force balance.

We now consider the first variation of W with respect to ψ ,

$$\begin{aligned} \delta W[\lambda, \psi; \delta \psi] &= \int_{\Omega} \left(\frac{\mathbf{B} \cdot \left(\nabla \delta \psi \times \nabla (\theta - \iota\phi + \lambda) + \nabla \psi \times \nabla \left(\left(-\iota'(\psi)\phi + \frac{\partial \lambda}{\partial \psi} \right) \delta \psi \right) \right)}{\mu_0} - p'(\psi)\delta \psi \right) d^3 x \\ &= \int_{\Omega} \delta \psi \left(\frac{\nabla \times \mathbf{B} \cdot \nabla (\theta - \iota\phi + \lambda) + \left(\iota'(\psi)\phi - \frac{\partial \lambda}{\partial \psi} \right) \nabla \times \mathbf{B} \cdot \nabla \psi}{\mu_0} - p'(\psi) \right) d^3 x. \end{aligned} \quad (223)$$

Here we have integrated by parts, noting that the boundary terms will vanish as $\delta\psi = 0$ on $\partial\Omega$. The second term in the above expression will vanish from (222), so we have the condition

$$\begin{aligned} \frac{1}{\mu_0} \nabla \times \mathbf{B} \cdot \nabla(\theta - \iota\phi + \lambda(\psi, \theta, \phi)) - p'(\psi) &= 0 \\ \mathbf{J} \times \mathbf{B} \cdot \frac{\partial \mathbf{r}}{\partial \psi} - p'(\psi) &= 0, \end{aligned} \quad (224)$$

since $\mathbf{J} \times \mathbf{B} = \nabla\psi(\mathbf{J} \cdot \nabla\alpha)$ due to (222). Thus we recover from the variational principle the $\mathbf{B} \times \nabla\psi$ component (222) and $\partial\mathbf{r}/\partial\psi$ component (224) of the force balance equation (216). Force balance parallel to \mathbf{B} is implied from the assumption of $\mathbf{B} \cdot \nabla\psi = 0$. We have therefore recovered each of the vector components of (216). Therefore, finding stationary points of W with respect to λ and ψ is equivalent to (216) under the above assumptions. This implies that an equilibrium magnetic field can be obtained efficiently from a variational method if the assumptions can be applied. Applications for 3D MHD calculations will be discussed in the following Section.

The discussion in this Section is similar to that in [60] and [36]. A discussion of numerical applications of energy principles for MHD equilibria is given in Section 4.5 of [51].

11.2 3D MHD equilibrium with assumption of surfaces

As discussed in Section 10, the assumption of continuously nested flux surfaces cannot generally be made in 3D. In addition, the assumption of continuously nested flux surfaces together with smooth pressure profiles gives rise to the possibility of singular currents at rational surfaces. Under these assumptions, however, equilibrium fields can be found by applying the variational approach explained in the previous Section by obtaining stationary points of W (217) via a gradient-descent method. This is the basis for the NSTAB [27] and VMEC [43] codes. Because of its computational efficiency, the VMEC code is routinely applied in stellarator design studies using numerical optimization tools [90]. A possible justification is to argue that, since the 3D solutions of physical interest must have good confinement properties, the desired solutions should have a set of magnetic surfaces of non-zero measure. The assumption should ultimately be checked with other methods described in the following Sections which do not assume the existence of surfaces.

For variational methods, several quantities need to be supplied:

- The pressure $p(\psi)$ is a given function depending only on the flux surface label (see Section 6.3). Thus from (110) it must be that $\mathbf{J} \cdot \nabla\psi = 0$ and $\mathbf{B} \cdot \nabla\psi = 0$.
- A second flux function, typically the toroidal current enclosed by a flux surface, $I_T(\psi)$, or the rotational transform, $\iota(\psi)$, is also given.
- Depending on whether the shape of the plasma boundary, $\partial\Omega$, is prescribed or not is referred to as either a fixed- or free-boundary calculation, respectively. For fixed-boundary, the outer boundary shape, $\partial\Omega$, is prescribed with a Neumann boundary condition $\mathbf{B} \cdot \hat{\mathbf{n}} = 0$ on $\partial\Omega$. The value of the toroidal flux (79) on $\partial\Omega$, Ψ_T , is also specified.

The shape of the flux surfaces must be determined from the equilibrium equations. Thus $\psi(\mathbf{r})$ is a result of the calculation.

For a free-boundary problem, the location of electro-magnetic coils and their currents are prescribed. Beginning with an initial guess for the boundary, the magnetic field and current can be determined as in the fixed boundary case. Through an iterative process, the boundary that is consistent with the coils can be obtained.

- Given the coil currents and positions, the vacuum magnetic field \mathbf{B}_0 , that exists in the absence of plasma currents, is determined.
- Given an initial guess for the boundary, $\partial\Omega$, the magnetic field (and thus current) can be determined in Ω using (110)-(111) and the same boundary conditions for the fixed boundary case, $\mathbf{B} \cdot \hat{\mathbf{n}}|_{\partial\Omega} = 0$.
- Given the plasma current from (111a) in Ω , the magnetic field in the region outside of Ω due to the plasma current, $\mathbf{B}_P = \nabla\Phi_B$, can be computed. Here Φ_B satisfies Laplace's equation for vacuum fields (see Section 11.6).

- The total field in the vacuum region is then obtained as $\mathbf{B}_V = \mathbf{B}_0 + \nabla\Phi_B$, and at the boundary we can evaluate $(p + B^2/2\mu_0)_{\partial\Omega}$, and $\mathbf{B}_V \cdot \hat{\mathbf{n}}|_{\partial\Omega}$.
- We desire the total field in the vacuum region, \mathbf{B}_V , to satisfy several conditions. The total pressure should be continuous across the boundary between the vacuum and plasma region, $(p + B^2/2\mu_0)_{\partial\Omega} = (B_V^2/2\mu_0)_{\partial\Omega}$, and $\mathbf{B}_V \cdot \hat{\mathbf{n}}|_{\partial\Omega} = 0$. The boundary $\partial\Omega$ is iterated until these conditions are satisfied. The assumption of continuity of total pressure arises from imposing force balance at the boundary.

This is the method used in the free-boundary VMEC code [41].

11.3 3D MHD equilibria without assumption of surfaces

As discussed in Section 10.2, in general 3D geometry continuously nested flux surfaces are not guaranteed to exist. In this Section we discuss models for computing equilibrium solutions with $\nabla p \neq 0$ without the assumption that magnetic surfaces exist.

The force balance condition (110) implies that $\mathbf{B} \cdot \nabla p = 0$ and $\mathbf{J} \cdot \nabla p = 0$, so that pressure is constant along field lines and streamlines of the current density. While models which assume surfaces can satisfy this condition by enforcing that pressure is a given flux function, in the absence of surfaces the pressure cannot be imposed, as it will not generally satisfy these conditions. Several numerical approaches for finding solutions in the absence of continuously nested flux surfaces have been developed, some of which are outlined in the proceeding discussion.

The approach employed by the PIES code [83] is to provide an initial guess for \mathbf{B} and p in Ω (for example, the field computed with the variational approach could be used) such that $\mathbf{B} \cdot \nabla p = 0$. Then, (110)-(111) are solved iteratively, as follows:

- The current density perpendicular to the magnetic field is known from (110),

$$\mathbf{J}_\perp = \frac{1}{B} \hat{\mathbf{b}} \times \nabla p. \quad (225)$$

- The parallel current can be computed by enforcing that $\nabla \cdot \mathbf{J} = 0$, which follows from (111b),

$$\mathbf{B} \cdot \nabla \left(\frac{J_\parallel}{B} \right) = -\nabla \cdot \left(\frac{1}{B} \hat{\mathbf{b}} \cdot \nabla p \right). \quad (226)$$

We note that this is an example of a magnetic differential equation which may have singular behavior at rational surfaces (see Section 10.3).

- Given $\mathbf{J} = \mathbf{J}_\perp + J_\parallel \hat{\mathbf{b}}$, the magnetic field can be determined from (111a).
- The perpendicular and parallel currents are again computed as described above, and the iteration continues until convergence.

The SIESTA [42] code, on the other hand, uses a variational method similar to that described in Section 11.1. Here a small term is added to (110) such that there is a small perturbation away from ideal MHD. In this way, the magnetic topology is no longer constrained, allowing the break-up of surfaces and island formation.

Another example is the HINT code [33], which evolves a set of time-dependent equations in order to arrive at a steady state solution which is then interpreted as an equilibrium state. As a first step, the magnetic field is held fixed while the pressure is allowed to evolve to satisfy $\mathbf{B} \cdot \nabla p = 0$. Second, the pressure is held fixed while the field evolves to satisfy force balance. Some small non-ideal terms are added to allow for changes in magnetic topology. These two steps are iterated until convergence is reached and force balance is achieved within a tolerable error.

11.4 Force-free fields

The magnetic fields in a stellarator are sometimes described by a force-free model. Force-free refers to the fact that $\mathbf{J} \times \mathbf{B}$ and ∇p vanish independently. As a consequence, the plasma current is everywhere parallel to the magnetic field. Such situations can arise in both laboratory and space plasmas. In this Section we provide some motivation for employing this model in magnetic confinement configurations as well as a variational principle for computing such states.

If $\mathbf{J} \times \mathbf{B} = 0$ in a given domain Ω , then from (111a) we must have

$$\nabla \times \mathbf{B} = \lambda \mathbf{B}, \quad (227)$$

for some scalar function λ . Note that λ is proportional to the parallel current density. Force-free magnetic fields are thus Beltrami fields, as will be discussed in Section 11.7. The value of the pressure is not constrained by this model, as long as it is a constant in Ω . Vacuum fields are a subset of force-free fields in the limit $\lambda = 0$.

In addition, from (111b) and (227) we require that

$$\mathbf{B} \cdot \nabla \lambda = 0. \quad (228)$$

Often λ is taken to be a constant in Ω to satisfy the above, sometimes called the linear force-free model. We will make this assumption throughout this discussion.

The force-free equation (227) with constant λ can be solved in a toroidal domain with the following conditions

$$\mathbf{B} \cdot \hat{\mathbf{n}} = 0 \quad \text{on } \partial\Omega \quad (229a)$$

$$\int_{S_T} \mathbf{B} \cdot \hat{\mathbf{n}} d^2x = \Psi_T \quad \text{on } \partial\Omega. \quad (229b)$$

Thus the boundary of the domain must be a magnetic surface. We note that the overall scale factor of \mathbf{B} is not determined from (227). Therefore, the toroidal flux enclosed by Ω can be specified to determine the overall scale. In (229b), S_T is a surface at constant poloidal angle bounded by $\partial\Omega$. Often instead of λ , the magnetic helicity is prescribed,

$$K = \int_{\Omega} \mathbf{A} \cdot \mathbf{B} d^3x, \quad (230)$$

where \mathbf{A} is the vector potential such that $\mathbf{B} = \nabla \times \mathbf{A}$. Then λ is chosen to achieve the desired value of the helicity. Rather analogously to helicity in fluid dynamics, K is a measure of the knottedness of magnetic field lines (see [10] for further discussion). Since the vector potential, \mathbf{A} , is gauge dependent (the gradient of a function can be added to \mathbf{A} without modifying $\mathbf{B} = \nabla \times \mathbf{A}$), the helicity must be defined carefully. In a specific choice of gauge for \mathbf{A} , known as the Coulomb gauge where $\nabla \cdot \mathbf{A} = 0$, K can be interpreted as the Gauss linking number which is studied in fields such as knot theory, algebraic topology, and differential geometry.

The force-free equations can also be solved within toroidal annuli rather than a full toroidal domain. We now consider the solution of (227) in a toroidal annulus $\Omega = \Omega_{\text{outer}} \setminus \Omega_{\text{inner}}$, where Ω_{outer} and Ω_{inner} are toroidal volumes such that $\Omega_{\text{inner}} \subset \Omega_{\text{outer}}$. These volumes are limited by toroidal surfaces, $\Gamma_{\text{outer}} = \partial\Omega_{\text{outer}}$ and $\Gamma_{\text{inner}} = \partial\Omega_{\text{inner}}$. Conditions (229a)-(229b) must be imposed as in the case of a toroidal domain, with the addition of a flux constraint,

$$\mathbf{B} \cdot \hat{\mathbf{n}} = 0 \quad \text{on } \Gamma_{\text{outer}} \text{ and } \Gamma_{\text{inner}} \quad (231a)$$

$$\int_{S_T} \mathbf{B} \cdot \hat{\mathbf{n}} d^2x = \Psi_T(\Gamma_{\text{outer}}) - \Psi_T(\Gamma_{\text{inner}}) \quad (231b)$$

$$\int_{S_P} \mathbf{B} \cdot \hat{\mathbf{n}} d^2x = \Psi_P(\Gamma_{\text{outer}}) - \Psi_P(\Gamma_{\text{inner}}). \quad (231c)$$

Here S_T is a surface at constant toroidal angle bounded by surfaces Γ_{outer} and Γ_{inner} , while S_P is a surface at constant poloidal angle bounded by surfaces Γ_{outer} and Γ_{inner} .

Force-free equilibria in a toroidal domain, Ω , can be found by minimizing an energy functional as in Section 11.1, but with a different set of constraints. In particular, we seek stationary points of,

$$W = \int_{\Omega} \frac{B^2}{2\mu_0} d^3x, \quad (232)$$

subject to the following constraints:

1. the total magnetic helicity (230) is given and constant;
2. the boundary of the domain, $\partial\Omega$, is a magnetic surface such that $\mathbf{B} \cdot \hat{\mathbf{n}}|_{\partial\Omega} = 0$;

3. the boundary of the domain is fixed such that the perturbation to the magnetic field satisfies $\delta\mathbf{B} \cdot \hat{\mathbf{n}}|_{\partial\Omega} = 0$;
4. the toroidal magnetic flux through Ω is fixed,

$$\int_{S_T} \mathbf{B} \cdot \hat{\mathbf{n}} d^2x = \Psi_T \quad \text{on } \partial\Omega. \quad (233)$$

This leads to the result that perturbations to the vector potential can be expressed as $\delta\mathbf{A} = \boldsymbol{\xi} \times \mathbf{B}$ on $\partial\Omega$, where $\boldsymbol{\xi}$ is known as the displacement vector [11, 29, 25].

Imposing constraint 1 with a Lagrange multiplier α and computing the first variation in W with respect to \mathbf{A} yields,

$$\delta W[\mathbf{A}; \delta\mathbf{A}] = \int_{\Omega} \left(\frac{\mathbf{B} \cdot \delta\mathbf{B}}{\mu_0} - \alpha (\mathbf{A} \cdot \delta\mathbf{B} - \delta\mathbf{A} \cdot \mathbf{B}) \right) d^3x, \quad (234)$$

where $\delta\mathbf{B} = \nabla \times \delta\mathbf{A}$. Integrating by parts, we obtain,

$$\delta W[\mathbf{A}; \delta\mathbf{A}] = \int_{\Omega} \delta\mathbf{A} \cdot \left(\frac{(\nabla \times \mathbf{B})}{\mu_0} - 2\alpha\mathbf{B} \right) d^3x + \int_{\partial\Omega} \delta\mathbf{A} \times \hat{\mathbf{n}} \cdot \left(\alpha\mathbf{A} - \frac{\mathbf{B}}{\mu_0} \right) d^2x. \quad (235)$$

The surface term vanishes under assumptions 2-4. Thus the field satisfies (227) with $\lambda = 2\alpha/\mu_0$.

The key assumption of force-free fields as energy minimizing equilibria is the conservation of total helicity (constraint 1). The veracity of this assumption as well as the dynamical process by which such states may form is a topic of some debate. The famous conjecture by J.B. Taylor [93, 94] argues that plasmas relax to such force-free states via turbulent processes under which K is approximately conserved. The states are therefore sometimes referred to as Taylor states within the literature. While this type of process is not relevant for stellarator confinement, this model has several features which may become important for computing 3D fields. These considerations will be described below.

Under ideal MHD evolution (Section 11.4), changes in magnetic topology are not allowed. Thus if a system begins in a state with closed, nested surfaces, the final state must also have the same topology, and no islands or stochastic regions can form. While the variational principle presented in Section 11.1 requires that the local topology of the magnetic field is fixed during variations, only the *global* helicity is fixed when performing variations of (235). Thus this model allows the calculation of energy minimized equilibria which differ in magnetic field topology from the initial state, and can allow for the formation of islands or stochastic field regions.

We also note that the force-free model is consistent with the assumption of a non-integrable magnetic field. If a given field line comes arbitrarily close to every point within a domain Ω , then from (110) we conclude that pressure must be constant within Ω . Therefore the magnetic field must satisfy (227). From the condition that the magnetic field must be divergence-free, (228) implies that λ is constant along field lines. Under the assumption that a given field line comes arbitrarily close to any point in Ω , we conclude that λ is a constant within Ω . We emphasize that this assumption on the field line structure is not required to invoke a force-free model, simply that it is consistent.

The existence and uniqueness of solutions to (227) has been shown for toroidal domains and toroidal annuli [59]. For more details on the constraints necessary for solving this set of PDEs in toroidal annuli and its implementation for axisymmetric geometry, see [81]. This formalism has been applied to stellarator geometry in the Boundary Integral Equation Solver for Taylor states (BIEST) code [71]. The extension of this model to describe multiple regions simultaneously is presented in the following Section.

11.5 Stepped pressure equilibrium (MRxMHD)

The multi-region relaxed MHD (MRxMHD) equilibrium model [44, 19] generalizes the single-volume force-free state by allowing discontinuous (stepped) pressure profiles and thus permitting the pressure to vary throughout the plasma volume. The plasma is partitioned into nested volumes in which the plasma is force-free (i.e. p is constant) and separated by interfaces which accommodate jumps in p . The geometry of the interfaces is not known *a priori* and must satisfy a specified set of jump and flux conditions which are described below. Note that these interface conditions are

similar to those used in immiscible fluid models or capillary interface models where the interfaces between phases or fluids are unknown².

Consider a toroidal domain, Ω , in which p and λ (227) are piecewise constant. The domain is partitioned into m nested toroidal sub-regions Ω_i for all i from 1 to m . The innermost volume, Ω_1 , is a genus one torus, otherwise Ω_i for $i \geq 2$ are genus two tori. Excepting Ω_1 , each Ω_i is bounded by two non-intersecting toroidal surfaces, Γ_{i-1} and Γ_i for i from 2 to m . Note that Ω_1 is bounded by a single toroidal surface, Γ_1 , and denote the outer most boundary $\Gamma_m = \partial\Omega$. The discontinuities which can arise in this model, including in p and λ , occur at the surfaces, Γ_i .

The components of the model can be described as follows:

- the parameters $\{\lambda_i\}_{1 \leq i \leq m}$ define the λ profile as $\lambda = \lambda_i$ in Ω_i for all i from 1 to m , while the magnetic field satisfies in each Ω_i

$$\nabla \times \mathbf{B}_i = \lambda_i \mathbf{B}_i \text{ in } \Omega_i, \quad (236)$$

where \mathbf{B}_i denotes the solution in Ω_i ;

- the parameters $\{p_i\}_{1 \leq i \leq m}$ define the stepped pressure profile as $p = p_i$ in Ω_i for all i from 1 to m , while the total pressure balance (including the plasma pressure p and the magnetic pressure $B^2/2\mu_0$) at the interfaces is expressed as:

$$[[p + B^2/2\mu_0]]_{\Gamma_i} = 0, \forall i \text{ between 1 and } m-1; \quad (237)$$

- the flux surface conditions hold at the interfaces:

$$\mathbf{B} \cdot \hat{\mathbf{n}} = 0 \text{ on } \Gamma_i, \forall i \text{ between 1 and } m; \quad (238)$$

- the parameters $\{\Psi_T^i, \Psi_P^i\}_{2 \leq i \leq m}$ define the toroidal and poloidal fluxes across each annular subdomain:

$$\int_{\mathcal{S}_{T_i}} \mathbf{B} \cdot \hat{\mathbf{n}} d^2x = \Psi_T^i, \forall i \text{ between 2 and } m \quad (239)$$

$$\int_{\mathcal{S}_{P_i}} \mathbf{B} \cdot \hat{\mathbf{n}} d^2x = \Psi_P^i, \forall i \text{ between 2 and } m. \quad (240)$$

Here \mathcal{S}_{T_i} is a surface at constant toroidal angle bounded by surfaces Γ_i and Γ_{i-1} , and \mathcal{S}_{P_i} is a surface at constant poloidal angle bounded by surfaces Γ_i and Γ_{i-1} ;

- the parameter Ψ_T^1 defines the toroidal flux across the innermost toroidal domain Ω_1 :

$$\int_{\mathcal{S}_{T_1}} \mathbf{B} \cdot \hat{\mathbf{n}} d^2x = \Psi_T^1, \quad (241)$$

where \mathcal{S}_{T_1} is a surface at constant toroidal angle bounded by Γ_1 .

In summary, given $\{\lambda_i, p_i, \Psi_T^i\}_{1 \leq i \leq m}$ and $\{\Psi_P^i\}_{2 \leq i \leq m}$, (236) can be solved, subject to the constraints (237)-(241), to determine the position of free surfaces $\{\Gamma_i\}_{1 \leq i \leq m}$ and value of the magnetic field \mathbf{B}_i in $\cup_{1 \leq i \leq m} \Omega_i$ which defines an MHD equilibrium. In place of $\{\lambda_i\}_{1 \leq i \leq m}$, the total helicity in each Ω_i may be prescribed and, in place of $\psi_T^1 \cup \{\Psi_T^i, \Psi_P^i\}_{2 \leq i \leq m}$, the value of the rotational transform on each Γ_i^- for $1 \leq i \leq m$ may be fixed.

An important characteristic of the model is that Γ_i , referred to as ideal interfaces and across which p is discontinuous, are magnetic surfaces. Recall from Section 10.3 that, in order to avoid the appearance of unphysical $1/x$ singular currents, pressure gradients must be avoided except at surfaces corresponding to sufficiently irrational values of the rotational transform. In the MRxMHD model, the pressure jump can be chosen to occur at interfaces which satisfy the Diophantine condition (186) and thus do not produce unphysical currents in 3D. Moreover, these magnetic surfaces may persist according to KAM theory (Section 10.2.4) if the perturbation from integrability is sufficiently small. Combined, this ensures the model produces well-defined equilibrium solutions, even in the absence of axisymmetry.

This model has been implemented numerically as Stepped Pressure Equilibrium Code (SPEC) [49], which solves for the magnetic field, iterating on the position of the interfaces until the constraints are satisfied.

²See for instance [39] for the introduction of a flux condition on an artificial boundary within the domain to ensure well-posedness for a Navier-Stokes problem, [40] for numerical aspects of a flow through an aperture in an infinite wall, or [50, 95] for a jump condition modeling force balance at an unknown interface.

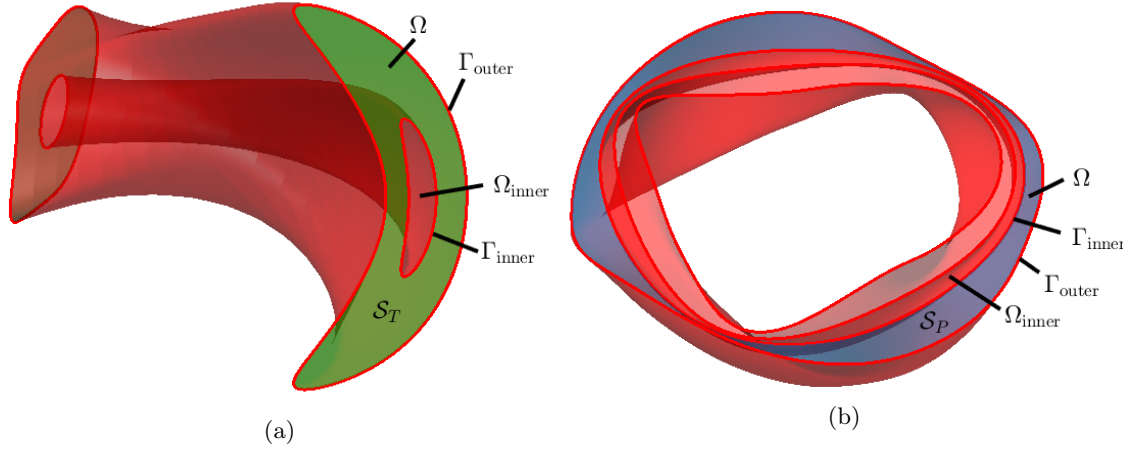


Figure 26: A force-free equilibrium can be computed in an annular region Ω bounded by toroidal surfaces Γ_{outer} and Γ_{inner} given the flux of magnetic field through a surface at constant toroidal angle, \mathcal{S}_T , (green in (a)) and the flux through a surface at constant poloidal angle, \mathcal{S}_P , (blue in (b)) bounded by Γ_{inner} and Γ_{outer}

11.6 Vacuum fields

As described in Section 3.4, the vacuum model for magnetic fields can be used if there is no current in a given domain. This implies that \mathbf{B} is curl-free from (111a), so it can be written in terms of a scalar potential (16), which must satisfy Laplace's equation (17).

In this Section we assume Laplace's equation is solved in a toroidal domain, Ω . The toroidal angle ϕ , will be taken to be the standard cylindrical angle (see Section 6.2). The poloidal angle, θ , will be some angle which increases by 2π on a poloidal loop about the torus. In general, the scalar potential can be separated into secular and periodic pieces,

$$\Phi_B = \tilde{\Phi}_B + A\phi + C\theta, \quad (242)$$

here $\tilde{\Phi}_B$ is periodic in θ and ϕ and A and C are constants. The scalar potential can generally be written as the form given in (242), as $\mathbf{B} = \nabla\Phi_B$ must be periodic in ϕ and θ . However, Φ_B can contain secular terms as it is not a physical quantity. We now enforce that the current enclosed by a poloidal loop about the torus vanishes, as there is no current inside Ω . We apply Ampere's law (111a), using a loop at constant ϕ on the boundary of the toroidal domain, $\partial\Omega$,

$$\oint_{\phi=\text{const.}} \mathbf{B} \cdot d\mathbf{l} = \mu_0 I_T = 0. \quad (243)$$

We can see that (243) implies that $C = 0$, using $d\mathbf{l} = (\partial\mathbf{r}/\partial\theta) d\theta$. The constant A can be determined by considering a loop at constant θ on $\partial\Omega$,

$$\oint_{\theta=\text{const.}} \mathbf{B} \cdot d\mathbf{l} = \mu_0 I_P. \quad (244)$$

The integrals in (243) and (244) are described in Section 9.2. From (244), we can see that $A = \mu_0 I_P / 2\pi$, using $d\mathbf{l} = (\partial\mathbf{r}/\partial\phi) d\phi$. As there is no current in Ω , I_P is the total coil current linking the plasma poloidally. The boundary condition for Φ_B on $\partial\Omega$ is determined by specifying $\mathbf{B} \cdot \hat{\mathbf{n}}$ on $\partial\Omega$,

$$\hat{\mathbf{n}} \cdot \nabla \tilde{\Phi}_B + \frac{\mu_0 I_P}{2\pi} \hat{\mathbf{n}} \cdot \nabla \phi = \mathbf{B} \cdot \hat{\mathbf{n}} \quad \text{on } \partial\Omega. \quad (245)$$

If $\partial\Omega$ is a magnetic surface, then $\mathbf{B} \cdot \hat{\mathbf{n}} = 0$. Otherwise, it can be computed from the Biot-Savart law (15) if all external currents are known. Laplace's equation subject to this Neumann boundary condition can be solved using a Green's function method, as is done in the NESTOR code [74].

The vacuum approximation is useful to model static fields in a stellarator, as they do not require plasma currents to produce a poloidal magnetic field. Even if the plasma current is not assumed to vanish, the vacuum model can be used to describe the region outside the confinement region.

Instead of solving Laplace's equation, the fields in a vacuum region can also be computed using the Biot-Savart law (15) applied to sources of current outside the vacuum region. Thus if the currents in electro-magnetic coils are provided, the magnetic field can be determined without the assumption of any magnetic surfaces under the vacuum model.

11.7 Summary and analogy with steady Euler flow

Below is a Table which summarizes the models used to describe equilibrium stellarator magnetic fields in a toroidal domain Ω , with flux surface boundary conditions on the boundary of Ω .

	MHD equilibrium (surfaces assumed)	Force-free fields	Vacuum fields
Hyp.	$\mathbf{J} \times \mathbf{B} \neq 0$ $\nabla p \neq 0$	$\mathbf{J} \times \mathbf{B} = 0$ $\nabla p = 0$ and $\lambda = \text{const.}$	$\mathbf{J} = 0$ $\nabla p = 0$
PDE model	$\mathbf{J} \times \mathbf{B} = \nabla p$ $\nabla \cdot \mathbf{B} = 0$ $\mu_0 \mathbf{J} = \nabla \times \mathbf{B}$	$\nabla \times \mathbf{B} = \lambda \mathbf{B}$ $\mu_0 \mathbf{J} = \nabla \times \mathbf{B}$	$\Delta \tilde{\Phi}_B = 0$
Given	$p(\psi), \iota(\psi), \Psi_T$	λ, Ψ_T	I_P
Unkn.	\mathbf{B}	\mathbf{B}	$\tilde{\Phi}_B$
With	\mathbf{J} function of \mathbf{B}	\mathbf{J} function of \mathbf{B}	$\mathbf{B} = \nabla \left(\tilde{\Phi}_B + (\mu_0 I_P / 2\pi) \phi \right)$
BC	$\mathbf{B} \cdot \hat{\mathbf{n}} = 0$	$\mathbf{B} \cdot \hat{\mathbf{n}} = 0$	$\hat{\mathbf{n}} \cdot \nabla \tilde{\Phi}_B + (\mu_0 I_P / 2\pi) \hat{\mathbf{n}} \cdot \nabla \phi = \mathbf{B} \cdot \hat{\mathbf{n}}$

Connections exist between MHD and fluid dynamics. In particular, the MHD equilibrium equations share many similarities with the steady Euler flow equations. Over the years, this has facilitated the exchange of ideas between the fluid dynamics and plasma physics communities (e.g. [75, 35, 15]).

The steady ($\partial/\partial t = 0$) incompressible Euler equations with constant and uniform density, ρ_0 , are equations for the flow velocity \mathbf{u} and pressure P . They can be written,

$$\mathbf{u} \cdot \nabla \mathbf{u} = -\nabla \left(\frac{P}{\rho_0} \right) \Leftrightarrow (\nabla \times \mathbf{u}) \times \mathbf{u} = -\nabla \left(\frac{P}{\rho_0} + \frac{u^2}{2} \right) \quad (246a)$$

$$\nabla \cdot \mathbf{u} = 0. \quad (246b)$$

Conservation of momentum density is expressed by (246a), while (246b) expresses incompressibility of the flow. The vorticity is defined as $\boldsymbol{\omega} = \nabla \times \mathbf{u}$. Beltrami flows describe states in which the vorticity is parallel to \mathbf{u} ; they are analogous to force-free fields. Flows with vanishing vorticity can be expressed in terms of a potential; they are analogous to vacuum fields.

Hyp.	Steady Euler models	MHD equilibrium models
	$(\nabla \times \mathbf{u}) \times \mathbf{u} = -\nabla \left(\frac{P}{\rho_0} + \frac{u^2}{2} \right)$ $\nabla \cdot \mathbf{u} = 0$	$(\nabla \times \mathbf{B}) \times \mathbf{B} = \mu_0 \nabla p$ $\nabla \cdot \mathbf{B} = 0$
Beltrami flows/fields (vorticity parallel to field)	$\nabla \times \mathbf{u} = \alpha \mathbf{u}$ $\nabla \cdot \mathbf{u} = 0$	$\nabla \times \mathbf{B} = \lambda \mathbf{B}$ $\nabla \cdot \mathbf{B} = 0$
Potential flows (zero vorticity)	$\mathbf{u} = \nabla \varphi$ $\Delta \varphi = 0$	$\mathbf{B} = \nabla \Phi_B$ $\Delta \Phi_B = 0$

12 Symmetries in stellarators

Although stellarators are non-axisymmetric, it is often possible to identify other symmetries which can become useful for confinement or efficient numerical discretization. In this Section we discuss several of these. These symmetries are properties of the equilibrium magnetic field and have been implemented in many stellarator configurations. In Section 12.1, an important symmetry which provides confinement of guiding center trajectories, quasisymmetry, is discussed. In Section 12.2, a periodicity in the number of field periods, often referred to as N_P symmetry, is presented. In Section 12.3, a discrete reflection symmetry, known as stellarator symmetry, is described. While N_P symmetry and stellarator symmetry may not result in improved confinement as quasisymmetry does, they are present in almost all stellarator configurations to date.

12.1 Quasisymmetry

Quasisymmetry is expressed in terms of Boozer coordinates, described in Section 9.3. Quasisymmetry is defined as a symmetry of the field strength, B , with respect to a linear combination of Boozer angles, ϑ_B and φ_B . More precisely, quasisymmetry means that there exists a change of coordinates $(\psi, \vartheta_B, \varphi_B) \rightarrow (\psi, \chi, \eta)$, where $\chi = M\vartheta_B - N\varphi_B$ and $\eta = M'\vartheta_B - N'\varphi_B$ with $M'/N' \neq M/N$,

$$B(\psi, \vartheta_B, \varphi_B) = \tilde{B}(\psi, \chi, \eta), \quad (247)$$

such that the magnetic field amplitude is independent of the coordinate η ,

$$\frac{\partial \tilde{B}(\psi, \chi, \eta)}{\partial \eta} = 0. \quad (248)$$

Thus there exists a symmetry direction when the field strength is expressed in Boozer coordinates. For example, quasi-axisymmetry corresponds to $M = 1$ and $N = 0$, and the field strength is independent of φ_B ,

$$\frac{\partial B(\psi, \vartheta_B, \varphi_B)}{\partial \varphi_B} = 0. \quad (249)$$

We can furthermore note that under the assumption of (248), the radial Boozer covariant component expressed in the (ψ, χ, η) system, $\tilde{K}(\psi, \chi, \eta) = K(\psi, \vartheta_B, \varphi_B)$, satisfies,

$$\frac{\partial \tilde{K}(\psi, \chi, \eta)}{\partial \eta} = 0. \quad (250)$$

This can be seen considering the expression obtained assuming an MHD equilibrium, (147). For the remainder of this Section, we consider $\iota \in \mathbb{R} \setminus \mathbb{Q}$ so that the δ -function term is zero, in which case,

$$K(\psi, \vartheta_B, \varphi_B) = \mathcal{K}(\psi) + i\mu_0 \frac{dp(\psi)}{d\psi} \sum_{m,n,mn \neq 0} \left(\frac{G(\psi) + \iota(\psi)I(\psi)}{n - \iota m} b_{m,n} \right) e^{i(m\vartheta_B - n\varphi_B)}, \quad (251)$$

where $b_{m,n}$ are the Fourier harmonics of $1/B^2$ defined in (144).

We now see that if $B(\psi, \vartheta_B, \varphi_B)$ varies on a surface only through $\chi = M\vartheta_B - N\varphi_B$, then so must K , as $b_{m,n}$ vanishes for $m/n \neq M/N$. Therefore, K has the same symmetry properties as B . This condition will become important for studying the guiding center motion in the following Section.

12.1.1 Guiding center motion in quasisymmetry

We will study the consequences of this symmetry on guiding center motion. The analysis will be similar to that in Section 7.2, where we saw that axisymmetry provided particle confinement under the assumption of a strong magnetic field. Again, the existence of a coordinate which does not appear in the Lagrangian will result in a constant of motion. Throughout this Section we assume the electrostatic potential, Φ , is a flux function, where the electric field $\mathbf{E} = -\nabla\Phi$. In practice, this is a good approximation for stellarator configurations [36].

In this Section we will assume that the fields are time-independent. We express the gyroaveraged Lagrangian, repeated here for convenience,

$$\mathcal{L}(\mathbf{R}, \rho, \dot{\mathbf{R}}, \dot{\varphi}) = \frac{m}{2} \left(\left(\dot{\mathbf{R}} \cdot \hat{\mathbf{b}}(\mathbf{R}) \right)^2 + \rho^2 \dot{\varphi}^2 \right) + q\mathbf{A}(\mathbf{R}) \cdot \dot{\mathbf{R}} - \frac{\dot{\varphi}\rho^2}{2} B(\mathbf{R}) - q\Phi(\mathbf{R}), \quad (252)$$

in Boozer coordinates $(\psi, \vartheta_B, \varphi_B)$. The time derivative of the guiding center position can be expressed in the Boozer contravariant form as

$$\dot{\mathbf{R}} = \dot{\psi} \frac{\partial \mathbf{r}}{\partial \psi} + \dot{\vartheta}_B \frac{\partial \mathbf{r}}{\partial \vartheta_B} + \dot{\varphi}_B \frac{\partial \mathbf{r}}{\partial \varphi_B}. \quad (253)$$

To compute the quantity $\dot{\mathbf{R}} \cdot \hat{\mathbf{b}}(\mathbf{R})$, we express $\dot{\mathbf{R}}$ as (253) and $\hat{\mathbf{b}} = \mathbf{B}/B$ in the covariant form using (137). To compute the quantity $\mathbf{A}(\mathbf{R}) \cdot \dot{\mathbf{R}}$, we first see that $\mathbf{B}(\mathbf{R}) = \nabla \times \mathbf{A}(\mathbf{R})$ implies that the vector potential \mathbf{A} can be written

$$\mathbf{A}(\psi, \vartheta_B, \varphi_B) = \psi \nabla \vartheta_B - \psi_P(\psi) \nabla \varphi_B, \quad (254)$$

where $\psi_P = \Psi_P/2\pi$ is the poloidal flux function such that $\psi'_P(\psi) = \iota(\psi)$. Upon application of a curl, we recover the Boozer contravariant form of \mathbf{B} (138). We will again express $\dot{\mathbf{R}}$ as in (253) to compute $\mathbf{A}(\mathbf{R}) \cdot \dot{\mathbf{R}}$. Doing so we obtain the following form for the gyroaveraged Lagrangian in Boozer coordinates,

$$\begin{aligned} \mathcal{L}(\psi, \vartheta_B, \varphi_B, \rho, \dot{\psi}, \dot{\vartheta}_B, \dot{\varphi}_B, \dot{\varphi}) &= \frac{m}{2B^2(\psi, \vartheta_B, \varphi_B)} \left(\dot{\psi} K(\psi, \vartheta_B, \varphi_B) + \dot{\vartheta}_B I(\psi) + \dot{\varphi}_B G(\psi) \right)^2 \\ &+ m \frac{\rho^2 \dot{\varphi}^2}{2} + q \left(\psi \dot{\vartheta}_B - \psi_P(\psi) \dot{\varphi}_B \right) - \frac{\dot{\varphi}\rho^2}{2} B(\psi, \vartheta_B, \varphi_B) - q\Phi(\psi). \end{aligned} \quad (255)$$

We now will assume that B and Φ are independent of $\chi = M\vartheta_B - N\varphi_B$. As discussed in Section 5.2.1, if the Lagrangian is independent of one coordinate, this implies the existence of a conserved quantity. Our aim will be to compute this conserved quantity and discuss the implications.

We perform a change of coordinates such that $(\psi, \vartheta_B, \varphi_B) \rightarrow (\psi, \chi, \eta)$ where $\chi = M\vartheta_B - N\varphi_B$ and $\eta = M'\vartheta_B - N'\varphi_B$ with $M'/N' \neq M/N$,

$$\mathcal{L}(\psi, \vartheta_B, \varphi_B, \rho, \dot{\psi}, \dot{\vartheta}_B, \dot{\varphi}_B, \dot{\varphi}) = \tilde{\mathcal{L}}(\psi, \chi, \eta, \rho, \dot{\psi}, \dot{\chi}, \dot{\eta}, \dot{\varphi}). \quad (256)$$

Here we note that $\vartheta_B = (N\eta - N'\chi)/(M'\eta - MN')$ and $\varphi_B = (M\eta - M'\chi)/(M'\eta - MN')$, so

$$\begin{aligned} \tilde{\mathcal{L}}(\psi, \chi, \eta, \rho, \dot{\psi}, \dot{\chi}, \dot{\eta}, \dot{\varphi}) &= \frac{m}{2\tilde{B}^2(\psi, \chi)} \left(\dot{\psi} \tilde{K}(\psi, \chi) - \frac{\dot{\chi}(N'I(\psi) + M'G(\psi))}{M'\eta - MN'} + \frac{\dot{\eta}(NI(\psi) + MG(\psi))}{M'\eta - MN'} \right)^2 \\ &+ m \frac{\rho^2 \dot{\varphi}^2}{2} + q \left(\frac{\dot{\chi}(M'\psi_P(\psi) - N'\psi)}{M'\eta - MN'} + \frac{\dot{\eta}(N\psi - M\psi_P(\psi))}{M'\eta - MN'} \right) - \frac{\dot{\varphi}\rho^2}{2} \tilde{B}(\psi, \chi) - q\tilde{\Phi}(\psi). \end{aligned} \quad (257)$$

The Euler-Lagrange equation corresponding to η is,

$$\frac{\partial \tilde{\mathcal{L}}}{\partial \eta} = \frac{d}{dt} \left(\frac{\partial \tilde{\mathcal{L}}}{\partial \dot{\eta}} \right) \Rightarrow \frac{dp_\eta(t)}{dt} = 0, \quad (258)$$

where p_η is the canonical momentum corresponding to η ,

$$p_\eta(\psi, \chi) := \frac{1}{M'N - MN'} \left(\frac{m\tilde{V}_\parallel(\psi, \chi)}{\tilde{B}(\psi, \chi)} (NI(\psi) + MG(\psi)) + q(N\psi - M\psi_P(\psi)) \right), \quad (259)$$

and the parallel guiding center velocity, \tilde{V}_\parallel , is defined in the following way,

$$\tilde{V}_\parallel(\psi, \chi)\tilde{B}(\psi, \chi) = \dot{\tilde{\mathbf{R}}} \cdot \tilde{\mathbf{B}}(\tilde{\mathbf{R}}) = \dot{\psi}\tilde{K}(\psi, \chi) - \frac{\dot{\chi}(N'I(\psi) + M'G(\psi))}{M'N - MN'} + \frac{\dot{\eta}(NI(\psi) + MG(\psi))}{M'N - MN'}. \quad (260)$$

Similar to the analysis in Section 7.2, we will consider the relative size of each term in p_η . Here we will approximate $V_\parallel \sim v_t$ where v_t is the thermal velocity, as was assumed in Section 5.1, and $\psi \sim r^2 B_T/2$, where r is an approximate scale of the minor radius and $B_T \sim \mathbf{B} \cdot \nabla\varphi_B/|\nabla\varphi_B|$ is an approximate scale of the toroidal field. In stellarators, the toroidal plasma current is much smaller than the poloidal current in the coils so we can assume that $I(\psi) \ll G(\psi)$, as the covariant components are defined such that $G(\psi) = \mu_0 I_P(\psi)/2\pi$ and $I(\psi) = \mu_0 I_T(\psi)/2\pi$. To compute an approximate scaling for the toroidal field, we assume $B_T \sim \mu_0 I_P/(2\pi R)$ where R is the approximate scale of the major radius (see Section 5.4), assuming that all of the poloidal current flows through the coils so that I_P is independent of ψ . Since the plasma current in a stellarator is often small, this is typically a valid approximation. Assuming the integers (N, M, N', M') are $\mathcal{O}(1)$ and that $\psi_P \sim \psi$, it follows that the ratio of the two terms in p_η scales as,

$$\frac{mV_\parallel(NI(\psi) + MG(\psi))/B}{q(N\psi - M\psi_P(\psi))} \sim \frac{v_t(\mu_0 I_P/(2\pi))}{\Omega(r^2 \mu_0 I_P/(4\pi R))} \sim \frac{\rho}{r} \sim \epsilon \ll 1, \quad (261)$$

where $\Omega = qB/m$ is the gyrofrequency and $\rho = v_t/\Omega$ is the gyroradius. In the above we have made the assumption that $r \sim R$, and $\epsilon \ll 1$ is the small parameter considered in Section 5.2, expressing the fact that the gyroradius is much smaller than typical length scales of our system.

Thus, we can approximate $p_\eta \sim q(N\psi - M\psi_P(\psi))$ to lowest order in ϵ . Since p_η is conserved along trajectories from the Euler-Lagrange equation (258), so is ψ to lowest order in ϵ . We can therefore conclude that guiding center orbits stay close to a flux surface, as they do in axisymmetry. In this way, guiding center motion exhibits good confinement properties when the magnetic field strength and electrostatic potential only varies on a surface through χ .

12.1.2 Remark on “quasi”

As seen from the analysis in Section 12.1.1, quasisymmetry refers to configurations for which the magnetic field strength, B , only varies on a surface through a given linear combination of Boozer angles. This symmetry implies that there exists a symmetry coordinate, η , (i.e. the field strength does not depend on η), which results in a conserved quantity upon application of the Euler-Lagrange equations. This is referred to as *quasisymmetry*, as it is a property of the field strength B rather than the vector field \mathbf{B} (that is, it is not a property of each of the vector components). In this way, quasisymmetry is distinct from axisymmetry, which implies a symmetry of each of the vector components of the field (see Section 7.1). Furthermore, some results suggest that quasisymmetry cannot be achieved globally, but only locally on a flux surface [28]. Finally, perfect quasisymmetry can never be achieved in practice, as other physics considerations must be accounted for when designing the magnetic field, and coils cannot be engineered to perfectly reproduce the desired field. However, several stellarators have been designed to be close to quasisymmetry due to its beneficial confinement properties. Several classes of quasisymmetric stellarators will be discussed in the following Section.

12.1.3 Types of quasisymmetry

Quasi-axisymmetry (QA) refers to the case when $N = 0$. Thus contours of B close toroidally without wrapping poloidally around the flux surface (see Figure 27). While there are currently no QA experiments in operation, the QA stellarator, NCSX [101], was designed and partially constructed at the Princeton Plasma Physics Laboratory. The CFQS [85] configuration has been designed and will be constructed at Southwest Jiaotong University in China. In addition, there have been several other configurations designed to be close to QA, including Aries-CS [78], ESTELL [22], and QuASDEX [38].

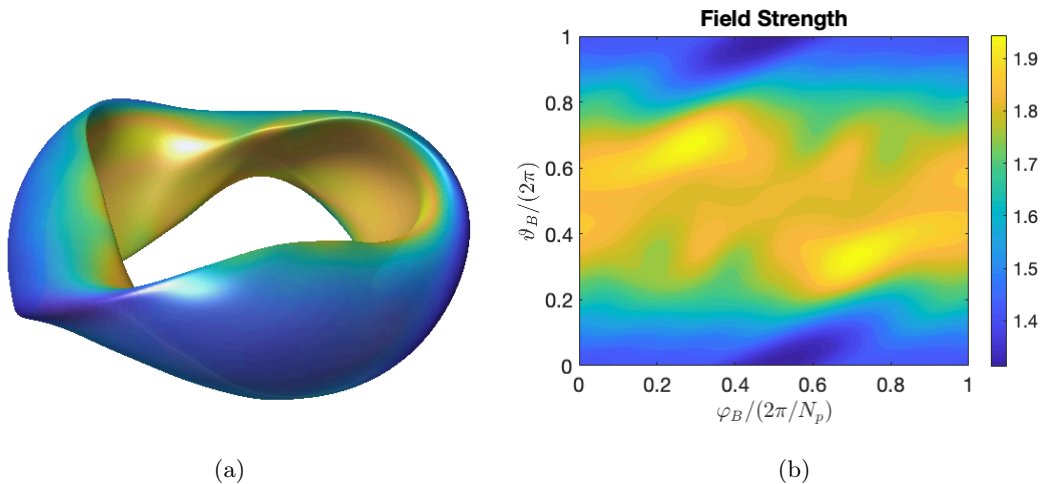


Figure 27: (a) The last magnetic surface of NCSX is shown with the colorscale indicating field strength. (b) The field strength on the last magnetic surface is plotted as a function of the two Boozer angles. As NCSX is quasi-axisymmetric, B is nearly constant along lines of constant φ_B .

Quasi-poloidal (QP) symmetry refers to the case when $M = 0$ so that contours of B close poloidally without wrapping toroidally around the flux surface. It should be noted that this type of symmetry cannot be achieved in practice near the axis due to the requirement that the pressure gradient vanishes on axis (see Section 2.7 in [62]). However, away from the axis, it may be possible to get close to QP symmetry. An example of a configuration designed for QP symmetry is the Quasi Poloidal Stellarator [91].

Quasi-helical (QH) symmetry implies that the field strength can be expressed as $B(\psi, M\vartheta_B - N\varphi_B)$ with $M \neq 0$ and $N \neq 0$. Thus contours of B close both toroidally and poloidally, or helically (see Figure 28). The Helically Symmetric Experiment (HSX) at the University of Wisconsin [7] is the only existing quasisymmetric stellarator. Several other QH configurations have been designed [80, 61] but not constructed.

12.2 N_P symmetry

While quasisymmetry is a continuous symmetry and results in a independent coordinate, many physical properties of stellarators can also exhibit discrete symmetries, for example, invariance with respect to reflection or translation.

Specifically, the magnetic field in stellarators often exhibits a (discrete) symmetry with respect to the number of periods, N_P , in a full toroidal turn, namely,

$$\mathbf{B}(\psi, \theta, \zeta + 2\pi/N_P) = \mathbf{B}(\psi, \theta, \zeta), \quad (262)$$

when expressed in flux coordinates (see Section 6.4), (ψ, θ, ζ) . The same periodicity holds in the cylindrical coordinate system (see Section 6.2), (R, ϕ, Z) .

The above notation in (262) indicates that each of the vector components obeys the symmetry. As a consequence, other quantities, such as the cylindrical coordinates describing magnetic surfaces, R and Z , exhibit the same periodicity when expressed in flux coordinates. As many physical quantities are periodic with respect to N_P , this yields computational savings for many problems. In the stellarator literature, this is referred to as N_P -symmetry or field period symmetry, referring to a periodicity with respect to a toroidal turn of $2\pi/N_P$.

For example, the W7-X stellarator has 5 field periods, and as a result, the same coil shapes can be used for each field period. In Figure 29, a magnetic surface of W7-X is shown, with the color scale indicating the field strength. As can be seen, the field strength exhibits 5 toroidal periods. The electro-magnetic coils are shown for one field period.

12.3 Stellarator symmetry

Stellarator symmetry refers to a discrete symmetry with respect to a specific transformation as defined below. Consider the cylindrical coordinates, (R, ϕ, Z) (see Section 6.2).

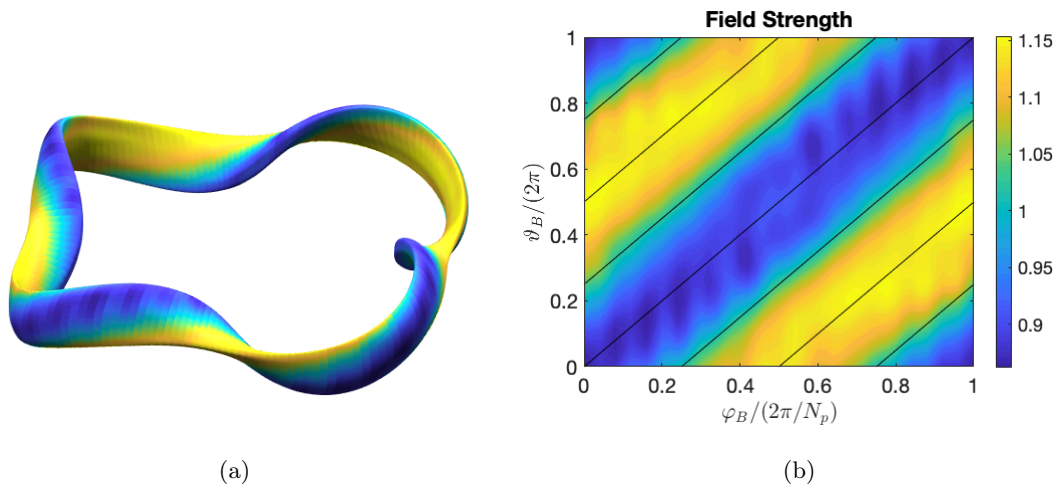


Figure 28: (a) The last magnetic surface of HSX is shown with the colorscale indicating field strength. (b) The field strength on the last magnetic surface is plotted as a function of the two Boozer angles. As HSX is quasi-helically symmetric, B is nearly constant along lines of constant $\vartheta_B + N_P\varphi_B$ (black), where N_P is the number of field periods (see Section 12.2).

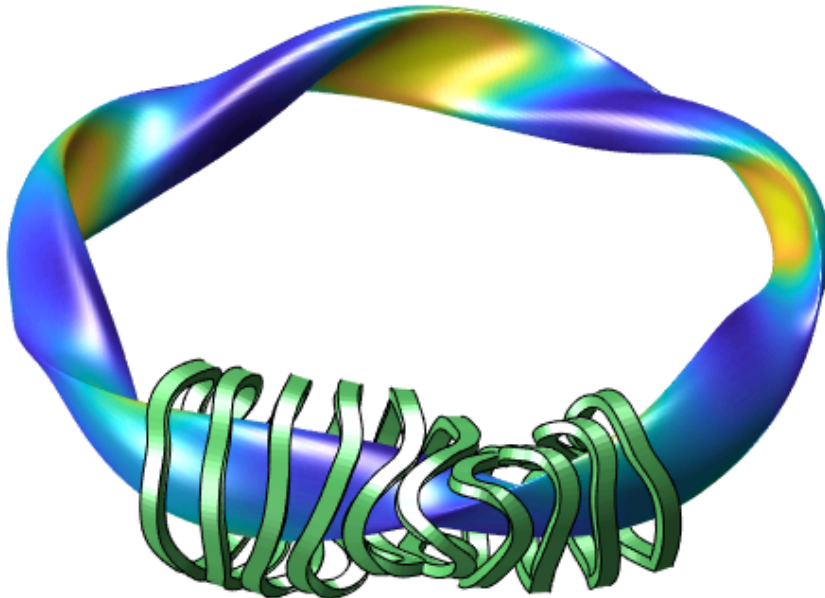


Figure 29: The last closed magnetic surface of the W7-X configuration is shown with the color scale indicating the field strength. The electro-magnetic coil shapes are shown for one field period of the device.

We define the transformation \mathcal{T} by

$$\mathcal{T} : \mathbf{F} = F_R \hat{\mathbf{R}} + F_\phi \hat{\boldsymbol{\phi}} + F_Z \hat{\mathbf{Z}} \mapsto \mathbf{G} = G_R \hat{\mathbf{R}} + G_\phi \hat{\boldsymbol{\phi}} + G_Z \hat{\mathbf{Z}} \quad (263)$$

such that

$$\begin{cases} G_R(R, \phi, Z) = F_R(R, -\phi, -Z) \\ G_\phi(R, \phi, Z) = F_\phi(R, -\phi, -Z) \\ G_Z(R, \phi, Z) = F_Z(R, -\phi, -Z) \end{cases} . \quad (264)$$

The transformation \mathcal{T} can be thought of as an inversion about the line $\phi = 0, Z = 0$ (see Figure 30). The term stellarator symmetry describes a vector field \mathbf{F} satisfying the following property

$$\mathcal{T}[\mathbf{F}] = -F_R \hat{\mathbf{R}} + F_\phi \hat{\boldsymbol{\phi}} + F_Z \hat{\mathbf{Z}}. \quad (265)$$

A given stellarator configuration is said to possess stellarator symmetry if the equilibrium magnetic field \mathbf{B} is stellarator symmetric according to (265). As will be discussed further at the end of this Section, stellarator symmetry provides computational efficiency, as many physical quantities have definite parity (are even or odd). It can be shown that if the magnetic field \mathbf{B} exhibits this symmetry, then so does the current density \mathbf{J} upon application of Ampere's law (13) in cylindrical coordinates.

Suppose a vector field \mathbf{F} possesses stellarator symmetry. This implies that the magnitude F of the vector field exhibits the following symmetry,

$$F(R, -\phi, -Z) = F(R, \phi, Z). \quad (266)$$

Thus the field strength B and magnitude of the current density J exhibit this property for a stellarator symmetric configuration.

Consider now what happens to the position vector which follows a field line, \mathbf{r} , under the assumption that \mathbf{B} is stellarator symmetric. The curve \mathbf{r} satisfies,

$$(\hat{\mathbf{b}} \cdot \nabla) \mathbf{r} = \hat{\mathbf{b}}, \quad (267)$$

where $\hat{\mathbf{b}} = \mathbf{B}/B$ is a unit vector in the direction of the magnetic field. Assume that \mathbf{r} is a curve parameterized by ϕ , $\mathbf{r}(\phi) = R(\phi) \hat{\mathbf{R}}(\phi) + Z(\phi) \hat{\mathbf{Z}}$, then in cylindrical coordinates (267) reads,

$$\frac{dR(\phi)}{d\phi} = \frac{R(\phi) B_R(R(\phi), \phi, Z(\phi))}{B_\phi(R(\phi), \phi, Z(\phi))} \quad (268a)$$

$$\frac{dZ(\phi)}{d\phi} = \frac{R(\phi) B_Z(R(\phi), \phi, Z(\phi))}{B_\phi(R(\phi), \phi, Z(\phi))}, \quad (268b)$$

where the notation $d/d\phi$ indicates the derivative with respect to ϕ along a field line and we have used $d\mathbf{r}/d\phi = dR/d\phi \hat{\mathbf{R}} + R \hat{\boldsymbol{\phi}} + dZ/d\phi \hat{\mathbf{Z}}$. If \mathbf{B} is stellarator symmetric, then under the transformation $Z \rightarrow -Z$ and $\phi \rightarrow -\phi$, we see that $dR/d\phi \rightarrow -dR/d\phi$ and $dZ/d\phi \rightarrow dZ/d\phi$. This implies that if $R(\phi)$ and $Z(\phi)$ parameterize a field line of a stellarator symmetric magnetic field, then so do $R(-\phi)$ and $-Z(-\phi)$. If in addition there exists a flux surface, this results in the same symmetry of the cylindrical components, R and Z , of the surface on which field lines lie.

Stellarator symmetry can also be expressed in general flux coordinates (ψ, θ, ζ) , where ψ is a flux label, θ is a poloidal angle, and ζ is a toroidal angle (see Section 6.4). We will now see that it can simplify the expression of some physical quantities of a stellarator symmetric field. For a coordinate system which preserves stellarator symmetry, the following property holds for the cylindrical components (R, ϕ, Z) ,

$$R(\psi, -\theta, -\zeta) = R(\psi, \theta, \zeta) \quad (269a)$$

$$\phi(\psi, -\theta, -\zeta) = -\phi(\psi, \theta, \zeta) \quad (269b)$$

$$Z(\psi, -\theta, -\zeta) = -Z(\psi, \theta, \zeta). \quad (269c)$$

Therefore the transformation \mathcal{T} defined in (263)-(264) can now be expressed in terms of flux coordinates as follows

$$\mathcal{T} : \mathbf{F} = F_R \hat{\mathbf{R}} + F_\phi \hat{\boldsymbol{\phi}} + F_Z \hat{\mathbf{Z}} \mapsto \mathbf{G} = G_R \hat{\mathbf{R}} + G_\phi \hat{\boldsymbol{\phi}} + G_Z \hat{\mathbf{Z}} \quad (270)$$

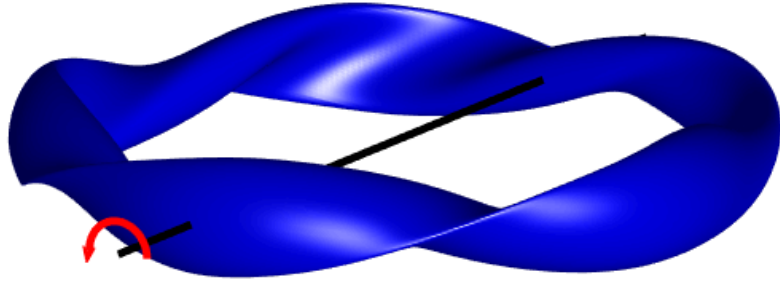


Figure 30: Stellarator symmetry describes an inversion about the line $Z = 0$, $\phi = 0$. The stellarator-symmetric W7-X configuration is shown.

defined by

$$\begin{cases} G_R(\psi, \theta, \zeta) = F_R(\psi, -\theta, -\zeta) \\ G_\phi(\psi, \theta, \zeta) = F_\phi(\psi, -\theta, -\zeta) \\ G_Z(\psi, \theta, \zeta) = F_Z(\psi, -\theta, -\zeta) \end{cases} . \quad (271)$$

We see that for a stellarator symmetric field, F_R is odd with respect to (θ, ζ) while F_Z and F_ϕ are even. Thus stellarator symmetry implies a definite parity of many physical quantities; these quantities are even or odd with respect to (θ, ζ) . Quantities with a definite parity can be expressed in terms of only a sine or cosine series rather than a generic Fourier series. For example, in a stellarator symmetric field the field strength can be expressed with just a cosine series from (266),

$$B(\psi, \theta, \zeta) = \sum_{m,n} B_{mn}(\psi) \cos(m\theta - n\zeta). \quad (272)$$

Unlike quasisymmetry, stellarator symmetry is not inherently beneficial for confinement. However, the assumption of stellarator symmetry has been made in the design of almost [64] every stellarator configuration to date. This is partly motivated by computational efficiency, as fewer Fourier coefficients are required to represent equilibrium quantities. A detailed discussion of stellarator symmetry is given in [18].

Appendices

A Debye shielding

As an example of the separation of scales that arise in plasma physics, we discuss the concept of Debye shielding.

Plasmas are dielectric, in that they tend to shield out electrostatic potentials. The Debye length, λ_D , is the characteristic length scale on which the electric field produced by a charge is screened by other mobile charges. It is defined, in the presence of species with number density n_s , temperature T_s and charge q_s , by

$$\lambda_D = \left(\sum_s \frac{n_s q_s^2}{\epsilon_0 T_s} \right)^{-1/2}. \quad (273)$$

If the plasma is cold ($T_s \rightarrow 0$), then the shielding is perfect and $\lambda_D \rightarrow 0$. In a hot plasma, some charges will have enough thermal energy to escape the electrostatic potential, resulting in a finite λ_D .

We can find this length scale by considering Poisson's equation (see Section 3.2) for a test charge q_T in the presence of species with number density n_1^s and charge q_s

$$\Delta\Phi = -\frac{1}{\epsilon_0} \left(\sum_s n_1^s q_s \right) - \frac{q_T}{\epsilon_0} \delta(\mathbf{r}). \quad (274)$$

Here $\delta(\mathbf{r})$ is the Dirac delta function. Note that n_1^s will differ from the density n_s that was introduced previously (as in (1) and (273)), as it was assumed then that one is looking at length scales longer than λ_D , such that the electrostatic potential is screened out. Here we will be considering the density at shorter length scales, so this assumption does not hold.

The densities n_1^s can be expressed in terms of distributions functions f_s as $n_1^s = \int d^3v f_s(\mathbf{v})$. The distribution function is normalized such that $f(\mathbf{v})d^3v$ is the number of particles per unit volume, so f describes the density of particles in phase space (position and velocity). The Maxwell-Boltzmann distribution can be applied to describe a plasma which has reached thermodynamic equilibrium, often through collisions, and we will make the assumption that both the distribution functions can be described by a Maxwell-Boltzmann distribution,

$$f_s(\mathbf{v}) = A \exp\left(\frac{m_s v^2}{2T_s} - \frac{q_s \Phi}{T_s}\right), \quad (275)$$

for normalization constant A . So, the densities can be written as $n_1^s = n_s e^{-q_s \Phi/T_s}$ where $n_s = A \int d^3v \exp\left(\frac{m_s v^2}{2T_s}\right)$ is the number density of species s in the limit $\Phi \rightarrow 0$. In other words, far away from the test charge the potential from the charge is shielded out so that quasineutrality holds, that is to say $\sum_s n_s q_s = 0$.

Assuming $q_s \Phi/T_s \ll 1$, we can Taylor expand the exponents,

$$\Delta\Phi = -\frac{1}{\epsilon_0} \sum_s n_s q_s \left(1 - \frac{q_s \Phi}{T_s}\right) - \frac{q_T}{\epsilon_0} \delta(\mathbf{r}). \quad (276)$$

Since $\sum_s n_s q_s = 0$,

$$\frac{1}{r^2} \frac{d}{dr} \left(r^2 \frac{d\Phi}{dr} \right) = \lambda_D^{-2} \Phi - \frac{q_T}{\epsilon_0} \delta(\mathbf{r}). \quad (277)$$

The solution for electrostatic potential is

$$\Phi = \frac{q_T}{r} \exp(-r/\lambda_D). \quad (278)$$

So on length scales longer than λ_D , the plasma is quasineutral. In typical fusion plasmas the number of particles in a sphere of radius λ_D is very large,

$$\frac{4\pi n \lambda_D^3}{3} \gg 1. \quad (279)$$

This allows one to consider the weak coupling assumption, such that the collective motion of the plasma dominates over the short-range electrostatic interaction between charges.

Acknowledgements

The authors would like to thank Matt Landreman, Per Helander, Stuart Hudson, Antoine Cerfon, Joaquim Loizu, Georg Stadler, Rogerio Jorge, Wrick Sengupta, Chris Smiet, and Allan Reiman for their valuable comments on the document.

References

- [1] *How NIF works*. <https://lasers.llnl.gov/about/how-nif-works>. Accessed: 2019-08-14.
- [2] *What will ITER do?* <https://www.iter.org/sci/Goals>. Accessed: 2019-08-14.
- [3] *The Hamiltonian formalism*. <http://www.damtp.cam.ac.uk/user/tong/dynamics/four.pdf>, 2015. Accessed: 2018-03-05.
- [4] *The Lagrangian formalism*. <http://www.damtp.cam.ac.uk/user/tong/dynamics/two.pdf>, 2015. Accessed: 2018-03-05.
- [5] *Magnetic Coils and Plasma from Wendelstein 7-X*. <https://www.ipp.mpg.de/2523775/konzeptentwicklung>, 2018. Accessed: 2018-10-04.

- [6] Tokamak. <http://www.ipp.mpg.de/14869/tokamak>, 2018. Accessed: 2018-10-04.
- [7] F. S. B. ANDERSON, A. F. ALMAGRI, D. T. ANDERSON, P. G. MATTHEWS, J. N. TALMADGE, AND J. L. SHOHEIT, *The Helically Symmetric Experiment (HSX): goals, design and status*, Fusion Technology, 27 (1995), pp. 273–277.
- [8] R. ANGELO, E. DUZZIONI, AND A. RIBEIRO, *Integrability in time-dependent systems with one degree of freedom*, Journal of Physics A: Mathematical and Theoretical, 45 (2012), p. 055101.
- [9] V. I. ARNOLD, *Proof of a theorem of AN Kolmogorov on the invariance of quasi-periodic motions under small perturbations of the Hamiltonian*, Collected Works: Representations of Functions, Celestial Mechanics and KAM Theory, 1957–1965, (2009), pp. 267–294.
- [10] M. A. BERGER AND G. B. FIELD, *The topological properties of magnetic helicity*, Journal of Fluid Mechanics, 147 (1984), pp. 133–148.
- [11] I. B. BERNSTEIN, E. FRIEMAN, M. D. KRUSKAL, AND R. KULSRUD, *An energy principle for hydromagnetic stability problems*, Proceedings of the Royal Society of London. Series A. Mathematical and Physical Sciences, 244 (1958), pp. 17–40.
- [12] A. S. BISHOP, *Project Sherwood - the US program in controlled fusion*, 1958.
- [13] A. H. BOOZER, *Evaluation of the structure of ergodic fields*, The Physics of Fluids, 26 (1983), pp. 1288–1291.
- [14] S. BOUQUET AND A. BOURDIER, *Notion of integrability for time-dependent Hamiltonian systems: illustrations from the relativistic motion of a charged particle*, Physical Review E, 57 (1998), p. 1273.
- [15] O. P. BRUNO AND P. LAURENCE, *Existence of three-dimensional toroidal MHD equilibria with nonconstant pressure*, Communications on Pure and Applied Mathematics, 49 (1996), pp. 717–764.
- [16] J. R. CARY AND R. G. LITTLEJOHN, *Noncanonical Hamiltonian mechanics and its application to magnetic field line flow*, Annals of Physics, 151 (1983), pp. 1–34.
- [17] D. DEL CASTILLO-NEGRETTE, J. GREENE, AND P. MORRISON, *Area preserving nontwist maps: periodic orbits and transition to chaos*, Physica D: Nonlinear Phenomena, 91 (1996), pp. 1–23.
- [18] R. DEWAR AND S. HUDSON, *Stellarator symmetry*, Physica D: Nonlinear Phenomena, 112 (1998), pp. 275–280.
- [19] R. L. DEWAR, Z. YOSHIDA, A. BHATTACHARJEE, AND S. R. HUDSON, *Variational formulation of relaxed and multi-region relaxed magnetohydrodynamics*, Journal of Plasma Physics, 81 (2015).
- [20] W. D. D’HAESELEER, W. N. HITCHON, J. D. CALLEN, AND J. L. SHOHEIT, *Flux Coordinates and Magnetic Field Structure: A Guide to a Fundamental Tool of Plasma Theory*, Springer, 1991.
- [21] C. T. DODSON, P. E. PARKER, AND P. PARKER, *A user’s guide to algebraic topology*, vol. 387, Springer Science & Business Media, 1997.
- [22] M. DREVLAK, F. BROCHARD, P. HELANDER, J. KISSLINGER, M. MIKHAILOV, C. NÜHRENBERG, J. NÜHRENBERG, AND Y. TURKIN, *ESTELL: A quasi-toroidally symmetric stellarator*, Contributions to Plasma Physics, 53 (2013), pp. 459–468.
- [23] K. ELSASSER, *Magnetic field line flow as a Hamiltonian problem*, Plasma Physics and Controlled Fusion, 28 (1986), p. 1743.
- [24] T. L. FERRELL, *Hamilton-Jacobi perturbation theory*, American Journal of Physics, 39 (1971), pp. 622–627.

- [25] J. FREIDBERG, *Ideal MHD*, Cambridge University Press, 2014.
- [26] J. P. FREIDBERG, *Plasma Physics and Fusion Energy*, Cambridge University Press, 2008.
- [27] P. GARABEDIAN, *Three-dimensional stellarator codes*, Proceedings of the National Academy of Sciences, 99 (2002), pp. 10257–10259.
- [28] D. GARREN AND A. H. BOOZER, *Existence of quasihelically symmetric stellarators*, Physics of Fluids B: Plasma Physics, 3 (1991), pp. 2822–2834.
- [29] J. GOEDBLOED AND S. POEDTS, *Principles of magnetohydrodynamics: with applications to laboratory and astrophysical plasmas*, Cambridge University Press, 2004.
- [30] H. GOLDSTEIN, C. POOLE, AND J. SAFKO, *Classical Mechanics*, Addison-Wesley, 2002.
- [31] R. J. GOLDSTON AND P. H. RUTHERFORD, *Introduction to plasma physics*, CRC Press, 1995.
- [32] H. GRAD, *Toroidal containment of a plasma*, The Physics of Fluids, 10 (1967), pp. 137–154.
- [33] K. HARAFUJI, T. HAYASHI, AND T. SATO, *Computational study of three-dimensional magnetohydrodynamic equilibria in toroidal helical systems*, Journal of computational physics, 81 (1989), pp. 169–192.
- [34] R. D. HAZELTINE AND J. D. MEISS, *Plasma Confinement*, Courier Corporation, 2003.
- [35] C. HEGNA AND A. BHATTACHARJEE, *Islands in three-dimensional steady flows*, Journal of Fluid Mechanics, 227 (1991), pp. 527–542.
- [36] P. HELANDER, *Theory of plasma confinement in non-axisymmetric magnetic field*, Reports of Progress in Physics, 77 (2014), p. 087001.
- [37] P. HELANDER AND D. J. SIGMAR, *Collisional Transport in Magnetized Plasmas*, vol. 4, Cambridge University Press, 2005.
- [38] S. HENNEBERG, M. DREVLAK, C. NÜHRENBURG, C. BEIDLER, Y. TURKIN, J. LOIZU, AND P. HELANDER, *Properties of a new quasi-axisymmetric configuration*, Nuclear Fusion, 59 (2019), p. 026014.
- [39] J. G. HEYWOOD, *Auxiliary flux and pressure conditions for Navier-Stokes problems*, in Approximation Methods for Navier-Stokes Problems, R. Rautmann, ed., Berlin, Heidelberg, 1980, Springer Berlin Heidelberg, pp. 223–234.
- [40] J. G. HEYWOOD, R. RANNACHER, AND S. TUREK, *Artificial boundaries and flux and pressure conditions for the incompressible Navier–Stokes equations*, International Journal for Numerical Methods in Fluids, 22 (1996), pp. 325–352.
- [41] S. HIRSHMAN, P. MERKEL, ET AL., *Three-dimensional free boundary calculations using a spectral Green’s function method*, Computer Physics Communications, 43 (1986), pp. 143–155.
- [42] S. HIRSHMAN, R. SANCHEZ, AND C. COOK, *SIESTA: A scalable iterative equilibrium solver for toroidal applications*, Physics of Plasmas, 18 (2011), p. 062504.
- [43] S. P. HIRSHMAN AND J. C. WHITSON, *Steepest descent moment method for three-dimensional magnetohydrodynamic equilibria*, The Physics of Fluids, 26 (1983), p. 3553.
- [44] M. HOLE, S. R. HUDSON, AND R. DEWAR, *Stepped pressure profile equilibria in cylindrical plasmas via partial Taylor relaxation*, Journal of Plasma Physics, 72 (2006), pp. 1167–1171.
- [45] J. D. HUBA, *NRL plasma formulary*, tech. rep., Naval Research Laboratory, 2006.
- [46] S. HUDSON, *A regularized approach for solving magnetic differential equations and a revised iterative equilibrium algorithm*, Physics of Plasmas, 17 (2010), p. 114501.

- [47] S. HUDSON, R. DEWAR, G. DENNIS, M. HOLE, M. MCGANN, G. VON NESSI, AND S. LAZERSON, *Computation of multi-region relaxed magnetohydrodynamic equilibria*, Physics of Plasmas, 19 (2012), p. 112502.
- [48] S. HUDSON AND N. NAKAJIMA, *Pressure, chaotic magnetic fields, and magnetohydrodynamic equilibria*, Physics of Plasmas, 17 (2010), p. 052511.
- [49] S. R. HUDSON, R. DEWAR, M. HOLE, AND M. MCGANN, *Non-axisymmetric, multi-region relaxed magnetohydrodynamic equilibrium solutions*, Plasma Physics and Controlled Fusion, 54 (2011), p. 014005.
- [50] S. HYSING, S. TUREK, D. KUZMIN, N. PAROLINI, E. BURMAN, S. GANESAN, AND L. TOBISKA, *Quantitative benchmark computations of two-dimensional bubble dynamics*, International Journal for Numerical Methods in Fluids, 60 (2009), pp. 1259–1288.
- [51] S. JARDIN, *Computational Methods in Plasma Physics*, CRC Press, 2010.
- [52] S. C. JARDIN, J. BRESLAU, AND N. FERRARO, *A high-order implicit finite element method for integrating the two-fluid magnetohydrodynamic equations in two dimensions*, Journal of Computational Physics, 226 (2007), pp. 2146–2174.
- [53] R. JORGE, P. RICCI, AND N. LOUREIRO, *A drift-kinetic analytical model for scrape-off layer plasma dynamics at arbitrary collisionality*, Journal of Plasma Physics, 83 (2017).
- [54] R. JORGE, W. SENGUPTA, AND M. LANDREMAN, *Near-axis framework for stellarator equilibrium at arbitrary order in the distance to the axis*. In preparation.
- [55] A. N. KOLMOGOROV, *On conservation of conditionally periodic motions for a small change in Hamilton's function*, in Dokl. Akad. Nauk SSSR, vol. 98, 1954, pp. 527–530.
- [56] A. KOMORI, T. MORISAKI, T. MUTOH, S. SAKAKIBARA, Y. TAKEIRI, R. KUMAZAWA, S. KUBO, K. IDA, S. MORITA, K. NARIHARA, ET AL., *Overview of progress in LHD experiments*, Fusion Science and Technology, 50 (2006), pp. 136–145.
- [57] M. G. KONG, G. KROESEN, G. MORFILL, T. NOSENKO, T. SHIMIZU, J. VAN DIJK, AND J. L. ZIMMERMANN, *Plasma medicine: an introductory review*, New Journal of Physics, 11 (2009), p. 115012.
- [58] V. V. KOZLOV, *Integrability and non-integrability in Hamiltonian mechanics*, Russian Mathematical Surveys, 38 (1983), p. 1.
- [59] R. KRESS, *On constant-alpha force-free fields in a torus*, Journal of Engineering Mathematics, 20 (1986), pp. 323–344.
- [60] M. D. KRUSKAL AND R. KULSRUD, *Equilibrium of a magnetically confined plasma in a toroid*, The Physics of Fluids, 1 (1958), pp. 265–274.
- [61] L. KU AND A. BOOZER, *New classes of quasi-helically symmetric stellarators*, Nuclear Fusion, 51 (2010), p. 013004.
- [62] M. LANDREMAN, *Electric Fields and Transport in Optimized Stellarators*, PhD thesis, MIT, 2011.
- [63] M. LANDREMAN AND W. SENGUPTA, *Direct construction of optimized stellarator shapes. Part 1. Theory in cylindrical coordinates*, Journal of Plasma Physics, 84 (2018).
- [64] M. LANDREMAN, W. SENGUPTA, AND G. G. PLUNK, *Direct construction of optimized stellarator shapes. Part 2. Numerical quasisymmetric solutions*, Journal of Plasma Physics, 85 (2019).
- [65] S. A. LAZERSON, J. LOIZU, S. HIRSHMAN, AND S. R. HUDSON, *Verification of the ideal magnetohydrodynamic response at rational surfaces in the VMEC code*, Physics of Plasmas, 23 (2016), p. 012507.

- [66] I. LEVCHENKO, S. XU, G. TEEL, D. MARIOTTI, M. WALKER, AND M. KEIDAR, *Recent progress and perspectives of space electric propulsion systems based on smart nanomaterials*, Nature Communications, 9 (2018), p. 879.
- [67] A. J. LICHTENBERG AND M. A. LIEBERMAN, *Regular and stochastic motion*, vol. 38, Springer Science & Business Media, 2013.
- [68] M. A. LIEBERMAN, A. J. LICHTENBERG, ET AL., *Principles of Plasma Discharges and Materials Processing*, vol. 2, Wiley Online Library, 2005.
- [69] R. G. LITTLEJOHN, *Variational principles of guiding centre motion*, Journal of Plasma Physics, 29 (1983), pp. 111–125.
- [70] J. LOIZU, S. HUDSON, A. BHATTACHARJEE, AND P. HELANDER, *Magnetic islands and singular currents at rational surfaces in three-dimensional magnetohydrodynamic equilibria*, Physics of Plasmas, 22 (2015), p. 022501.
- [71] D. MALHOTRA, A. CERFON, L.-M. IMBERT-GÉRARD, AND M. O’NEIL, *Taylor states in stellarators: A fast high-order boundary integral solver*, Journal of Computational Physics, 397 (2019), p. 108791.
- [72] K. MCCORMICK, P. GRIGULL, R. BURHENN, R. BRAKEL, H. EHMLER, Y. FENG, F. GADELMEIER, L. GIANNONE, D. HILDEBRANDT, M. HIRSCH, ET AL., *New advanced operational regime on the W7-AS stellarator*, Physical Review Letters, 89 (2002), p. 015001.
- [73] C. MERCIER, *Equilibrium and stability of a toroidal magnetohydrodynamic system in the neighbourhood of a magnetic axis*, Nuclear Fusion, 4 (1964), p. 213.
- [74] P. MERKEL, *An integral equation technique for the exterior and interior Neumann problem in toroidal regions*, Journal of Computational Physics, 66 (1986), pp. 83–98.
- [75] H. MOFFATT, *Magnetostatic equilibria and analogous euler flows of arbitrarily complex topology. Part 1. Fundamentals*, Journal of Fluid Mechanics, 159 (1985), pp. 359–378.
- [76] P. J. MORRISON, *Hamiltonian description of the ideal fluid*, Reviews of Modern Physics, 70 (1998), p. 467.
- [77] J. MÖSER, *On invariant curves of area-preserving mappings of an annulus*, Nachr. Akad. Wiss. Göttingen, II, (1962), pp. 1–20.
- [78] F. NAJMAADI, A. RAFFRAY, S. ABDEL-KHALIK, L. BROMBERG, L. CROSATTI, L. EL-GUEBALY, P. GARABEDIAN, A. GROSSMAN, D. HENDERSON, A. IBRAHIM, ET AL., *The ARIES-CS compact stellarator fusion power plant*, Fusion Science and Technology, 54 (2008), pp. 655–672.
- [79] D. R. NICHOLSON AND D. R. NICHOLSON, *Introduction to Plasma Theory*, Wiley New York, 1983.
- [80] J. NÜHRENBERG AND R. ZILLE, *Quasi-helically symmetric toroidal stellarators*, Physics Letters A, 129 (1988), pp. 113–117.
- [81] M. O’NEIL AND A. J. CERFON, *An integral equation-based numerical solver for Taylor states in toroidal geometries*, Journal of Computational Physics, 359 (2018), pp. 263–282.
- [82] E. OTT, *Chaos in Dynamical Systems*, Cambridge University Press, 2002, ch. 7.
- [83] A. REIMAN AND H. GREENSIDE, *Calculation of three-dimensional MHD equilibria with islands and stochastic regions*, Computer Physics Communications, 43 (1986), p. 157.
- [84] W. SENGUPTA, *Stellarator equilibrium axis-expansion to all orders in distance from the axis for arbitrary plasma beta*. In preparation.
- [85] A. SHIMIZU, H. LIU, M. ISOBE, S. OKAMURA, S. NISHIMURA, C. SUZUKI, Y. XU, X. ZHANG, B. LIU, J. HUANG, ET AL., *Configuration property of the chinese first quasi-axisymmetric stellarator*, Plasma and Fusion Research, 13 (2018), pp. 3403123–3403123.

- [86] L. SOLOVÈV AND V. SHAFRANOV, *Plasma confinement in closed magnetic systems*, in Reviews of Plasma Physics, Springer, 1970, pp. 1–247.
- [87] C. SOVINEC, A. GLASSER, T. GIANAKON, D. BARNES, R. NEBEL, S. KRUGER, S. PLIMPTON, A. TARDITI, M. CHU, AND THE NIMROD TEAM, *Nonlinear magnetohydrodynamics with high-order finite elements*, J. Comp. Phys., 195 (2004), p. 355.
- [88] M. SPADA AND H. WOBIG, *On the existence and uniqueness of dissipative plasma equilibria in a toroidal domain*, Journal of Physics A: Mathematical and General, 25 (1992), p. 1575.
- [89] L. SPITZER JR, *The stellarator concept*, The Physics of Fluids, 1 (1958), pp. 253–264.
- [90] D. SPONG, S. P. HIRSHMAN, L. BERRY, J. LYON, R. FOWLER, D. STRICKLER, M. COLE, B. NELSON, D. WILLIAMSON, A. WARE, ET AL., *Physics issues of compact drift optimized stellarators*, Nuclear Fusion, 41 (2001), p. 711.
- [91] D. J. STRICKLER, S. P. HIRSHMAN, D. A. SPONG, M. J. COLE, J. F. LYON, B. E. NELSON, D. E. WILLIAMSON, AND A. S. WARE, *Development of a robust quasi-poloidal compact stellarator*, Fusion Science and Technology, 45 (2004), pp. 15–26.
- [92] T. SUNN PEDERSEN, A. DINKLAGE, Y. TURKIN, R. WOLF, S. BOZHENKOV, J. GEIGER, G. FUCHERT, H.-S. BOSCH, K. RAHBARNIA, H. THOMSEN, ET AL., *Key results from the first plasma operation phase and outlook for future performance in Wendelstein 7-X*, Physics of Plasmas, 24 (2017), p. 055503.
- [93] J. B. TAYLOR, *Relaxation of toroidal plasma and generation of reverse magnetic fields*, Physical Review Letters, 33 (1974), p. 1139.
- [94] J. B. TAYLOR, *Relaxation and magnetic reconnection in plasmas*, Rev. Mod. Phys., 58 (1986), pp. 741–763.
- [95] S. TUREK, O. MIERKA, AND K. BÄUMLER, *Numerical benchmarking for 3D multiphase flow: New results for a rising bubble*, in Numerical Mathematics and Advanced Applications ENUMATH 2017, F. A. Radu, K. Kumar, I. Berre, J. M. Nordbotten, and I. S. Pop, eds., Cham, 2019, Springer International Publishing, pp. 593–601.
- [96] H. WEITZNER, *Ideal magnetohydrodynamic equilibrium in a non-symmetric topological torus*, Physics of Plasmas, 21 (2014), p. 022515.
- [97] H. WEITZNER, *Expansions of non-symmetric toroidal magnetohydrodynamic equilibria*, Physics of Plasmas, 23 (2016), p. 062512.
- [98] J. WESSON AND D. J. CAMPBELL, *Tokamaks*, vol. 149, Oxford University Press, 2011.
- [99] J.-C. YOCCOZ, *An Introduction To Small Divisors Problems*, Springer Berlin Heidelberg, Berlin, Heidelberg, 1992, pp. 659–679.
- [100] L. E. ZAKHAROV, *Implementation of Hamada principle in calculations of nested 3-D equilibria*, Journal of Plasma Physics, 81 (2015).
- [101] M. ZARNSTORFF, L. BERRY, A. BROOKS, E. FREDRICKSON, G. FU, S. HIRSHMAN, S. HUDSON, L. KU, E. LAZARUS, D. MIKKELSEN, ET AL., *Physics of the compact advanced stellarator NCSX*, Plasma Physics and Controlled Fusion, 43 (2001), p. A237.